AN ANALYSIS OF THE APPLICATION OF SELF-ADAPTING CONTROL TO THE LATERAL RESPONSE OF A HIGH PERFORMANCE, SUPERSONIC AIRCRAFT

JOHN F. FROST, III
AND
RONALD A. GURNSEY

AN ANALYSIS OF THE APPLICATION OF SELF-ADAPTING CONTROL TO THE LATERAL RESPONSE OF A HIGH PERFORMANCE, SUPERSONIC AIRCRAFT

by

John F. Frost, III.

Lieutenant, United States Navy

and

Ronald A. Gurnsey

Lieutenant, United States Navy

Submitted in partial fulfillment of
the requirements for the degree of

MASTER OF SCIENCE
IN
ELECTRICAL ENGINEERING

United States Naval Postgraduate School
Monterey, California

1 9 5 9

AN ANALYSIS OF THE APPLICATION OF SELF-ADAPTING CONTROL TO THE LATERAL RESPONSE OF A HIGH PERFORMANCE, SUPERSONIC AIRCRAFT

* * * * * * * *

John F. Frost, III.

and

Ronald A. Gurnsey

AN ANALYSIS OF THE APPLICATION OF SELF-ADAPTING CONTROL TO THE LATERAL RESPONSE OF A HIGH PERFORMANCE SUPERSONIC AIRCRAFT

by

John F. Frost, III.

and

Ronald A. Gurnsey

This work is accepted as fulfilling

the thesis requirements for the degree of

MASTER OF SCIENCE

IN

ELECTRICAL ENGINEERING

from the

United States Naval Postgraduate School

ABSTRACT

In the modern, high performance, supersonic aircraft, varying conditions of flight produce airframe transfer functions whose parameters also vary. Fixed parameter, servo control loops in general cannot provide satisfactory control over the entire region of flight. Self-adapting control loops which automatically alter their parameters in order to provide the most satisfactory control response are becoming increasingly important. The analysis of several lateral airframe responses in order to determine which is most favorable for adaptive control is discussed. The design, analysis and description of a method for self-adaptive control of the yaw augmentation control loop of a high performance aircraft are then discussed with appropriate conclusions and recommendations as to further research or development.

ACKNOWLEDGEMENT

The authors wish to express their appreciation for the assistance and encouragement given them by their faculty advisor, Professor George J. Thaler, Dr. Eng., of the Electrical Engineering Department, United States Naval Postgraduate School. In addition, the authors desire to express their gratitude and appreciation for the kind cooperation and assistance rendered by personnel of the Flight Control Section of the Autonetics Division of North American Aviation, Incorporated, during the period of research. In particular, we wish to thank Mr. Richard K. Smyth under whose supervision and guidance the research was conducted, and, Mr. Robert E. Chandos and Mr. Thomas Morton who performed the analog computer mechanization and assisted in the computer study.

TABLE OF CONTENTS

LIST OF ILLUSTRATIONS

Chapter I

Introduction

In the development of modern weapons systems, during the years following World War II, certain rapid strides in engineering techniques as well as technologies have resulted in weapons concepts which were heretofore unimaginable. The development of the jet engine for aircraft and the rocket engine for missiles or experimental aircraft have created demands for system control in the regions and environments of flight which occur at velocities several times the speed of sound.

With the advent of the supersonic aircraft and its increased operational capabilities, numerous problems never before encountered in such magnitude and importance are foremost in the designer's mind. He must reckon with aircraft velocities which are subsonic as well as supersonic, and dynamic pressures, q, whose magnitudes range from those normally encountered with conventional aircraft to those associated with smaller types of missiles and rockets. The designer must take into account the high maneuvering rates possible under such flight conditions and the inherent sensitivity of such an aircraft to control surface forces in the extreme conditions of flight. Control measures must be supplied which will operate to minimize the large forces which could occur on the aircrafts' structure and cause its destruction. In addition, these control measures must account for the human factors which unfortunately enter the picture in high performance, high velocity situations. Human response time to instantaneous accelerations and disturbance forces is prohibitively slow. The human is also relatively insensitive as to the proper magnitude of an input command to the control surfaces. In a high performance supersonic aircraft, these improper inputs could result in large forces which

might exceed the structural load limits. In addition, the lag in human response time could result in corrective action reinforcing a rapid oscillatory disturbance so as to create less stable, or perhaps unstable, operation.

The inherent increase in the performance capabilities briefly mentioned has created additional problems in terms of aircraft stability and response. No longer does the aircraft's dynamic response vary slightly under all possible conditions of flight. The variance in dynamic response at extreme conditions of flight, i.e.; landing characteristics as compared to high altitude high velocity flight, is large. The aircraft may conceivably exhibit good stability under one flight environment and at another altitude and velocity the airframe may become unstable. Clearly, such an aircraft dominates the pilot's capabilities to control and command. There is established a need for some type of automatic control to assist the pilot in his function.

Automatic control systems were developed to provide stable aircraft response characteristics in the pitch, yaw and roll modes of motion. The basic requirements being that the autopilot provide the ability for the aircraft to remain steadily on the commanded course or maneuver, while providing the necessary stability in the response modes mentioned above. These requirements pertain to any disturbances which may occur as inputs to the airframe. Such inputs may include undesirable oscillations or rates due to commanded inputs, gust disturbances and random force inputs, such as buffeting, in the transonic region.

Generally, autopilots augment the commands generated by the pilot. The pilot possesses complete control of the aircraft's command inputs. The autopilot in this instance serves to provide stable airframe maneuver

to the desired attitude and heading. Recently, however, in the development of automatic control systems for supersonic, high performance aircraft, certain command functions normally handled by the pilot have necessarily been programmed into the autopilot which automatically applies the aircraft command to achieve the desired response. This paper concerns itself with such an instance in the yaw control channel of the autopilot for supersonic aircraft. [1]

As previously indicated, the aerodynamic characteristics of this particular type of aircraft vary over the entire region of flight capabilities. There must be some compromise in the designer's planning to account for the necessary stability required at landing as well as at high velocity, high altitude flight. Obviously the physical dimensions of the aircraft cannot be modified so as to always present an ideal design with respect to air flow at any and all flight conditions. It follows, then, that the automatic control system must be capable of providing a control which is satisfactory for all of the flight conditions, and therefore any changing aircraft characteristics which may occur. In many instances this control is satisfactorily achieved by servo loops, containing constant parameters, which provide acceptable response regardless of the flight condition. However, in the case of the aircraft considered by this report, a constant parameter control loop was not sufficient to insure acceptable response throughout the regions of flight. A variation of one or more parameters of the control loops were considered necessary to provide the desired stability requirements. Such a control loop would then adopt itself to each flight condition by sensing its inadequacy and providing the necessary changes in its parameters to improve the response.

[ ] Shall refer to references listed at the end of this report.

The research on the adaptive controller, which refers to this entire unit with the capability of varying control system characteristics, has been carried out principally in recent years. The United States Air Force became interested in the development of advanced aircraft design which indicated a need for relatively more sophisticated control methods. Soon leading laboratories in the control systems development field were contributing to the problems' solution. Many approaches were made to the problem. Some strived to obtain satisfactory response by single parameter variation as a function of perhaps mach number, M, and altitude, h. In such a method some switching was incorporated to set a predetermined loop gain which would provide satisfactory airframe response over some region defined by limits expressed as some function of M and h. Other systems, certainly more sophisticated, used the model reference system whereby an analog model of the aircraft received the same inputs as the airframe. By measuring the airframe's response and comparing this to the model's response, which was considered the ideal response, an error signal was generated which served to provide some measure of the system changes necessary to match the physical to the ideal model response. This error signal was handled in numerous ways by the research and development units. By developing and applying criteria of optimum response to this error, input signals could be processed and shaped so as to provide forcing functions which, when applied to the airframe, caused it to reproduce the model's response; or, the error criterion could provide the impetus for varying loop gains and/or time constants. Clearly there are many variations and applications of these and other principles not discussed. From the summary of these systems, it can be readily appreciated that there are requirements for accurate data input in order to predict switching

function values, usually provided by air data computers, or, analog computers are necessary to provide the model reference and integrate, in cases, functions which modify the input signal's shape. Digital computers, by numerical methods, could handle some of these analog functions but the need for some computer remains.

Many of these systems have been satisfactorily flight tested or undergone extensive tests under simulation conditions. Applications of adaptive controls in processes are becoming prevalent in industry as automation becomes more evident. Their future application in fields where human inadequacies are detrimental to control is insured. [2,3,4,7,8,9]

The material presented by the authors in this thesis is the analysis of a high performance and velocity aircraft with intentions of providing a satisfactory response over all flight conditions by simply the introduction of a gain change in the control loop. Furthermore, the impetus for furnishing the gain change is to be entirely derived from the airframe response and is therefore a self adapting scheme. No exterior inputs, such as M and h, were considered. No computers were utilized in the scheme. The aircraft response was to approach the "selected ideal" as closely as possible in order to define the optimum response.

The study was carried out at the Autonetics Division of North American Aviation, Incorporated under the direction of Mr. Richard K. Smyth, senior research engineer and supervisor of the Advanced Analysis Unit of the Flight Control Section. The study was conducted in June and July, 1959.

Chapter II

General Approaches to the Problem

The development of the adaptive controller as an integral part of an automatic flight control system has been briefly mentioned in Chapter I. Generally the systems evolved from basically simple ideas and techniques associated with obtaining the "optimum" performance from a servomechanism or control system. Just what is meant by the term "optimum" depends primarily on the user of the word. Reference 5 uses the word optimum to define the most commonly acceptable second order system damping ratio, 0.7. Still other authors define the system as optimum when certain mathematical relationships are introduced which alter the forcing function, and/or the system parameters, giving a "desired" response. An example of this would be the least squares criterion proposed in reference 6. It seems evident then that the field of adaptive servomechanisms and optimum design research are inter-related. Furthermore, the basis of adaptive control is some method of attaining the most desirable response under variable operating conditions or inputs. Hence, the most desirable response is often referred to as the "optimum response" under these imposed conditions. Therefore, it is a recognized fact that the "state of the art" of adaptive mechanisms to date have relied upon these techniques.

The first portion of this report concerns itself with the analysis of several recommended airframe lateral responses with the object in mind that these chosen transfer functions satisfy the following requirements. First, the response must furnish oscillatory stability over the entire region of flight. Furthermore, any divergent instability from a real root must be slight enough to permit the pilot or autopilot to remain on course by command inputs. Secondly, the response characteristics should provide

some similarity to the response of a second order system in order that the human pilot preference, 3 rad/sec and a damping ration of 0.7, as well as second order optimizing principles might be attempted. [11,12]

The recommended responses to be investigated as indicative of lateral aircraft motion were lateral acceleration of the aircraft center of gravity, N_y, yaw rate, $\frac{d\psi}{dt}$ or r, and yaw acceleration, $\frac{d^2\psi}{dt^2}$ or $\dot{r}$, in combination with r or N_y. These functions are the descriptive characteristics of an airframe's lateral motion and are capable of measurement by instrumentation perfected and existing as useable hardware. Fig. 1 indicates the basis for measurement of the quantities by relation to the basic stability axes contained in the airframe with their origin at the c.g. or center of gravity. Positive N_y is measured along the positive y axis and is the result of a left rudder deflection. Positive ψ , r and $\dot{r}$ are measured in a clockwise direction about the vertical axis.

The stability analysis was carried out with the following basic assumptions. The analysis was to be linear with all responses as a function of rudder deflection only. All other control surfaces were assumed to remain at zero deflection. The aircraft was allowed three degree freedom as a result of these rudder deflections and was assumed initially in steady level flight prior to application of a forcing function. Six indicative flight conditions representing the extremes of the designed region of flight were chosen as the basis of requirements for stability. These six flight conditions represent individual transfer functions and therefore varying responses.

The basic control loop is shown in Fig. 2. The loop consists of the transfer functions for the airframe, necessary instrumentation, compensation if required, and provision for variable gain adjustment.

To summarize, the analysis was necessary in order to determine which

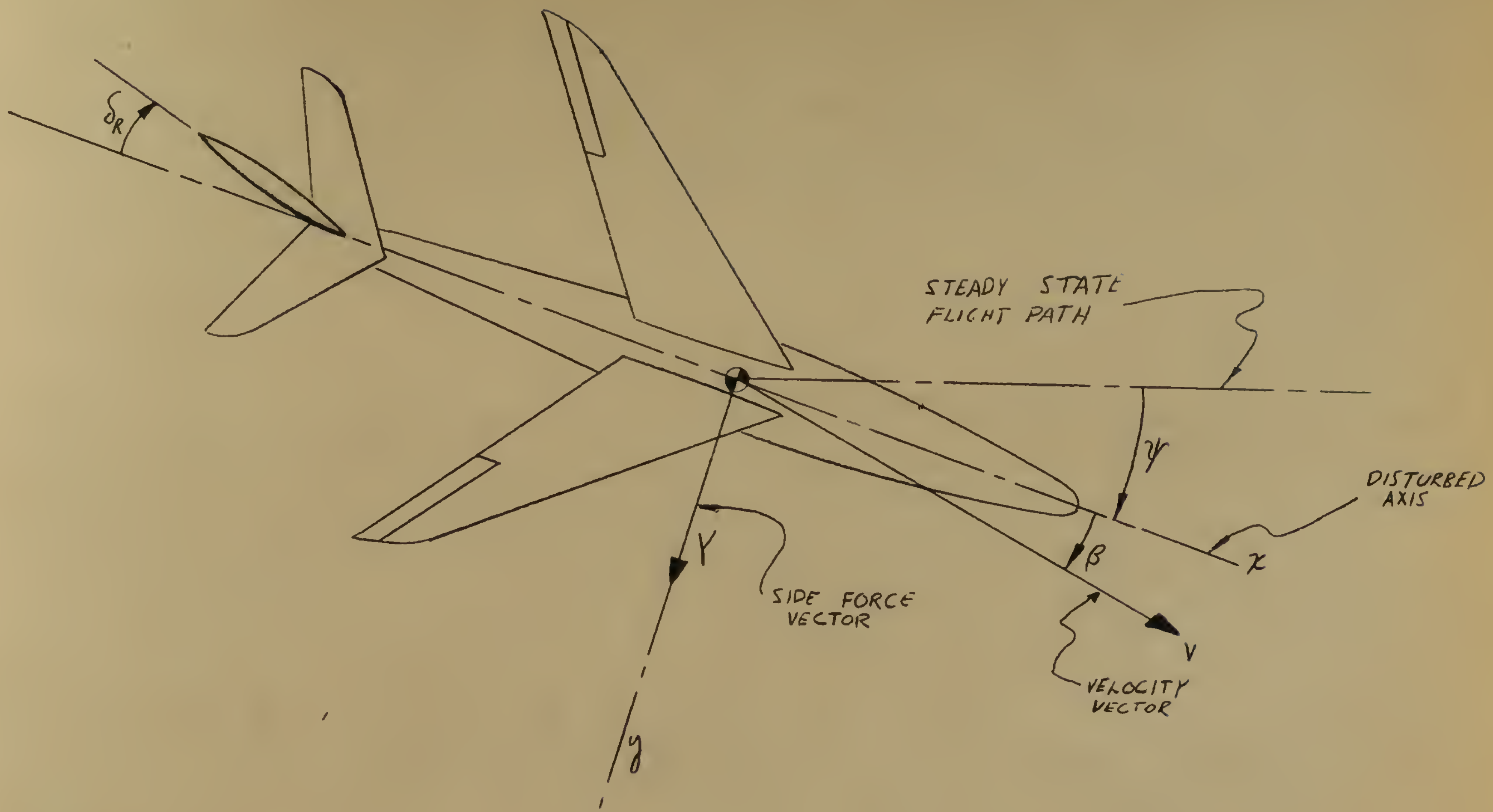

Fig. 1

LATERAL BODY AXIS REFERENCE SYSTEM

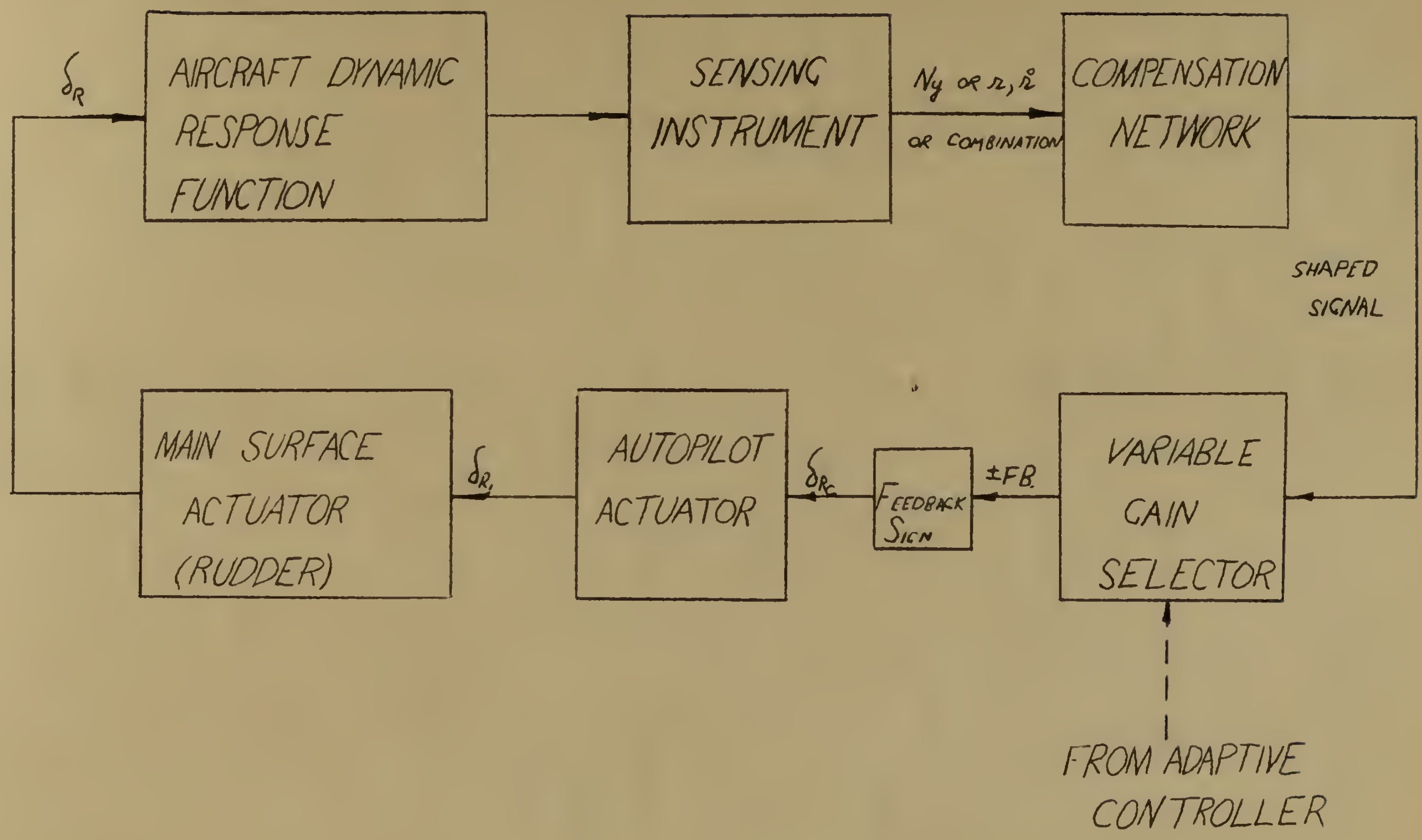

FIG. 2

BASIC YAW STABILITY AUGMENTATION LOOP

of the lateral aircraft responses at extreme conditions of flight provided a response to rudder deflection, only, which was stable in oscillation and approximated a second order system at all six flight conditions. This was necessary to permit application of basic optimum criterion to provide satisfactory adaptive control.

The design of the adaptive control circuits was based on the following desired characteristics. The designed scheme was to be simple and easily mechanized. The scheme was required to base its own adjustments on an error criterion which exhibited selectivity of an acceptable damping ratio based on information obtained from the control loop and not from sources external to the loop. The adaptive controller was to achieve this damping ratio by a gain variation only. Therefore, effectively the adaptive control system would be capable of sensing the requirements for stable response by looking at the contemporary airframe dynamics.

The various chapters contained within the Scope of This Investigation are logically arranged to provide introductions and explanations of the sequential development of the stability analysis, self adaptive design and test of the entire system. Specific Appendices are referenced as their need arises in the report text. Conclusions of this report and recommendations for further design, test and analysis are presented as a final summary of the material.

Chapter III

Scope of This Investigation: Stability Loop

Referring to Fig. 2, it is considered appropriate to detail the make-up and function of the loop parameters. The basic control loop, as briefly explained in Chapter II, serves as the yaw augmentation loop for the aircraft's autopilot or automatic flight control system. There are no external command inputs to the yaw loop for this purpose. Therefore, the loop becomes one in which the airframe is disturbed by some force which imparts a measurable lateral response. The measured response is fed back, with the appropriate sign of feedback, to actuate the rudder in order to reduce the response to zero. Since the control loop is a single closed loop, and referring to Fig. 3, we may combine the loop transfer functions into a single function with a variable gain factor and unity feedback. Fig. 4 indicates, however, that to obtain the response of the airframe, as an example, the problem reverts to one in which there is a direct, feed forward function and a feedback function.

The instrumentation contained within the control loop was as follows:

a. autopilot actuator
b. main rudder actuator
c. measuring instrument (rate gyro, accelerometer, or angular accelerometer)

The autopilot actuator was a closed loop servo, hydraulic control valve which regulated the hydraulic pressure fed to the main rudder actuator. The main rudder actuator controlled the displacement of this vertical control surface. The servo valve used in the autopilot actuator exhibited a closed loop second order response function of

$$\frac{\theta_c(s)}{\theta_R(s)}_{AA} = \frac{800}{(s + 20 \pm j20}$$

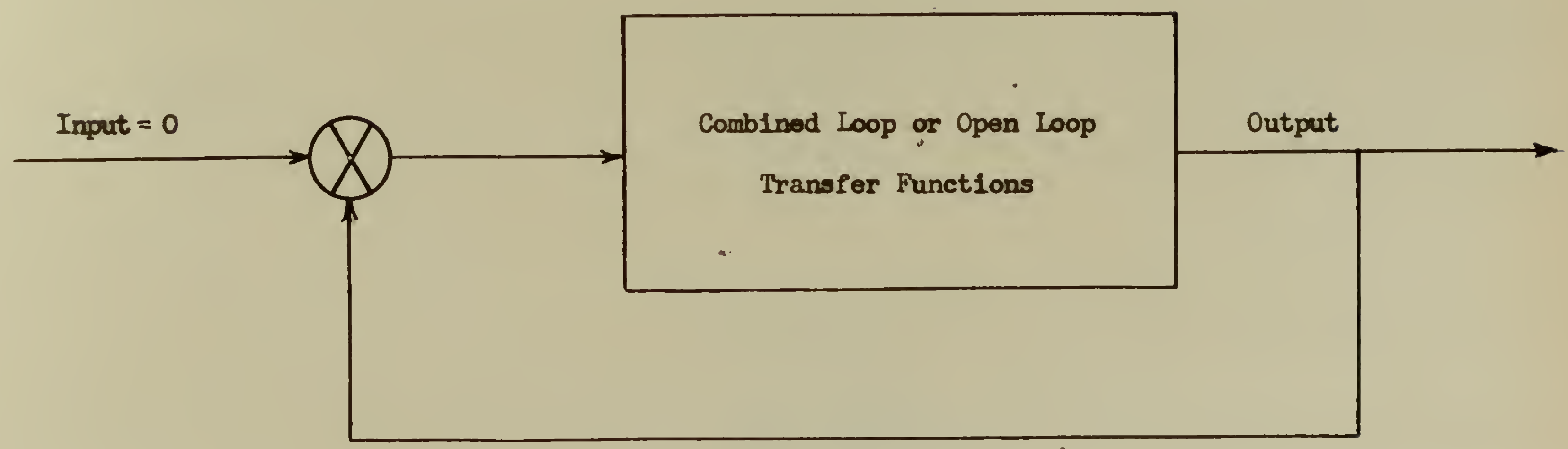

Fig. 3

Block Diagram Presentation For Stability Analysis

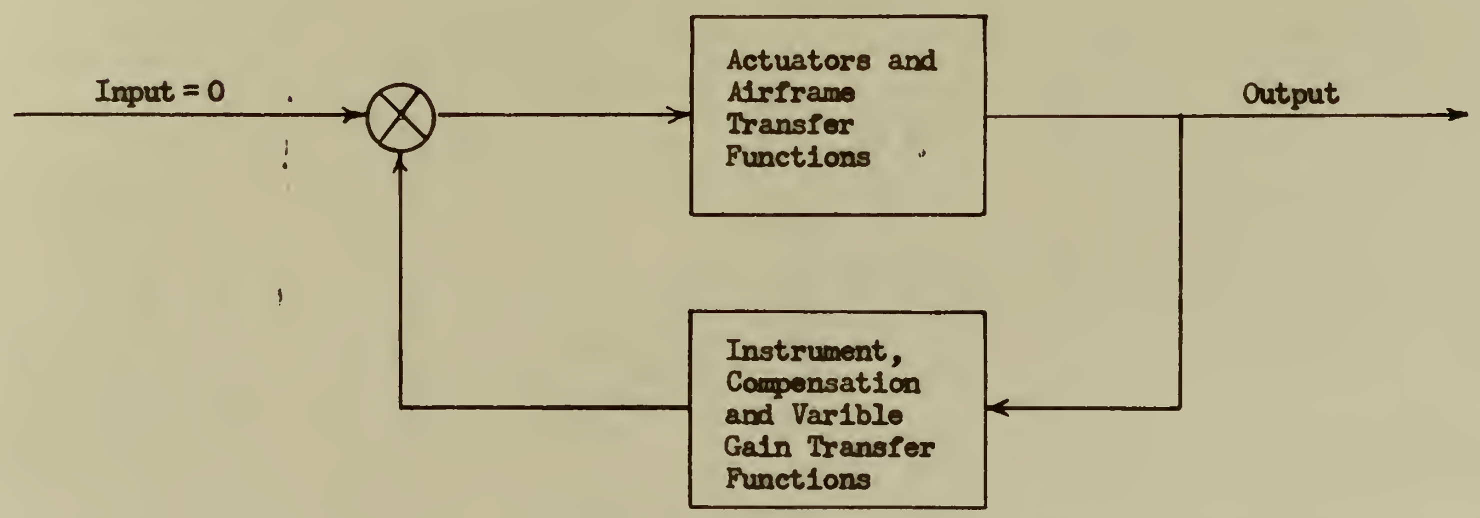

Fig. 4

Block Diagram of Loop To Determine An Airframe Response To A Command Actuating the Rudder.

while the main rudder actuator had a response characterized by the function

$$\frac{\theta_c(s)}{\theta_R(s)}_{MA} = \frac{10}{(s + 10)}$$

Investigation of these functions by an application of the final value theorem, for any particular input, shows that for the autopilot actuator where the input function is given by $\theta_R(s)$ and the output function by $\theta_c(s)$, we find that

$$\theta_c(s)_{AA} = \frac{800\ \theta_R(s)_{AA}}{(s + 20 \pm j20)} = \frac{800\ \theta_R(s)_{AA}}{s^2 + 40s + 800}$$

then;

$$\lim_{t \to \infty} \theta_c(t) = \lim_{s \to 0} s\cdot\theta_c(s) = \lim_{s \to 0} s \circ \frac{800\ \theta_R(s)}{s^2 + 40s + 800}$$

$$= \lim_{s \to 0} \frac{800}{s^2 + 40s + 800} \cdot \lim_{s \to 0} s \cdot \theta_R(s)$$

$$= \lim_{s \to 0} s \cdot \theta_R(s)$$

and observe that the steady state value of the instrument is unity. This also holds true for the main rudder actuator and the measuring instruments. The measuring instruments used in the analysis were a rate gyro in order to measure yaw rate; an accelerometer to measure lateral acceleration at the c.g. of the airframe; and an eccentric angular accelerometer developed by North American Aviation Corporation which was capable of measuring the lateral acceleration at the c.g. and some desired proportion of $\dot{r}$. The signals were essentially combined to give a single output value from the device. In each instance the identical transfer function was used since it provided a measure of simplicity and was a fair approximation to all three instances. The transfer function used was

$$\frac{\theta_c(s)}{\theta_R(s)} = \frac{15795}{(s + 87.9 \pm j89.7)}$$

and is second order with a steady state value of unity. Its dynamic characteristics were a natural frequency of 20 cps and a damping ratio of 0.7.

In addition to the instrumentation contained in the loop was the appropriate transfer function of the airframe as a function of rudder deflection, δ_R. A particular aircraft function was inserted into the loop equation for each of the desired lateral responses at every condition of flight. This required analysis then of a minimum of eighteen airframe functions. These functions will be given and explained in detail in the following Chapters.

Finally, the loop provided for the insertion of recommended compensation, a variable gain adjustment and some means for reversing the phase of the loop signal, if required.

Chapter IV

Scope of this Investigation: Lateral Acceleration as a Dynamic Response

By referring to Fig. 2 which indicates the control loop for yaw augmentation the transfer functions for lateral acceleration as a function of rudder deflection, N_y/δ_R , may be inserted as the particular aircraft function. Since it is customary to express the function δ_R in degrees, the gain variable in the loop will be expressed as degrees/g and designated K_{Ny}.

The transfer functions of N_y/δ_R at the specific conditions of flight are listed in Table I. The extreme flight conditions chosen to represent the limits of aircraft performance are:

Condition 1: low altitude, low dynamic pressure, landing condition

Condition 2: low altitude, low dynamic pressure

Condition 3: low altitude, high dynamic pressure

Condition 4: medium altitude, high dynamic pressure

Condition 5: high altitude, low dynamic pressure

Condition 6: high altitude, high dynamic pressure

and are specifically referred to as conditions 1 through 6 in the remainder of the report.

Insertion of the appropriate transfer function into the control loop results in an expression for the open loop function KG(s) which is, of course, merely a combination of the loop transfer functions into a single expression

$$KG(s) = K_{Ny} \cdot \frac{\theta_c(s)}{\theta_R(s)}\,AA \cdot \frac{\theta_c(s)}{\theta_R(s)}\,MA \cdot \frac{\theta_c(s)}{\theta_R(s)}\,INST.$$

TABLE I

Three Degree Lateral Transfer Functions for N_y/δ_R at Indicated Conditions of Flight

Condition 1:

$$N_y/\delta_R = \frac{0.1479(s-0.9468)(s-0.0844)(s+1.3209 \pm j0.5214)}{(s+0.0657)(s+0.7322)(s+0.4715 \pm j1.5798)}$$

Condition 2:

$$N_y/\delta_R = \frac{0.5315(s-0.0184)(s+2.9354)(s-2.1236)(s+2.0986)}{(s+0.0189)(s+2.3972)(s+0.3376 \pm j1.7172)}$$

Condition 3:

$$N_y/\delta_R = \frac{3.3985(s+0.0063)(s-4.1672)(s+5.2181 \pm j0.4958)}{(s-0.0007)(s+5.209)(s+0.532 \pm j3.4933)}$$

Condition 4:

$$N_y/\delta_R = \frac{0.2184(s-0.0128)(s+0.8625)(s-1.2238)(s+1.0598)}{(s+0.0194)(s+0.3334)(s+0.187 \pm j1.6679)}$$

Condition 5:

$$N_y/\delta_R = \frac{3.3106(s-0.0073)(s+4.6913)(s-5.9673)(s+6.4883)}{(s+0.044)(s+4.7792)(s+0.3571 \pm j2.3784)}$$

Condition 6:

$$N_y/\delta_R = \frac{0.8405(s-0.001)(s+0.9195)(s-3.3749)(s+3.489)}{(s+0.0079)(s+0.7404)(s+0.1706 \pm j1.706)}$$

which may be examined by root locus or frequency response techniques to determine the linear characteristics of stability and response.

Primary investigations of the characteristic responses were made by the root locus method. Since the characteristic equation of a closed loop system is given by

$$1 \pm KG(s) = 0$$

where the overall gain constant K is the open loop gain and G(s) represents the overall open loop function in La Place Transform notation. It should be noted that the sign of K may be either positive or negative depending upon the chosen positive response directions in Fig. 1. The $\pm$ sign results from the combination of the sign of K and the feedback sign used to close the loop.

Open loop functions for each flight condition are indicated in Table II for the case of the aircraft's lateral response being N_y/δ_R. The subscripts on each of the functions refer to the previously designated flight condition. In the interest of brevity in all tables which follow and list lateral transfer functions, the denominators of the open loop functions contained in Table II shall be designated by $\Delta(s)_n$ where the subscript n specifies the condition of flight.

TABLE II

Open Loop Transfer functions for the Lateral Response

N_y/δ_R at Indicated Conditions of Flight

Condition 1:

$$KG(s)_1 = \frac{0.1869\times10^{8} K_{Ny}(s-0.9468)(s-0.0844)(s+1.3209\pm j0.5214)}{(s+0.0657)(s+0.7322)(s+0.4715\pm j1.5798)(s+10)(s+20\pm j20)(s+87.9\pm j89.7)}$$

Condition 2:

$$KG(s)_2 = \frac{0.6716\times10^{8} K_{Ny}(s-0.0184)(s+2.9354)(s-2.1236)(s+2.0986)}{(s+0.0189)(s+2.3972)(s+0.3376\pm j1.7172)(s+10)(s+20\pm j20)(s+87.9\pm j89.7)}$$

Condition 3:

$$KG(s)_3 = \frac{4.2943\times10^{8} K_{Ny}(s+0.0063)(s-4.1672)(s+5.2181\pm j0.4958)}{(s-0.0007)(s+5.209)(s+0.532\pm j3.4933)(s+10)(s+20\pm j20)(s+87.9\pm j89.7)}$$

Condition 4:

$$KG(s)_4 = \frac{0.276\times10^{8} K_{Ny}(s-0.0128)(s+0.8625)(s-1.2238)(s+1.0598)}{(s+0.0194)(s+0.3334)(s+0.187\pm j1.6679)(s+10)(s+20\pm j20)(s+87.9\pm j89.7)}$$

Condition 5:

$$KG(s)_5 = \frac{4.1833\times10^{8} K_{Ny}(s-0.0073)(s+4.6913)(s-5.9673)(s+6.4883)}{(s+0.044)(s+4.7792)(s+0.3571\pm j2.3784)(s+10)(s+20\pm j20)(s+87.9\pm j89.7)}$$

Condition 6:

$$KG(s)_6 = \frac{1.062\times10^{8} K_{Ny}(s-0.001)(s+0.9195)(s-3.3749)(s+3.489)}{(s+0.0079)(s+0.7404)(s+0.1706\pm j1.706)(s+10)(s+20\pm j20)(s+87.9\pm j89.7)}$$

Preliminary root locus plots were made on these functions in Table II and they were found to be unsuitable for both positive and negative feedback. For positive feedback the locus emanating from the complex poles immediately entered the right half plane, or, the unstable region of the S-plane. The situation for negative feedback produced stability as concerned the locus leaving the complex poles. However, for one flight condition, a real root was present, for all values of loop gain, in the right half plane. The root locus sketches are not contained in this report but mentioned to indicate that the use of lateral acceleration as the principal dynamic response required compensation.

At this point it is interesting to note the aircraft function poles and zeros since these exist in the critical portion of the S-plane and are predominant in determining the closed loop characteristics of the system. Fig. 5 indicates the characteristic arrangement of the airframe poles and zeros for a supersonic aircraft. These differ from the conventional aircraft in that the latter case usually exhibits two complex pole pairs. The complex pole pair for the supersonic vehicle is indicated as the short period or dutch roll pair since the locus emerging from this set usually are dominant in fixing the short period, higher frequency oscillation. The real pair occasionally give rise to a complex locus resulting in a low frequency, long period oscillation and are referred to as the phugoid or long period pair. Characteristically, roots contained in the phygoid locus are lightly damped while short period roots may attain much more favorable damping ratios. Characteristically, real roots may also exist. Usually, one real root is contained in the negative real axis and one real root occurs about the origin either in the positive or negative real axis. The former root locus segment gives rise to a root called the roll damping factor which controls the stiffness of response in roll to a rudder deflection.

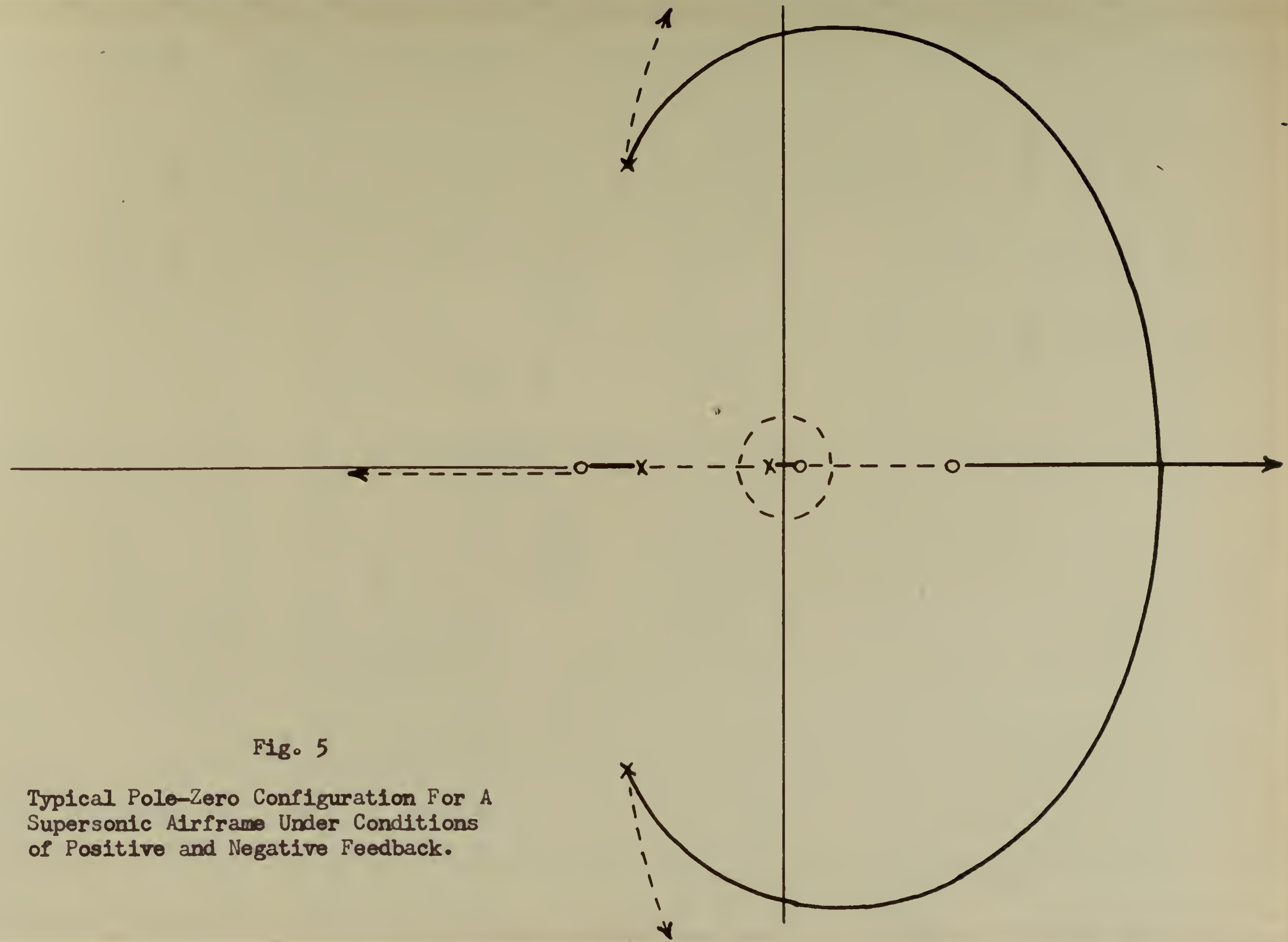

Fig. 5

Typical Pole-Zero Configuration For A Supersonic Airframe Under Conditions of Positive and Negative Feedback.

The root about the origin determines the spiral characteristics of the aircraft. As long as the residue or coefficient of this particular root is small, and should the root exist in the unstable half-plane, the spiral instability is easily compensated for by the pilot or autopilot. Should this residue be significantly large, the aircraft is obviously spirally unstable. Referring to the list of transfer functions for N_y/δ_R in Table I, it may be noted that these poles and zeros generally conform to the above cases. The zeros may appear as complex but generally as real points. [10]

Since compensation was desirable the suggested scheme derived from basic design research conducted by Autonetics design personnel was analyzed. This consisted of inserting a lead filter network into the loop with transfer function

$$\frac{\theta_c(s)}{\theta_R(s)}\text{ FILTER 1} = \frac{(s+1)}{(0.1s+1)}$$

and, it may be noted, a steady state gain of unity. By insertion of the filter it was desired that the locus would be shaped so that oscillatory response was determined largely by the dominant complex roots and therefore second order assumptions could be applied to regulate damping ratio and natural frequency.

By methods contained and illustrated in Appendix A, solution of the basic equation defining the root locus, the characteristic equation, (where $KG(s)_n$ now is defined as $KG(s)_n \cdot KG(s)$ filter)

$$1 \pm KG(s)_n = 0$$

was carried out for both conditions of feedback. In this instance, the case of negative feedback proved to be undesirable since the locus emanating from the complex poles directly entered the unstable or right half plane.

However, the condition of positive feedback produced loci which were stable over some variable gain region and whose complex short period loci indicated that a variable damping ratio, with varying loop gain, could be achieved. The root loci plots of the Ny plus lead filter or filter 1 response for positive feedback are included as Figs. 6 through 11. Gain points on these plots are marked as values of the variable loop gain, K_{Ny}, inserted into the loop and not the open loop gain as is normally the case. Furthermore, the variable gain, K_{Ny}, is expressed in the units deg/g on all plots and references in this report. Since all transfer functions were given in terms of radian measure, K_{Ny} was expressed as rad./g for all computations. This convention was incorporated because of the aircraft industry's practice of referring to control surface deflections in degree units.

In an attempt to provide increased dominance by the complex roots, additional compensation was proposed by the authors in the form of an additional lag pole in the lead filter at s equal to - 0.5. This filter took the form

$$\frac{\theta_c(s)}{\theta_R(s)} \text{ FILTER 2} = \frac{(s+1)}{(.1s+1)(2s+1)}$$

In addition it was desirous to perturbate the pole at - 10.0 and the zero at - 1.0 in filter 2 to investigate the effects. The following filter was proposed:

$$\frac{\theta_c(s)}{\theta_R(s)} \text{ FILTER 3} = \frac{(s+2)}{(.125s+1)(2s+1)}$$

Filters 2 and 3 were examined under conditions of negative and positive feedback by the methods contained in Appendix A. Root locus plots with these filters inserted as loop compensators are contained in Figs. 12 through 17 for filter 2 and Figs. 18 through 23 for filter 3. In each of these cases satisfactory loci shaping, was obtained for negative feedback

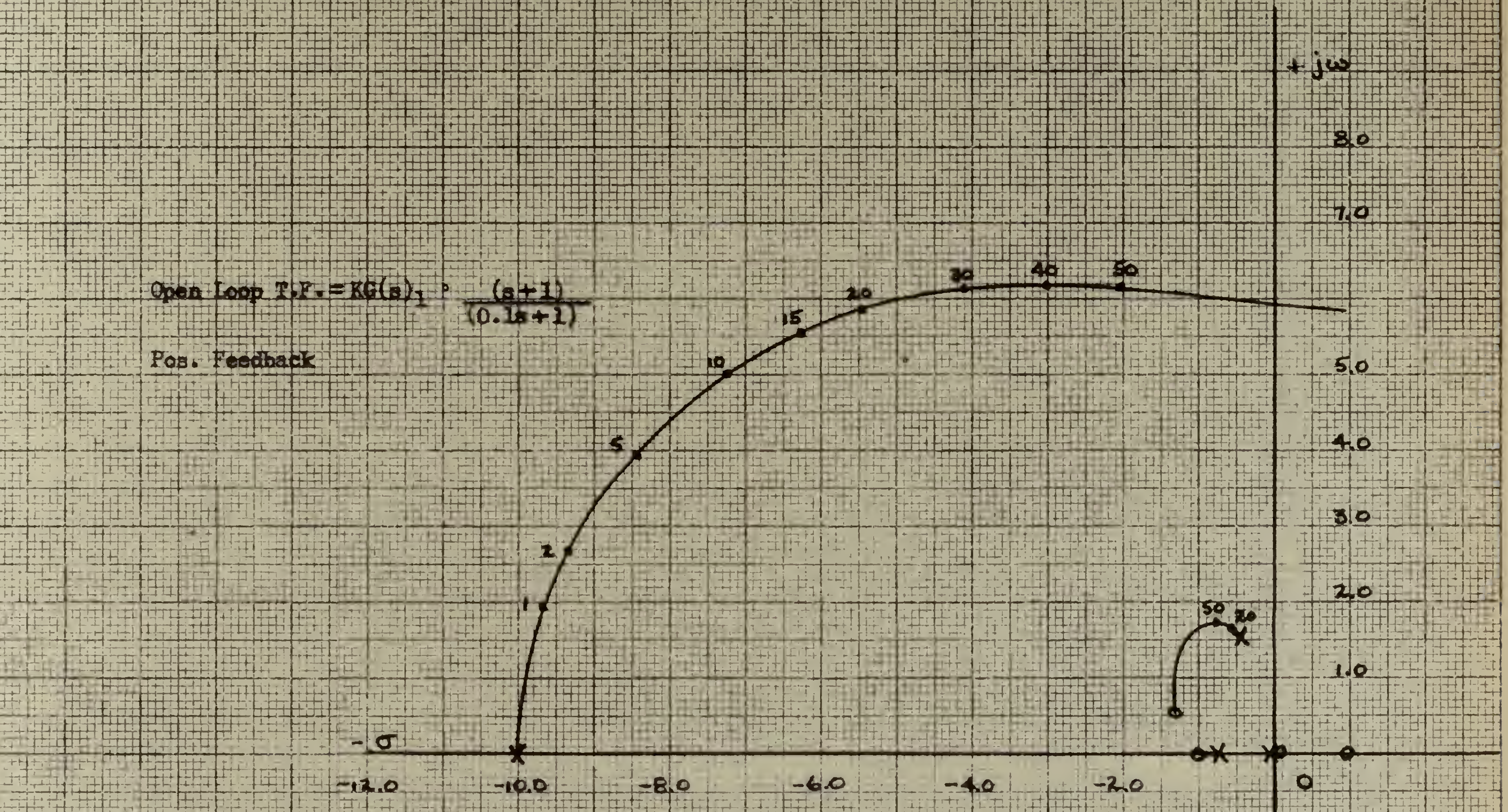

Fig. 6

Root Locus Plot for N_y with filter 1, Flight Condition 1.

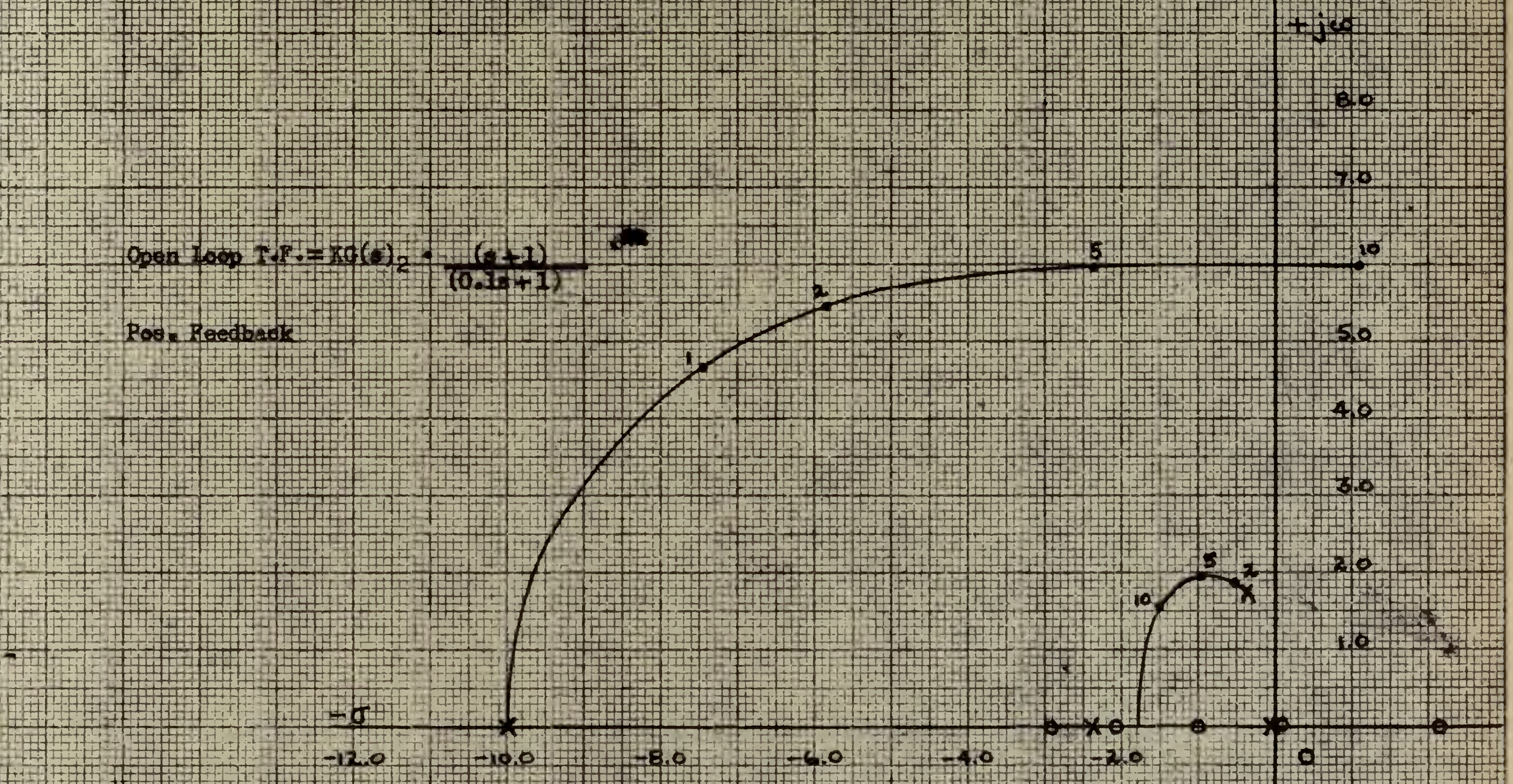

Fig. 7

Root Locus Plot for N_y with filter 1, Flight Condition 2.

Open Loop T.F. = $KG(s)_3 \cdot \frac{(s+1)}{(0.1s+1)}$

Pos. Feedback

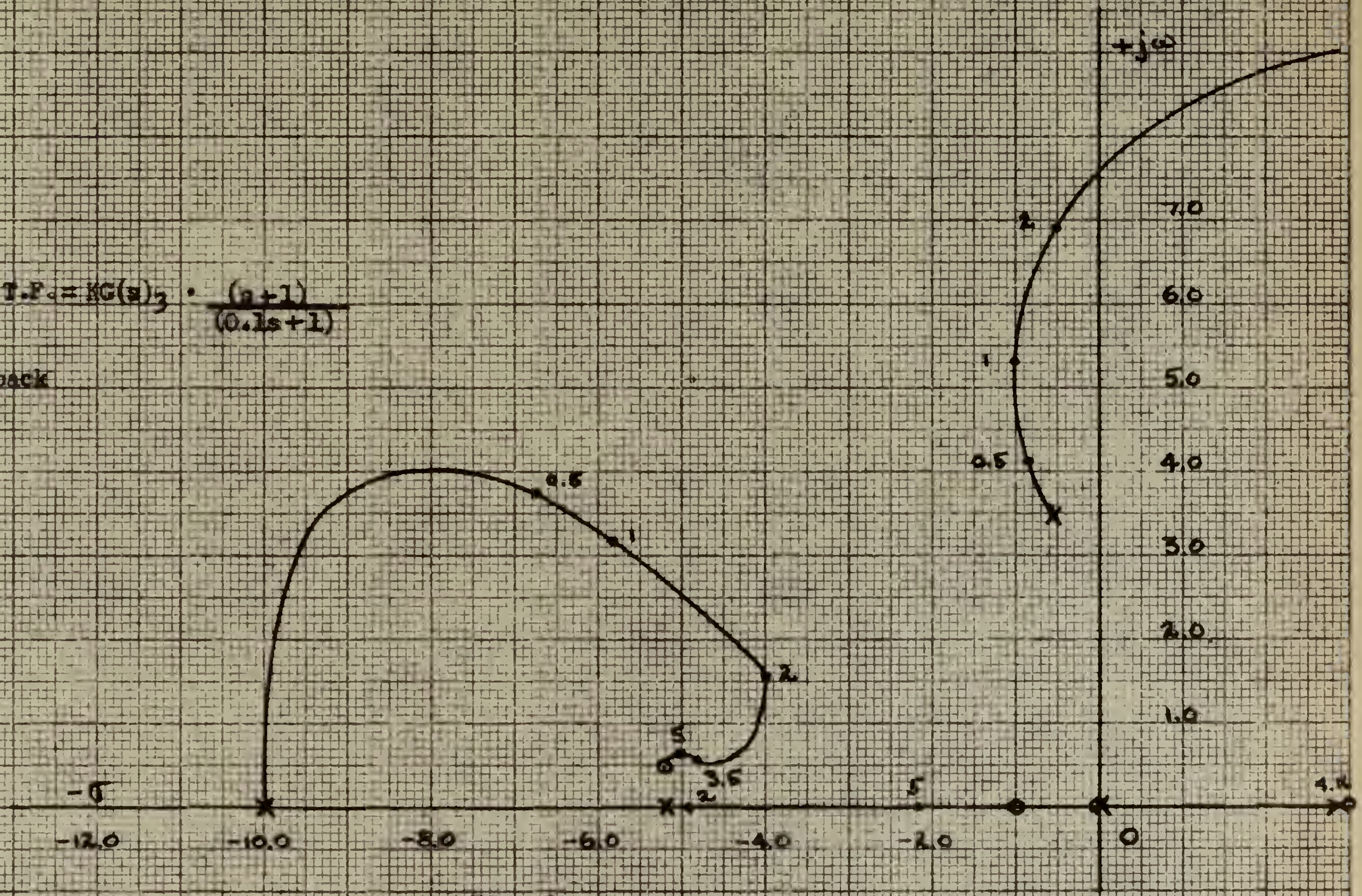

Fig. 8

Root Locus Plot for N_y with filter 1, Flight Condition 3.

Open Loop T.F. = $KG(s)_4 \cdot \frac{(s+1)}{(0.1s+1)}$

Pos. Feedback

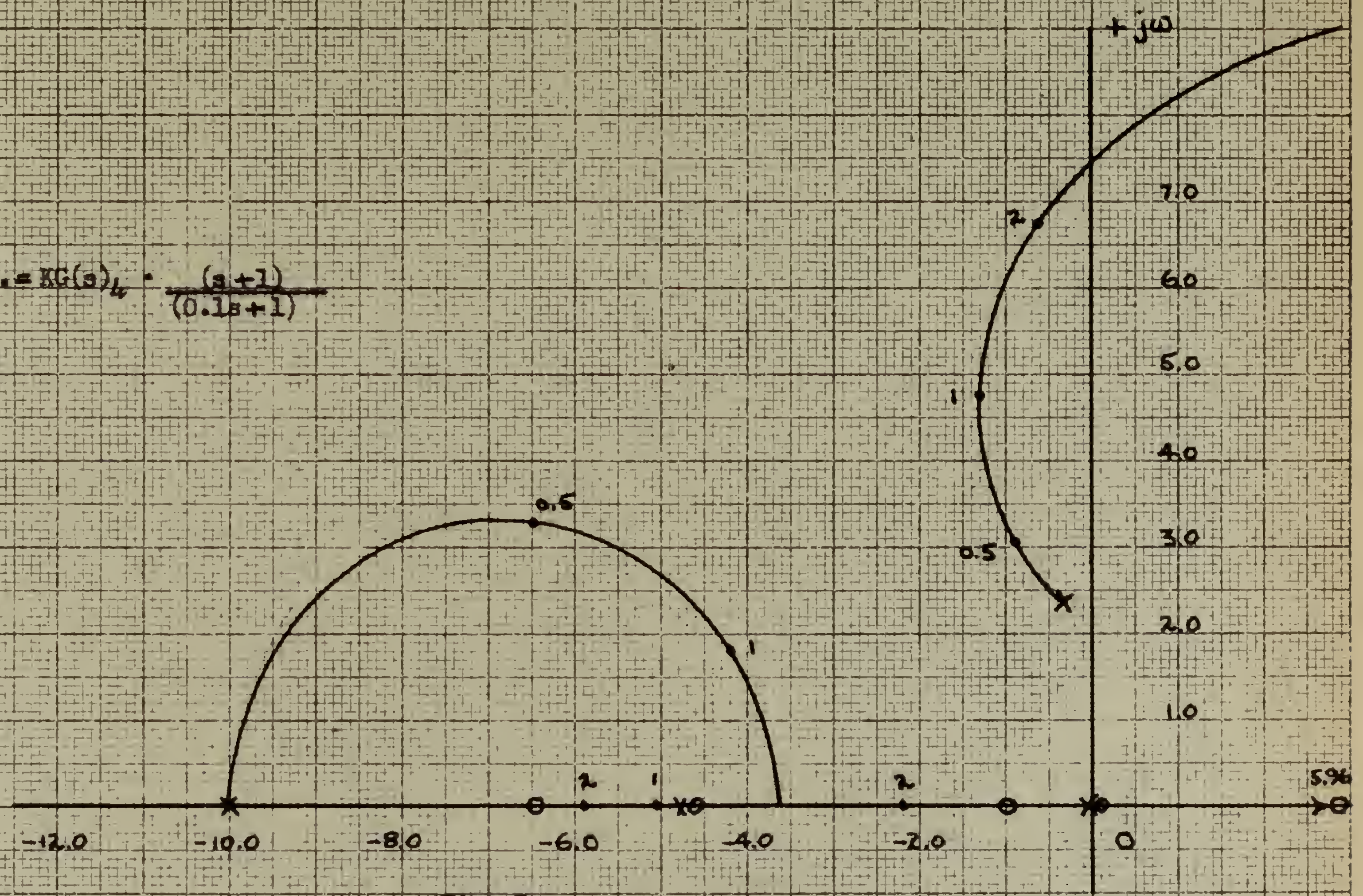

Fig. 9

Root Locus Plot for N_y with filter 1, Flight Condition 4.

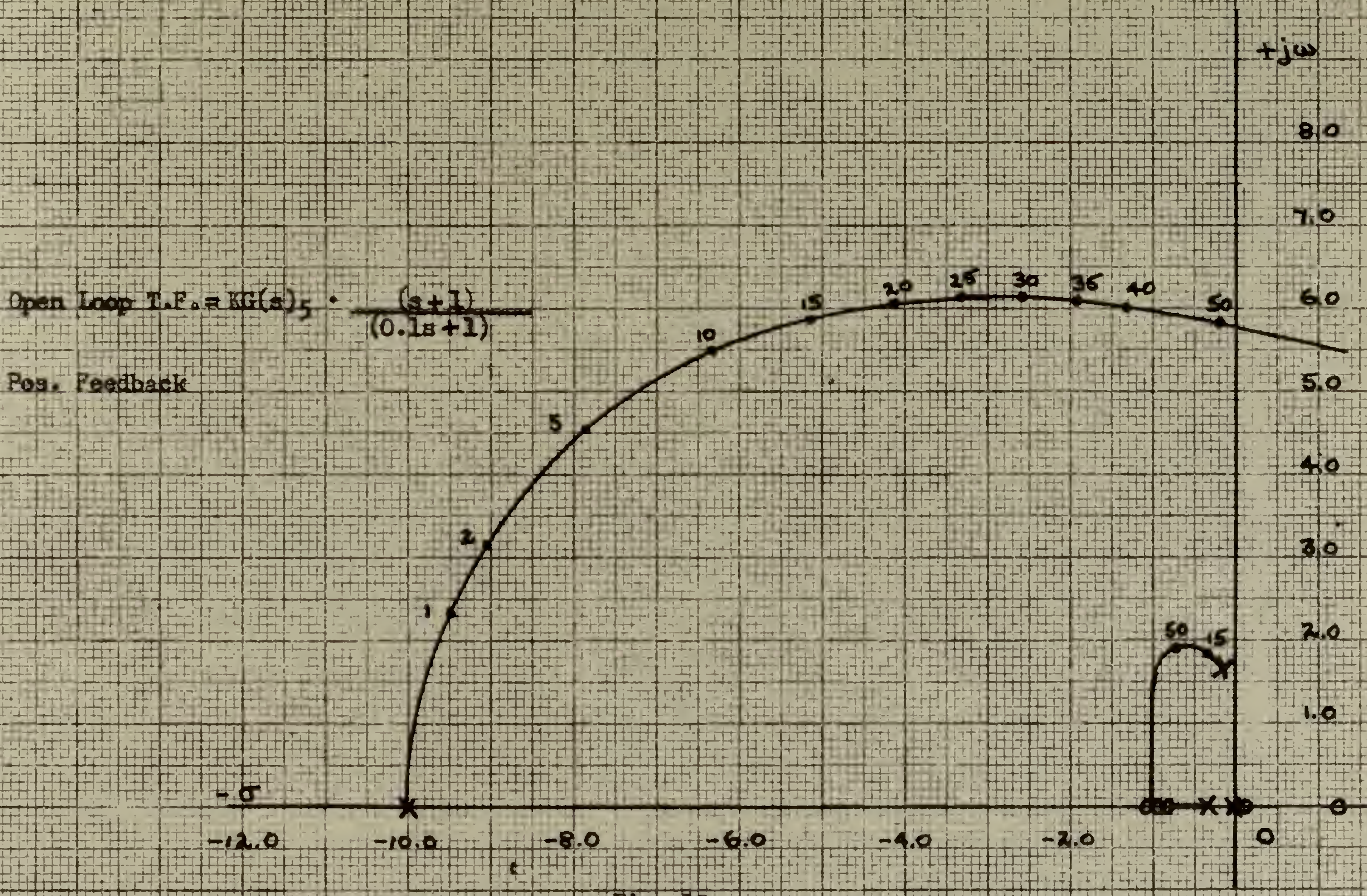

Fig. 10

Root Locus Plot for N_y with filter 1, Flight Condition 5.

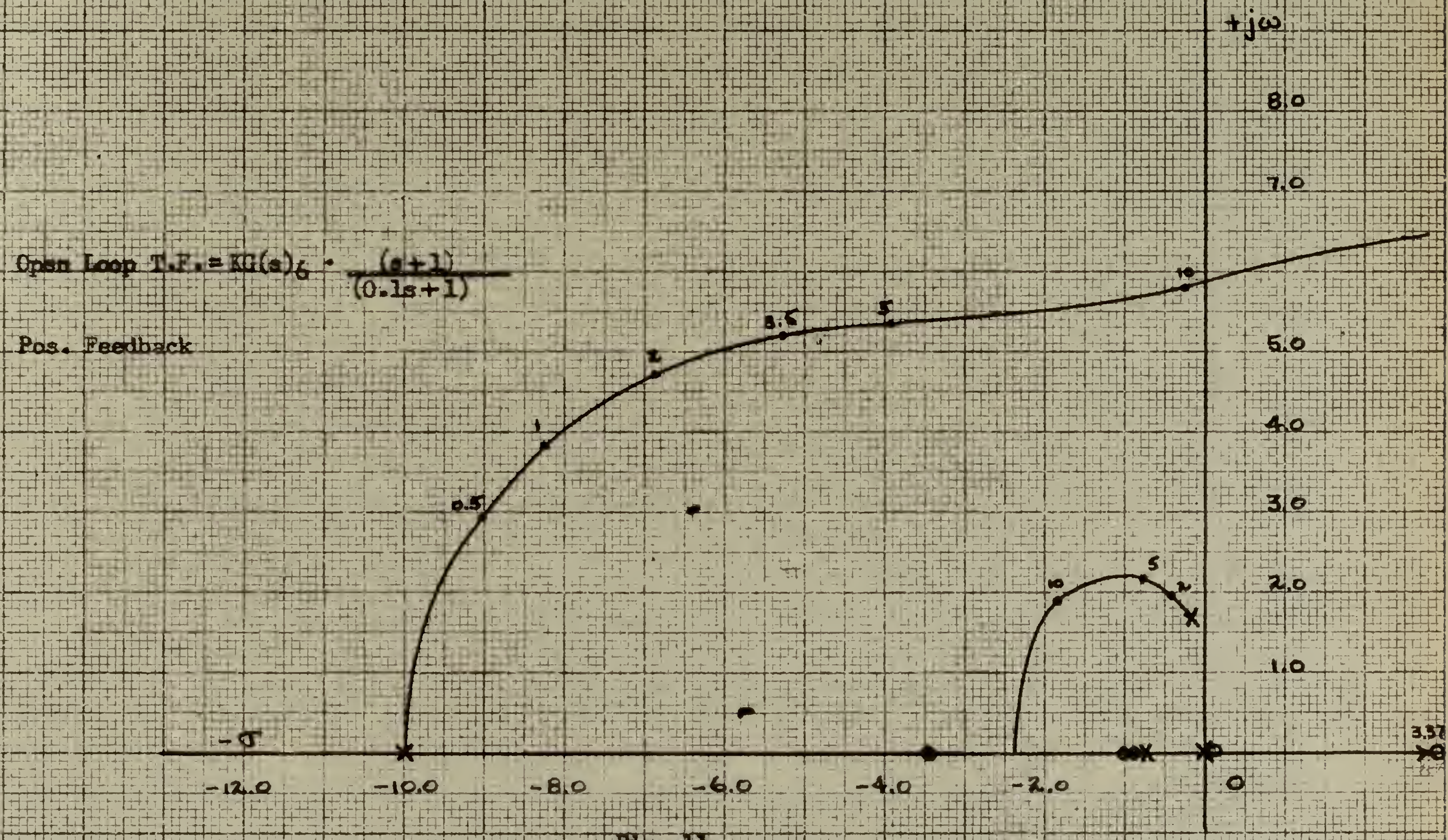

Fig. 11

Root Locus Plot for N_y with filter 1, Flight Condition 6.

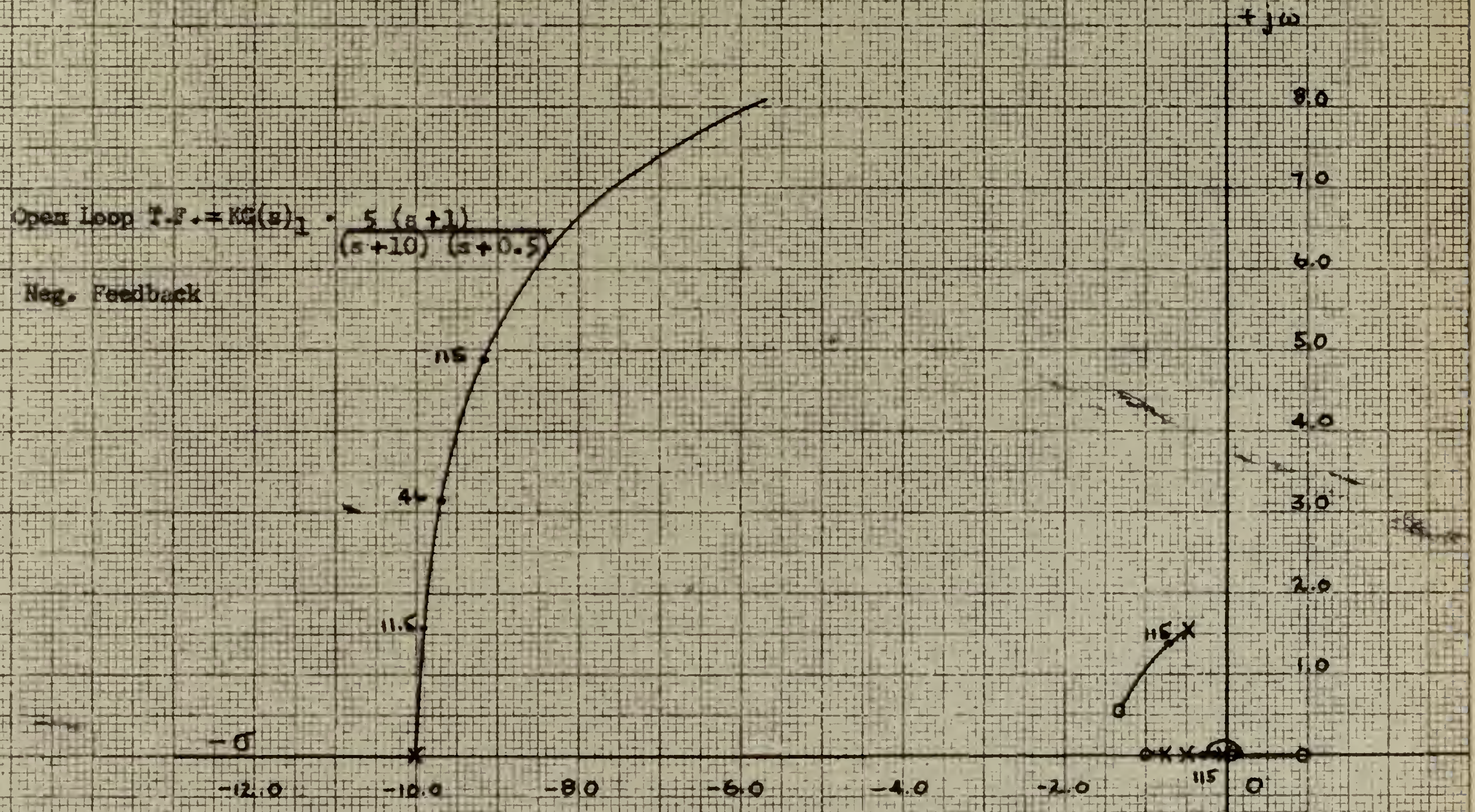

Fig. 12

Root Locus Plot for N_y with filter 2, Flight Condition 1.

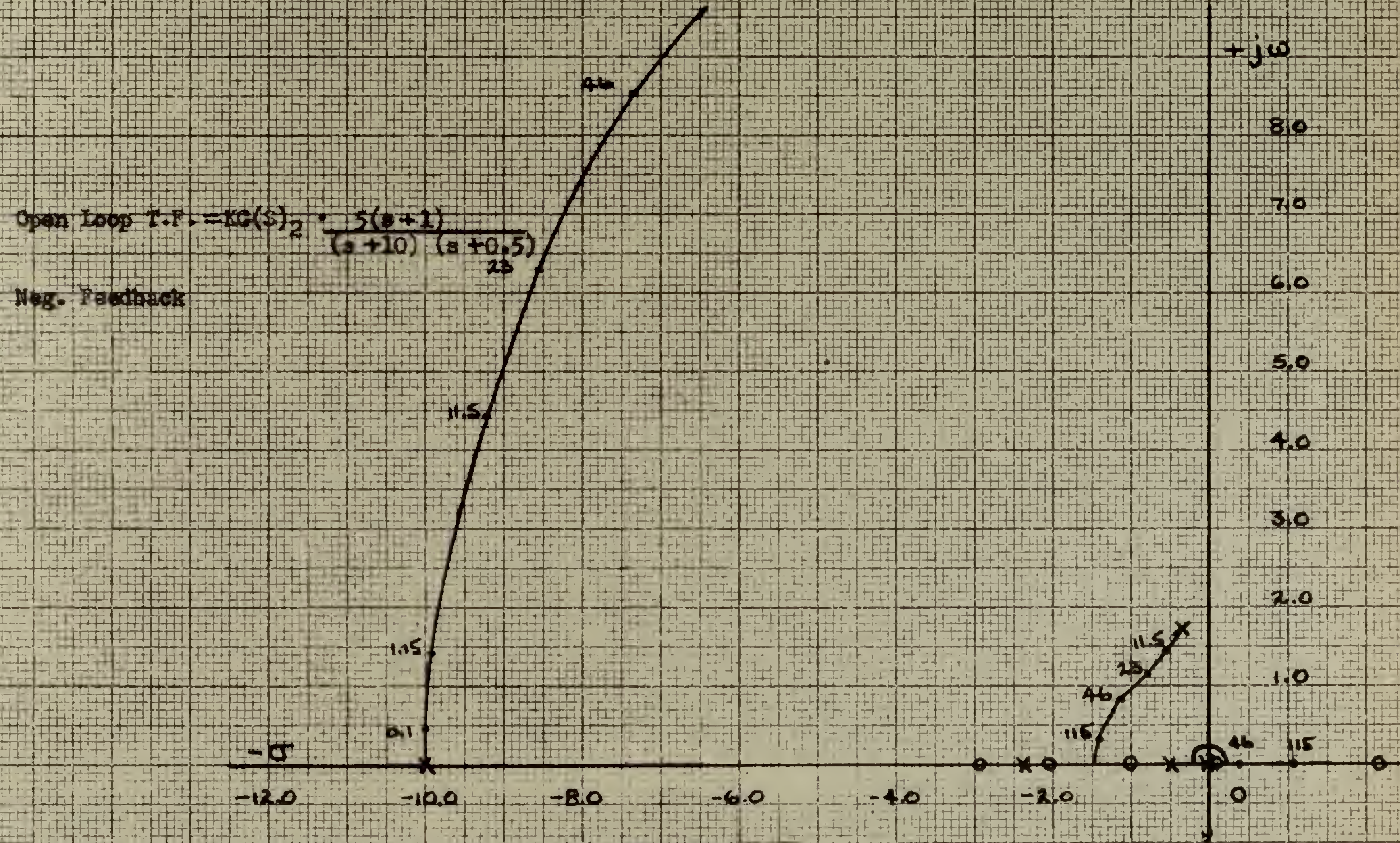

Fig. 13

Root Locus Plot for N_y with filter 2, Flight Condition 2.

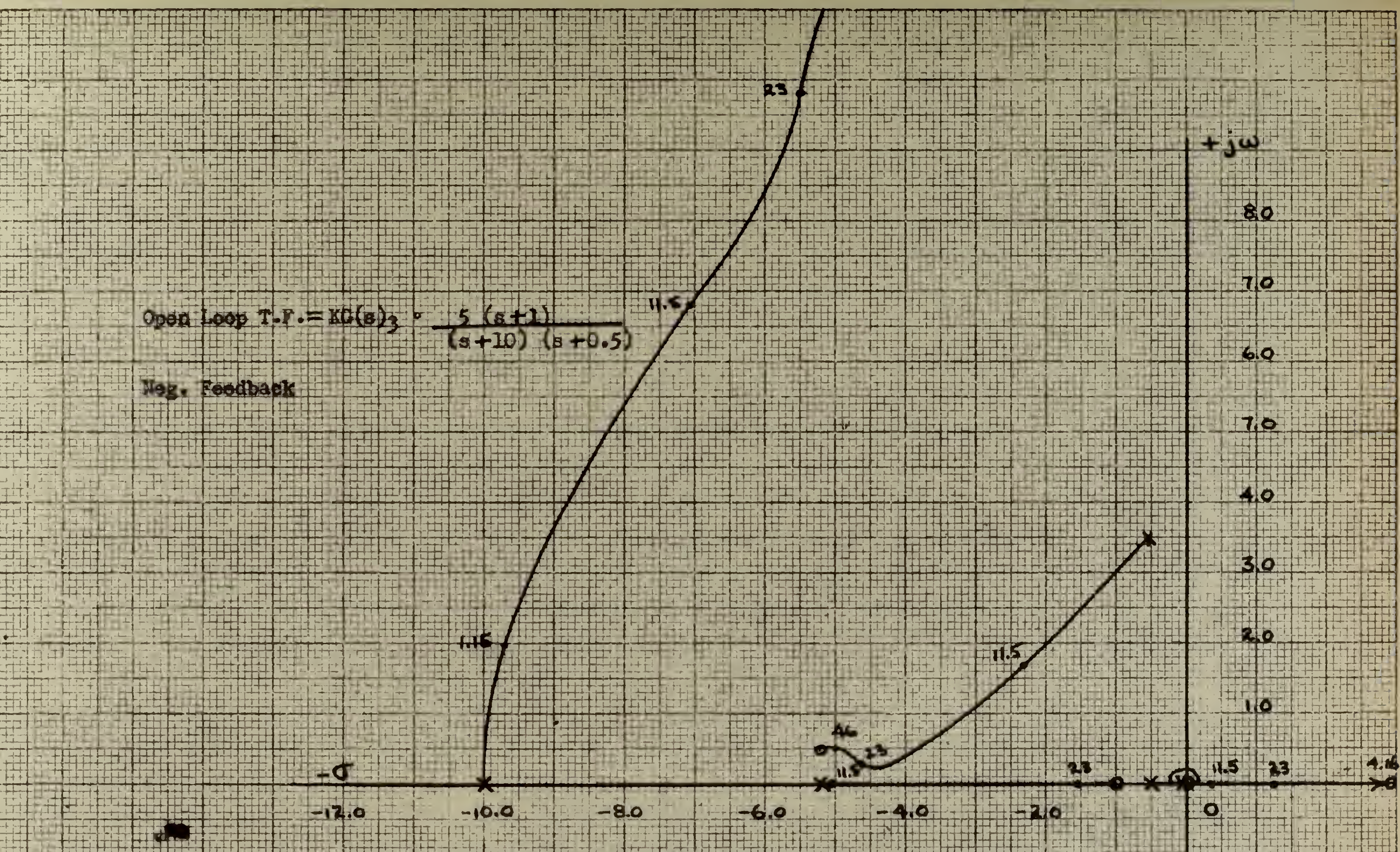

Fig. 14

Root Locus Plot for N_y with filter 2, Flight Condition 3.

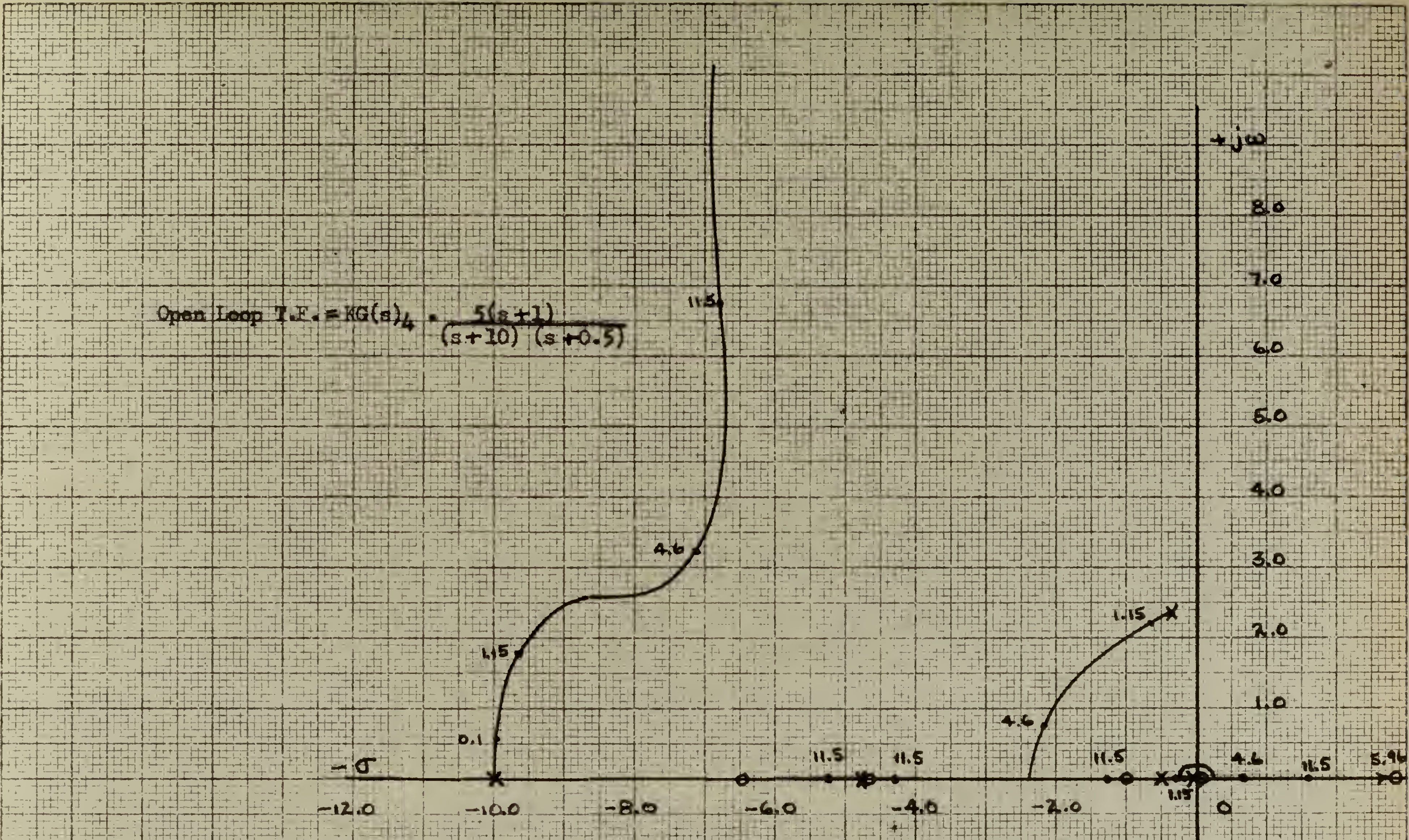

Fig. 15

Root Locus Plot for N_y with filter 2, Flight Condition 4.

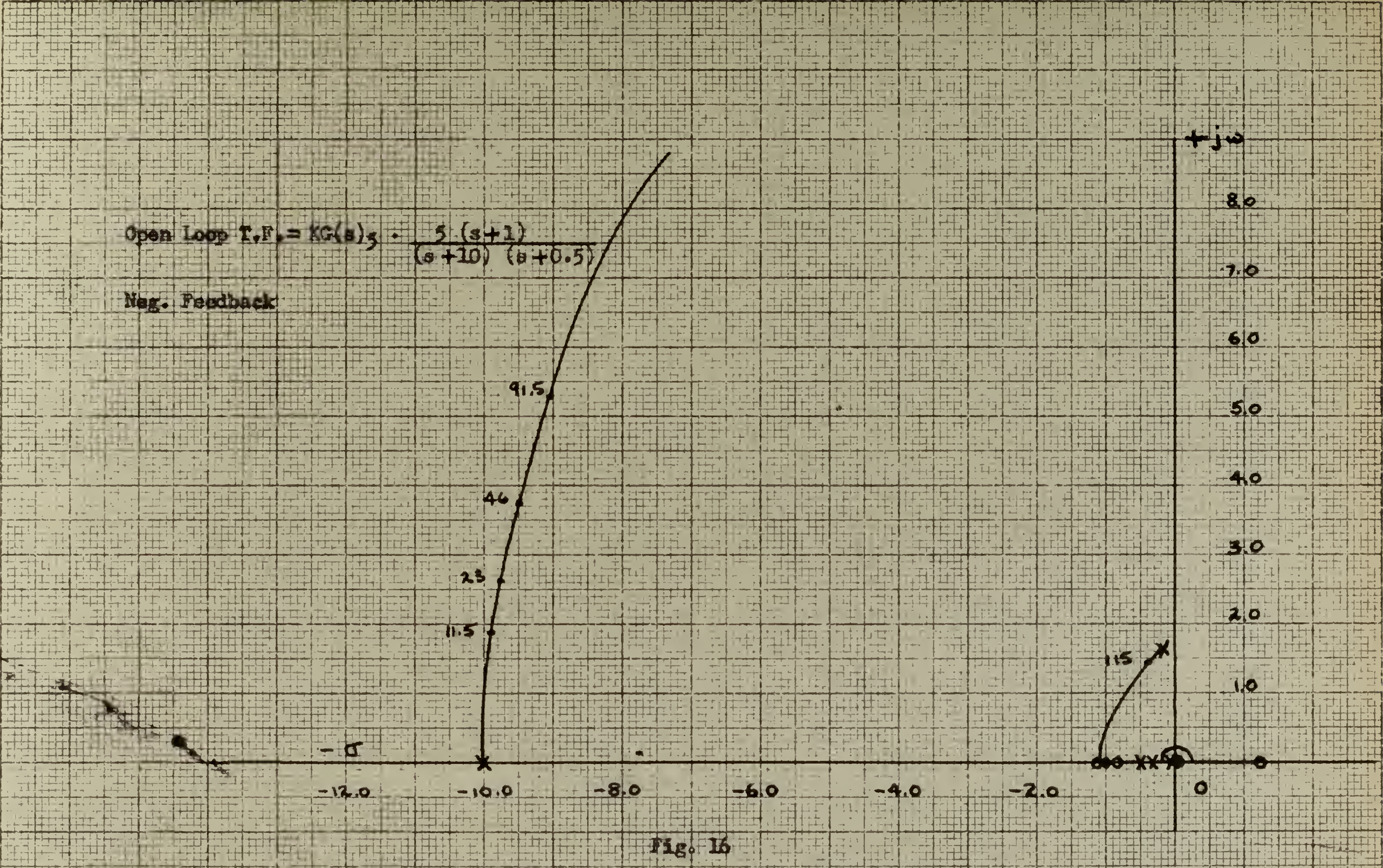

Fig. 16

Root Locus Plot for N_y with filter 2, Flight Condition 5.

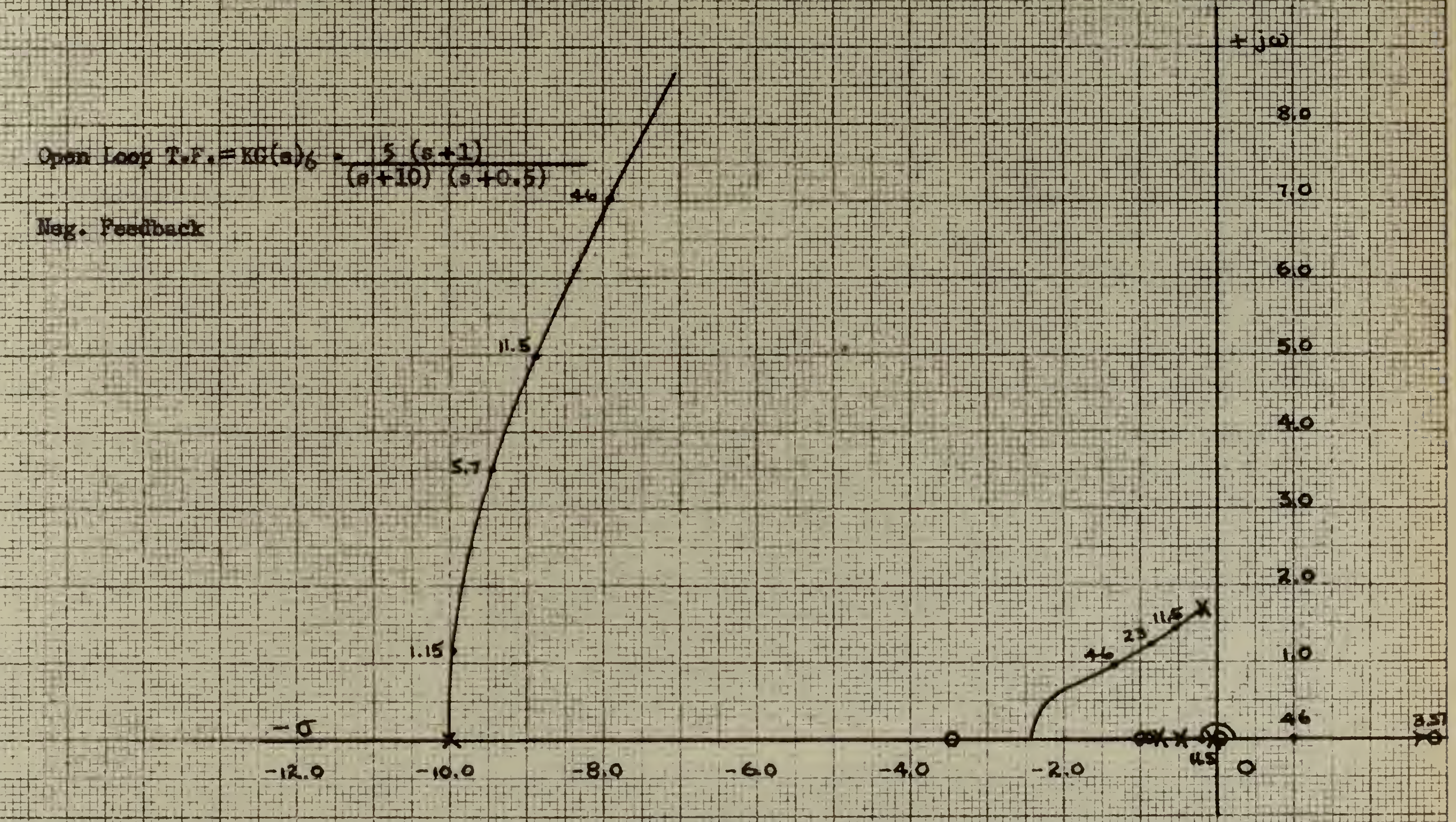

Fig. 17

Root Locus Plot for N_y with filter 2, Flight Condition 6.

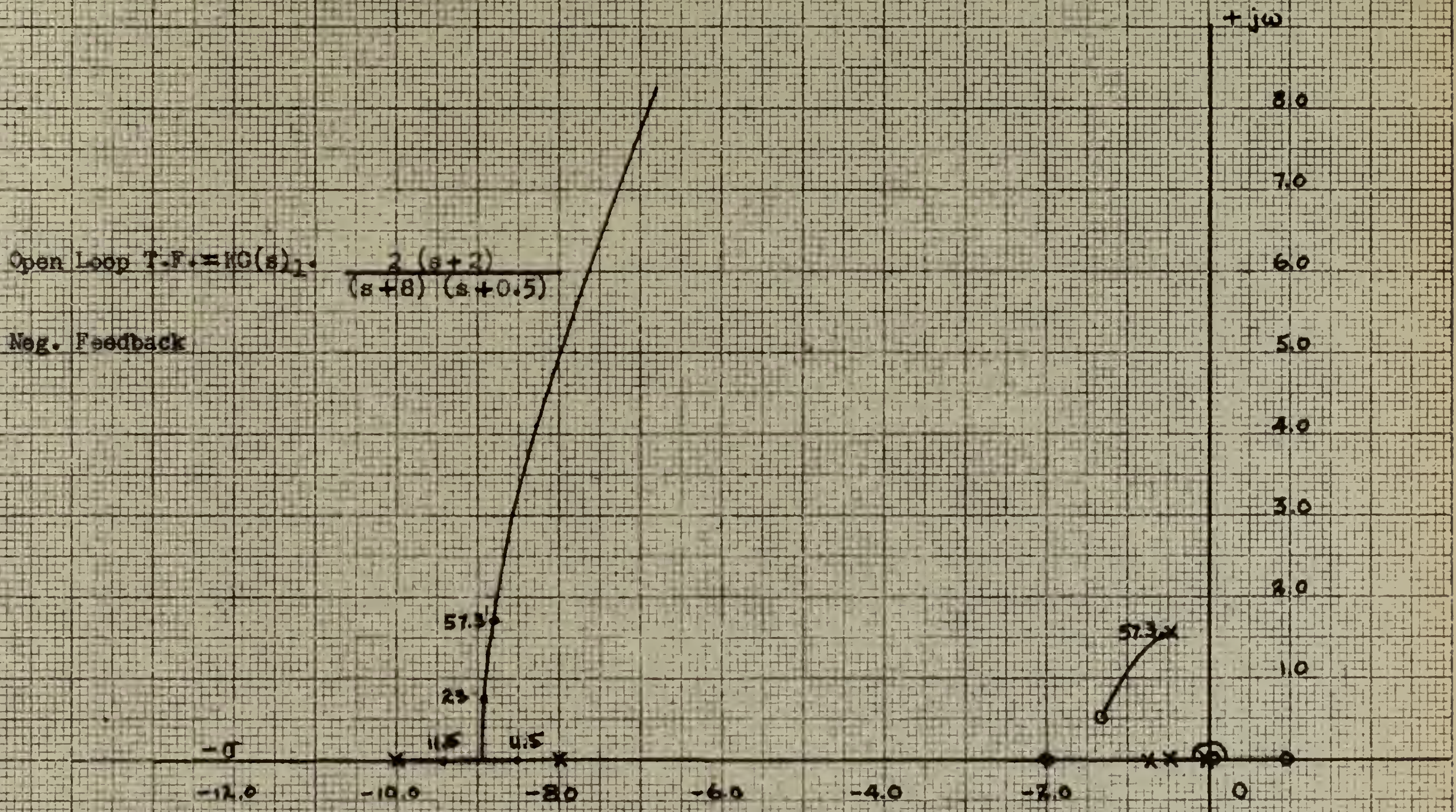

Fig. 18

Root Locus Plot for N_y with filter 3, Flight Condition 1.

Open Loop T.F. = $KG(s)_2 = \frac{2\,(s+2)}{(s+8)\,(s+0.5)}$

Neg. Feedback

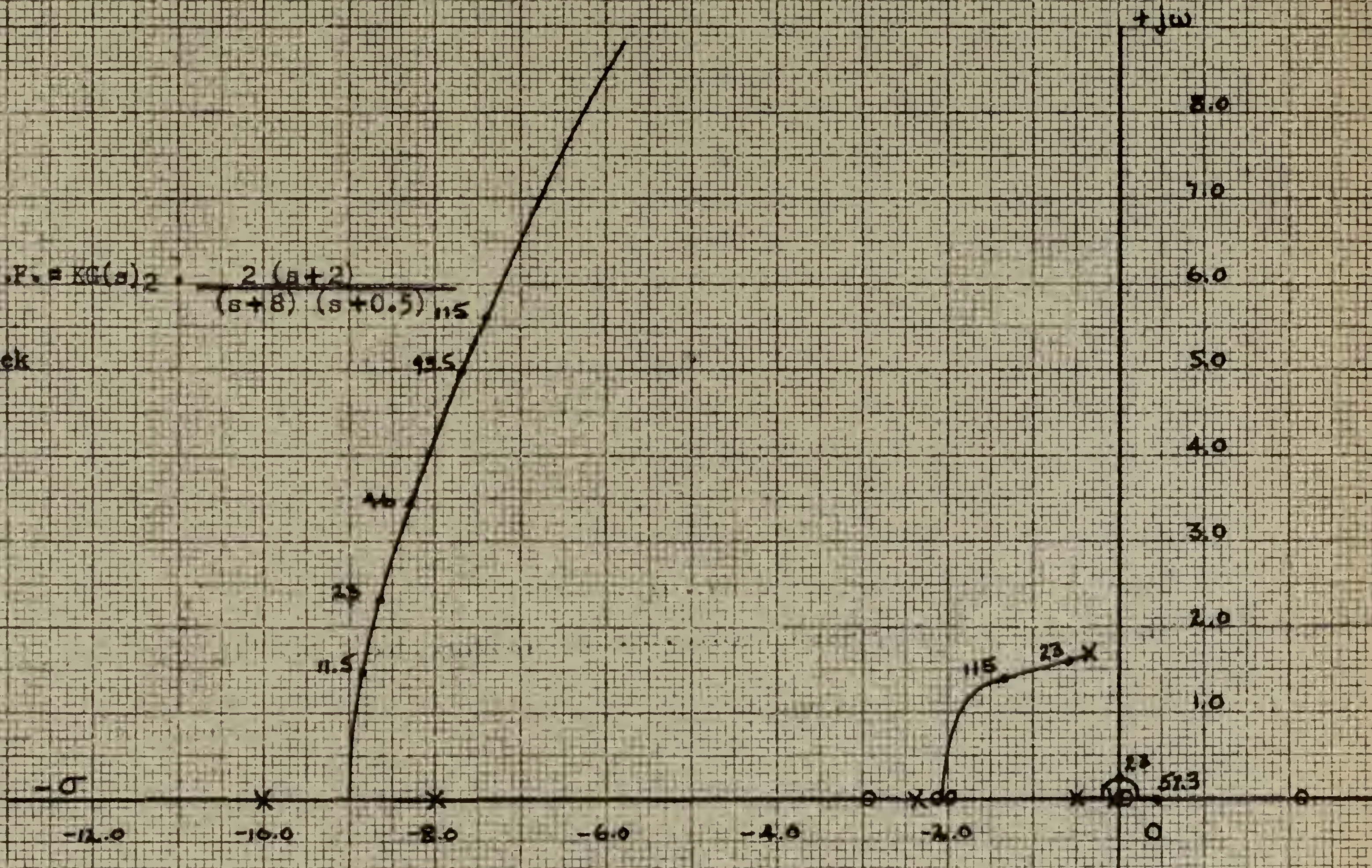

Fig. 19

Root Locus Plot for N_y with filter 3, Flight Condition 2.

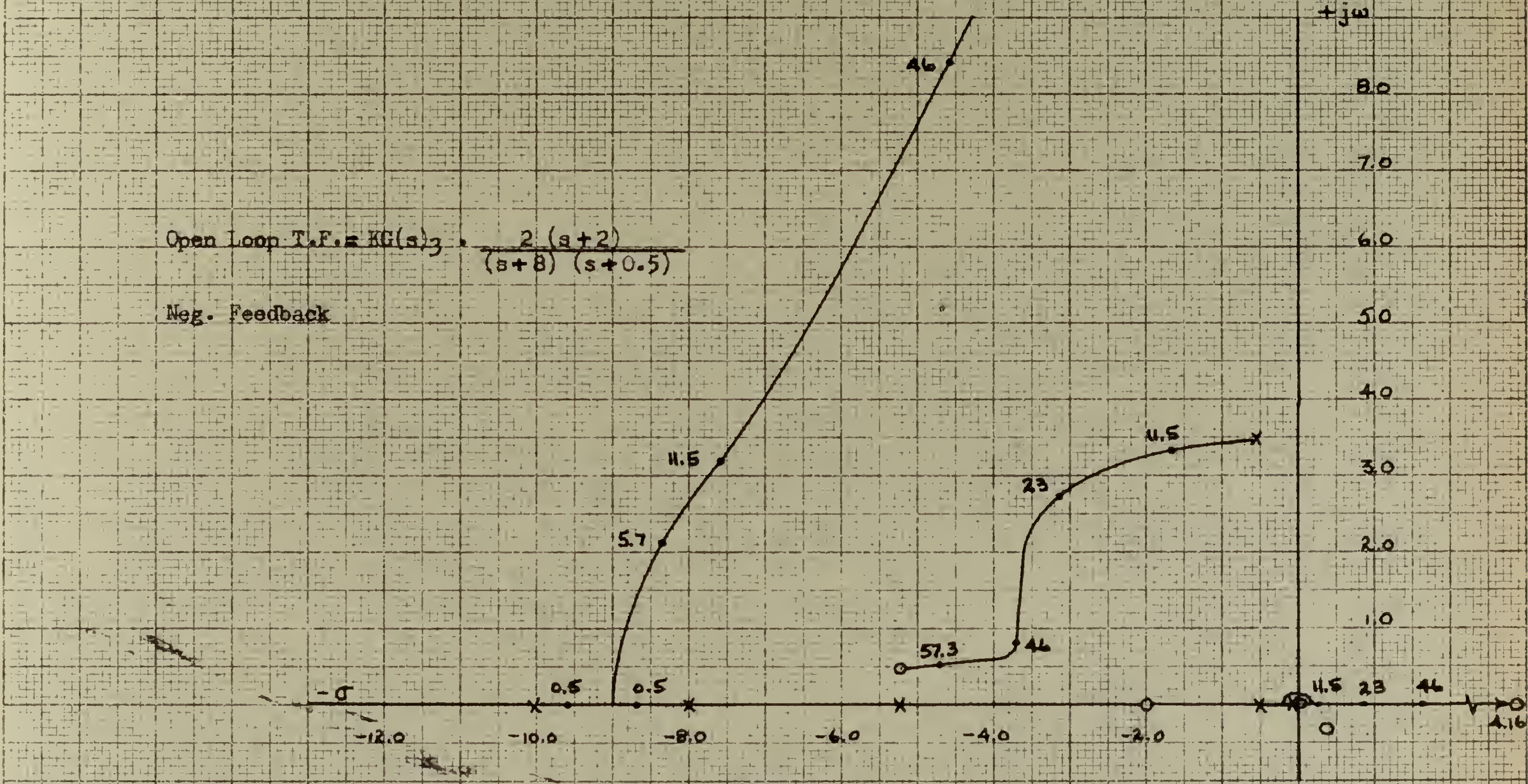

Fig. 20

Root Locus Plot for [illegible] with Filter 3, Flight Condition 3.

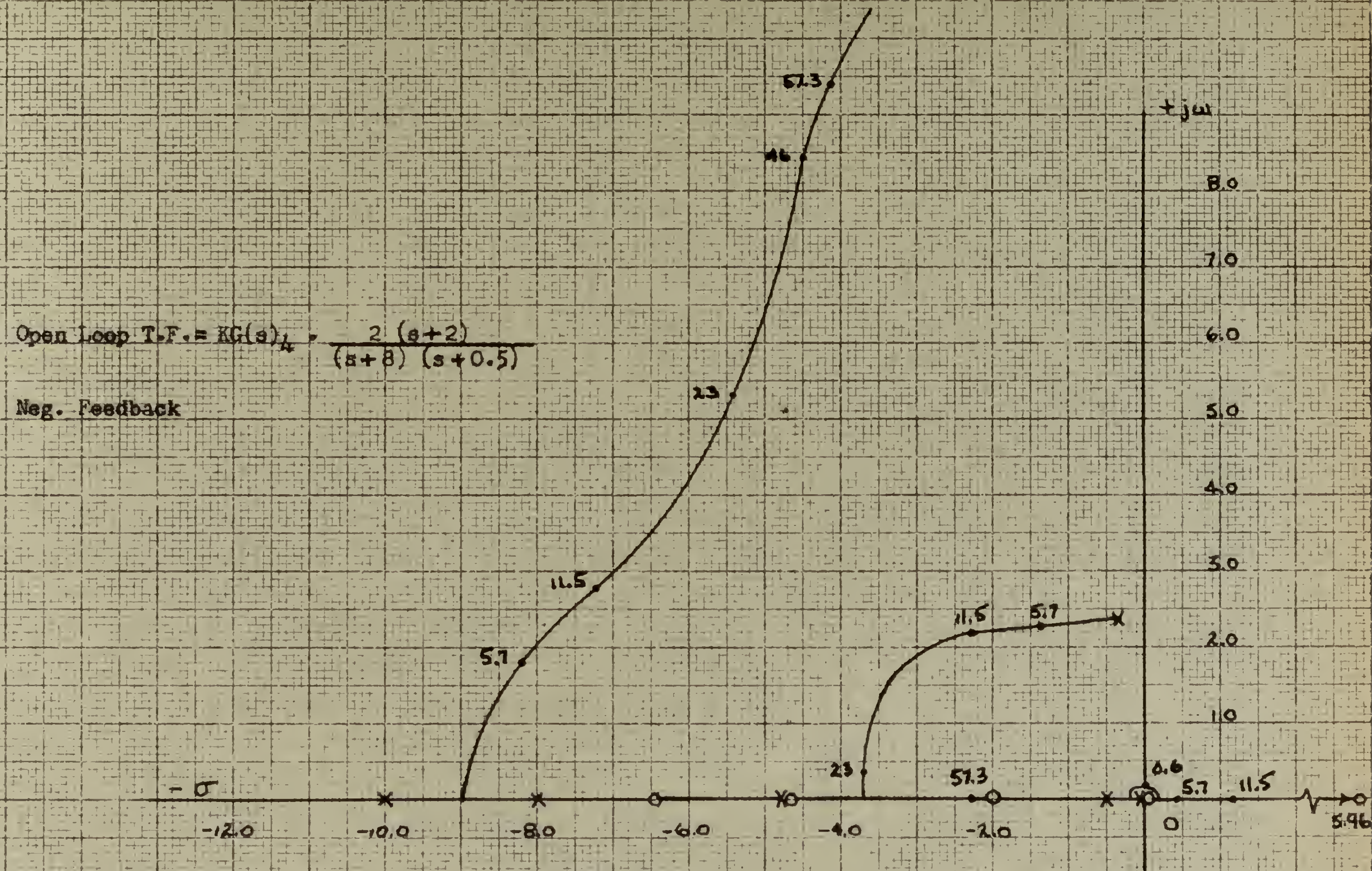

Fig. 21

Root Locus Plot for N_y with filter 3, Flight Condition 4.

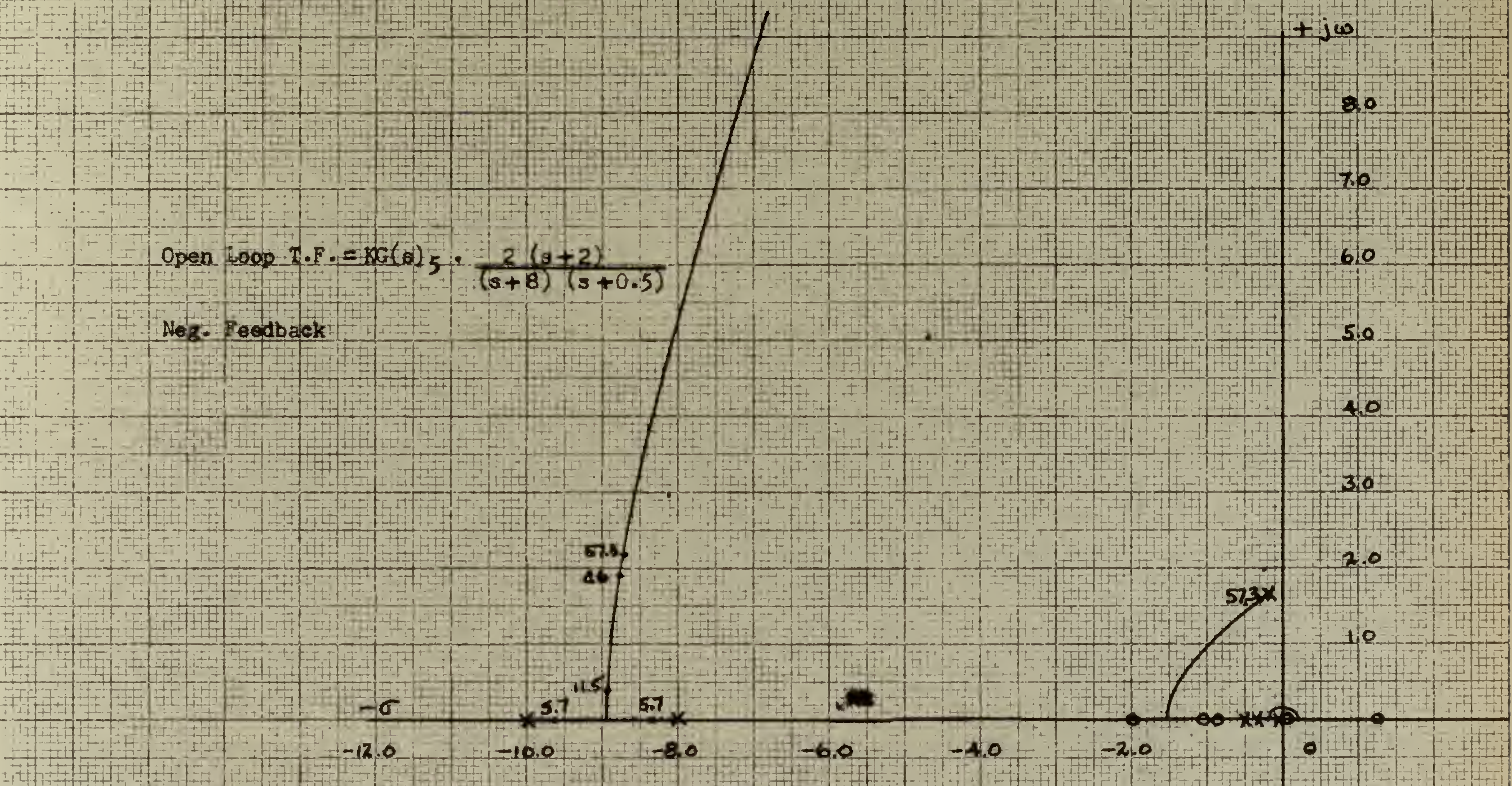

Fig. 22

Root Locus Plot for N_y with filter 3, Flight Condition 5.

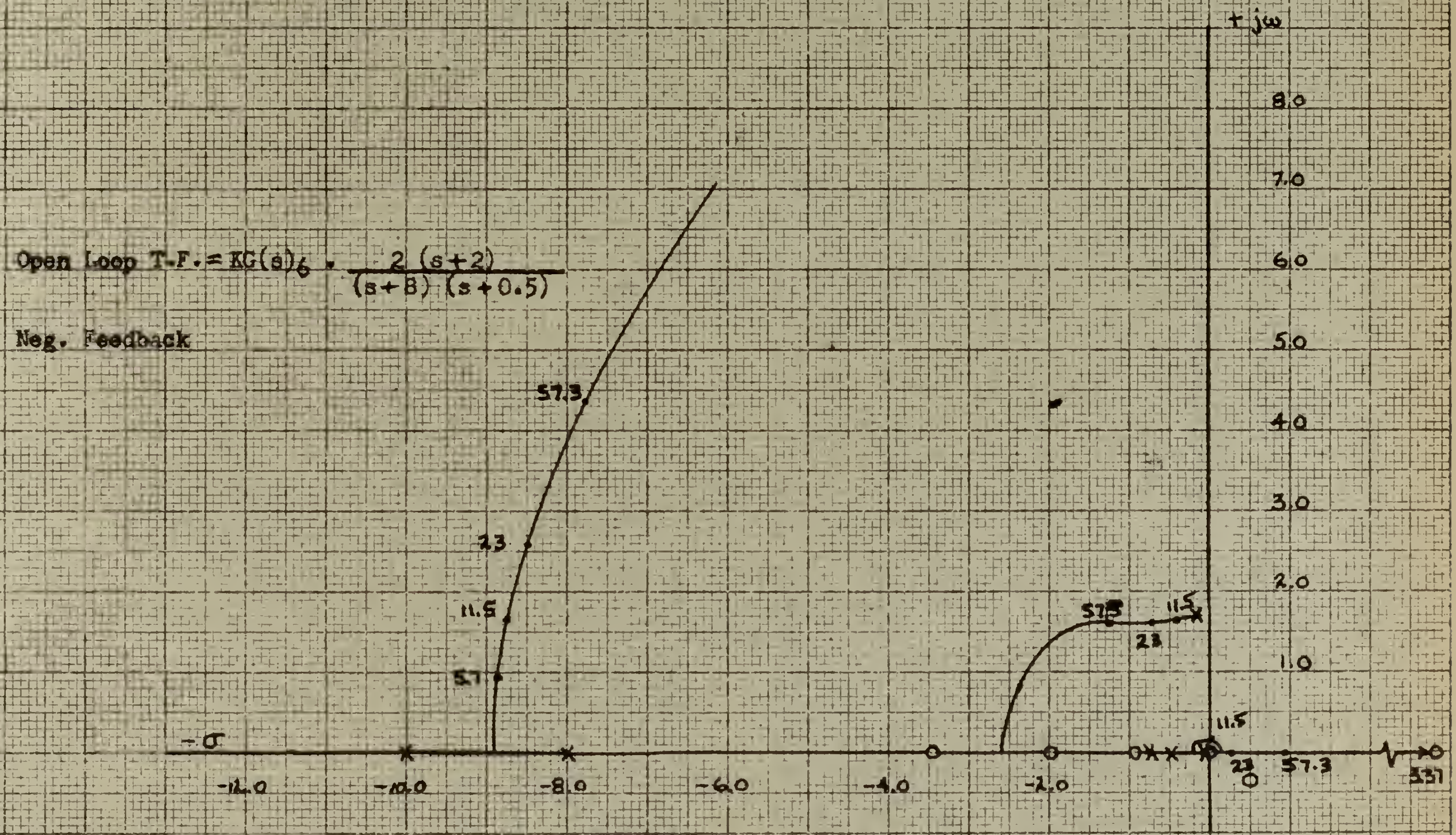

Fig. 23

Root Locus Plot for N_y with filter 3, Flight Condition 6.

conditions. Positive feedback was undesirable since complex roots processed directly into the right half plane.

The final suggested implementation of N_y was in combination with some proportional amount of $\dot{r}$, yaw acceleration, resulting in a transfer function $(N_y + K_{\dot{r}}\,\dot{r})/\delta_R$. The selected value of $K_{\dot{r}}$ determined the offset distance of the measuring accelerometer from the c.g. Positive $K_{\dot{r}}$ indicated positioning of the instrument or the center-line of the airframe forward of the c.g. while negative $K_{\dot{r}}$ placed the instrumentation aft of c.g.

The open loop transfer functions for $(N_y + K_{\dot{r}}\,\dot{r})/\delta_R$ are listed in Table III. According to selected values of $K_{\dot{r}}$ equal to $\pm$ 0.1, $\pm$ 0.2 and 0.31 These values were chosen as indicative of the probable offset distance of the accelerometer from the c.g. The variable loop gain was designated as K_{Ny} and expressed in the units deg./g.

Root locus solutions were obtained using these functions as open loop transfer functions. Due to the enormity of the investigation of these functions and the fact that N_y with compensation was being thoroughly analyzed, studies only of the feasibility of this combination were carried out. Family plots indicating the paths of the loci in the regions of the origin and imaginary axis are contained in Figs. 24 through 30 for each of the values of $K_{\dot{r}}$ mentioned above.

TABLE III

Open Loop Lateral Transfer Functions for $(N_y + K_{\dot{r}}\dot{r})/\delta_R$

with Varying Values of $K_{\dot{r}}$ for Each Flight Condition

$K_{\dot{r}} = +0.1$;

Condition 1:

$$KG'(s)_1 = \frac{0.1102 \times 10^8 K_{N_y}(s-0.0738)(s-1.198)(s+1.7077 \pm j0.4112)}{\Delta(s)_1}$$

Condition 2:

$$KG'(s)_2 = \frac{0.4718 \times 10^8 K_{N_y}(s-0.0182)(s+2.191)(s-2.5106)(s+3.434)}{\Delta(s)_2}$$

Condition 3:

$$KG'(s)_3 = \frac{3.1716 \times 10^8 K_{N_y}(s-4.801)(s+0.0063)(s+5.674 \pm j0.261)}{\Delta(s)_3}$$

Condition 4:

$$KG'(s)_4 = \frac{3.0736 \times 10^8 K_{N_y}(s-0.0073)(s+4.719)(s-6.965)(s+7.435)}{\Delta(s)_4}$$

Condition 5:

$$KG'(s)_5 = \frac{0.1755 \times 10^8 K_{N_y}(s-0.02)(s+0.8308)(s-1.505)(s+1.5214)}{\Delta(s)_5}$$

Condition 6:

$$KG'(s)_6 = \frac{0.7566 \times 10^8 K_{N_y}(s-0.001)(s+1.089)(s-4.988)(s+2.813)}{\Delta(s)_6}$$

TABLE III (Cont'd)

$K_r = -0.1;$

Condition 1:

$$KG'(s)_1 = \frac{0.2636 \times 10^8 K_{Ny}(s-0.0979)(s-0.785)(s+1.135 \pm j0.4413)}{\Delta(s)_1}$$

Condition 2:

$$KG'(s)_2 = \frac{0.884 \times 10^8 K_{Ny}(s-0.0187)(s+2.611)(s-1.864)(s+2.013)}{\Delta(s)_2}$$

Condition 3:

$$KG'(s)_3 = \frac{5.417 \times 10^8 K_{Ny}(s-3.733)(s+0.0063)(s+4.92 \pm j0.376)}{\Delta(s)_3}$$

Condition 4:

$$KG'(s)_4 = \frac{5.293 \times 10^8 K_{Ny}(s-0.0073)(s+4.644)(s-5.289)(s+5.811)}{\Delta(s)_4}$$

Condition 5:

$$KG'(s)_5 = \frac{0.376 \times 10^8 K_{Ny}(s+0.84)(s-0.1066)(s-1.0499)(s-0.0236)}{\Delta(s)_5}$$

Condition 6:

$$KG'(s)_6 = \frac{1.367 \times 10^8 K_{Ny}(s-0.0009)(s+0.9162)(s-2.979)(s+3.066)}{\Delta(s)_6}$$

TABLE III (Cont'd)

$K_r = +0.2;$

Condition 1:

$$KG'(s)_1 = \frac{0.033 \times 10^8 K_{N_y} (s-1.702)(s+1.486)(s-0.066)(s+5.419)}{\Delta(s)_1}$$

Condition 2:

$$KG'(s)_2 = \frac{0.2468 \times 10^8 K_{N_y} (s-0.0179)(s+2.175)(s-3.297)(s+5.1076)}{\Delta(s)_2}$$

Condition 3:

$$KG'(s)_3 = \frac{2.049 \times 10^8 K_{N_y} (s+0.0063)(s+7.631)(s-5.86 \pm j5.356)}{\Delta(s)_3}$$

Condition 4:

$$KG'(s)_4 = \frac{1.964 \times 10^8 K_{N_y} (s-0.0073)(s+4.74)(s-8.691)(s+9.409)}{\Delta(s)_4}$$

Condition 5:

$$KG'(s)_5 = \frac{0.0752 \times 10^8 K_{N_y} (s-0.0186)(s+0.8216)(s-2.142)(s+2.716)}{\Delta(s)_5}$$

Condition 6:

$$KG'(s)_6 = \frac{0.451 \times 10^8 K_{N_y} (s-0.0009)(s+0.9263)(s-5.1295)(s+5.42)}{\Delta(s)_6}$$

TABLE III (Cont'd)

$K_r = -0.2;$

Condition 1:

$$KG'(s)_1 = \frac{0.3404 \times 10^8 K_{N_y} (s-0.65)(s-0.1175)(s+1.0163 \pm j0.3523)}{\Delta(s)_1}$$

Condition 2:

$$KG'(s)_2 = \frac{1.096 \times 10^8 K_{N_y} (s-0.0189)(s+2.454)(s-1.677)(s+1.891)}{\Delta(s)_2}$$

Condition 3:

$$KG'(s)_3 = \frac{6.54 \times 10^8 K_{N_y} (s-3.411)(s+4.915)(s+0.0063)(s+4.496)}{\Delta(s)_3}$$

Condition 4:

$$KG'(s)_4 = \frac{6.4027 \times 10^8 K_{N_y} (s-0.0073)(s-4.8033)(s+5.806)(s+4.559)}{\Delta(s)_4}$$

Condition 5:

$$KG'(s)_5 = \frac{0.477 \times 10^8 K_{N_y} (s-0.926)(s-0.026)(s+0.759)(s-0.096)}{\Delta(s)_5}$$

Condition 6:

$$KG'(s)_6 = \frac{1.673 \times 10^8 K_{N_y} (s-0.0009)(s+0.912)(s-2.695)(s+2.767)}{\Delta(s)_6}$$

TABLE III (Cont'd)

$K_{\dot{r}} = +0.3;$

Condition 1:

$$KG'(s)_1 = \frac{-.0433 \times 10^8 K_{N_y}(s-0.059)(s+1.394)(s-1.896)(s+2.191)}{\Delta(s)_1}$$

Condition 2:

$$KG'(s)_2 = \frac{0.0343 \times 10^8 K_{N_y}(s-0.0177)(s+2.192)(s-6.477)(s+18.78)}{\Delta(s)_2}$$

Condition 3:

$$KG'(s)_3 = \frac{0.926 \times 10^8 K_{N_y}(s+0.0063)(s+5.292)(s-8.266 \pm j12.096)}{\Delta(s)_3}$$

Condition 4:

$$KG'(s)_4 = \frac{0.8542 \times 10^8 K_{N_y}(s-0.0072)(s+4.747)(s+14.409)(s-13.091)}{\Delta(s)_4}$$

Condition 5:

$$KG'(s)_5 = \frac{-0.0253 \times 10^8 K_{N_y}(s-0.0174)(s+0.817)(s-1.622 \pm j4.001)}{\Delta(s)_5}$$

Condition 6:

$$KG'(s) = \frac{0.146 \times 10^8 K_{N_y}(s-0.0009)(s+0.93)(s-8.821)(s+9.775)}{\Delta(s)_6}$$

TABLE III (Cont'd)

$K_{\dot{r}} = -0.3$

Condition 1:

$$KG'(s)_1 = \frac{0.4171 \times 10^8 K_{N_y}(s-0.526)(s-0.1482)(s+0.931 \pm j0.2412)}{\Delta(s)_1}$$

Condition 2:

$$KG'(s)_2 = \frac{1.309 \times 10^8 K_{N_y}(s-0.0193)(s+2.382)(s-1.534)(s+1.7585)}{\Delta(s)_2}$$

Condition 3:

$$KG'(s)_3 = \frac{7.662 \times 10^8 K_{N_y}(s+4.046)(s+5.038)(s-3.159)(s+0.0063)}{\Delta(s)_3}$$

Condition 4:

$$KG'(s)_4 = \frac{7.512 \times 10^8 K_{N_y}(s-0.0073)(s+4.674)(s+4.8805)(s-4.4395)}{\Delta(s)_4}$$

Condition 5:

$$KG'(s)_5 = \frac{0.577 \times 10^8 K_{N_y}(s-0.0287)(s+0.668)(s-0.829)(s+0.73)}{\Delta(s)_5}$$

Condition 6:

$$KG'(s)_6 = \frac{1.978 \times 10^8 K_{N_y}(s-0.0009)(s+0.9086)(s-2.4794)(s+2.542)}{\Delta(s)_6}$$

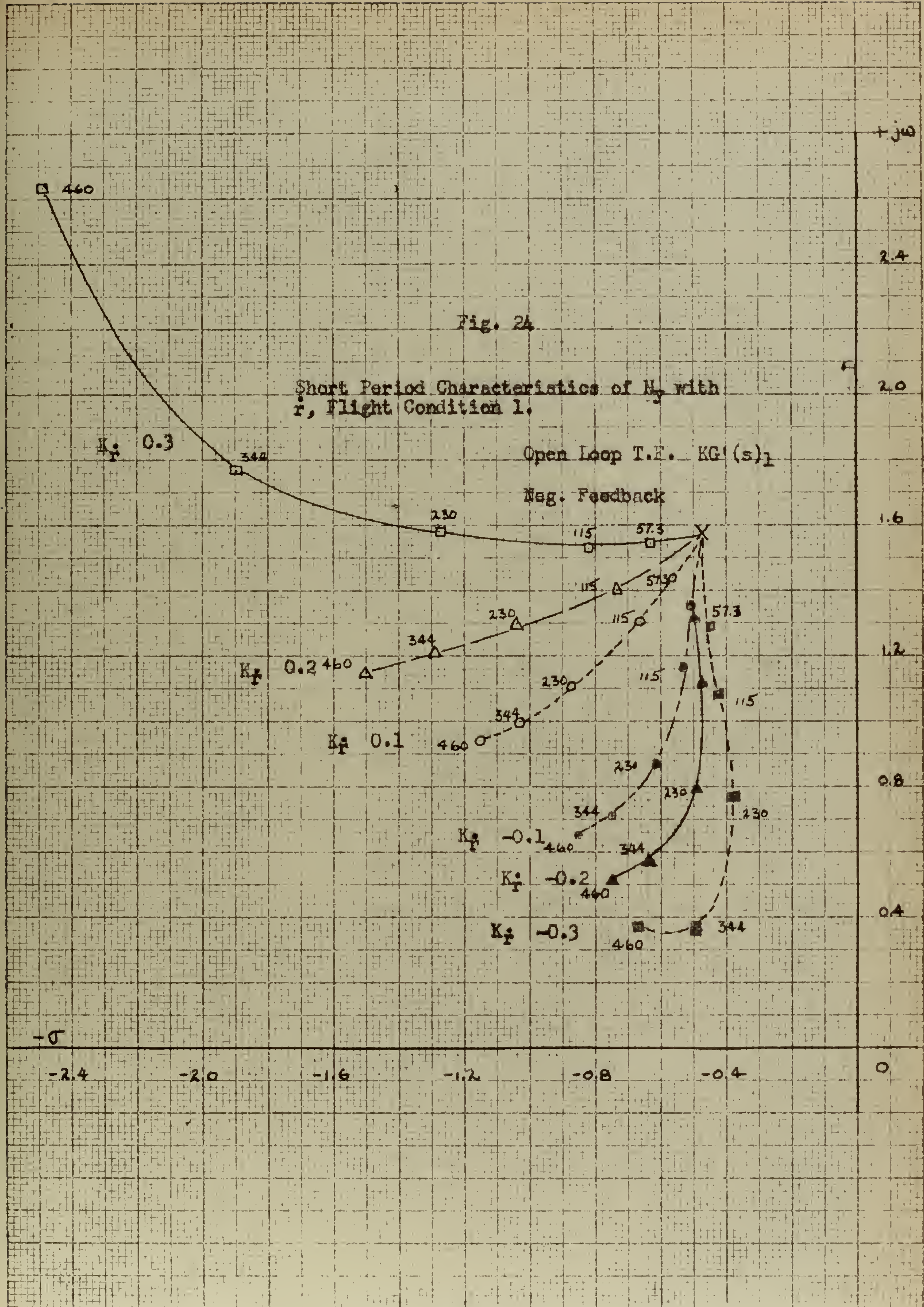
Fig. 24
Short Period Characteristics of N_y with $\dot{r}$, Flight Condition 1.
Open Loop T.F. $KG'(s)_1$
Neg. Feedback
$K_{\dot{r}}$ 0.3
$K_{\dot{r}}$ 0.2
$K_{\dot{r}}$ 0.1
$K_{\dot{r}}$ -0.1
$K_{\dot{r}}$ -0.2
$K_{\dot{r}}$ -0.3
460
344
230
115
57.3
+jω
2.4
2.0
1.6
1.2
0.8
0.4
-σ
-2.4
-2.0
-1.6
-1.2
-0.8
-0.4
0

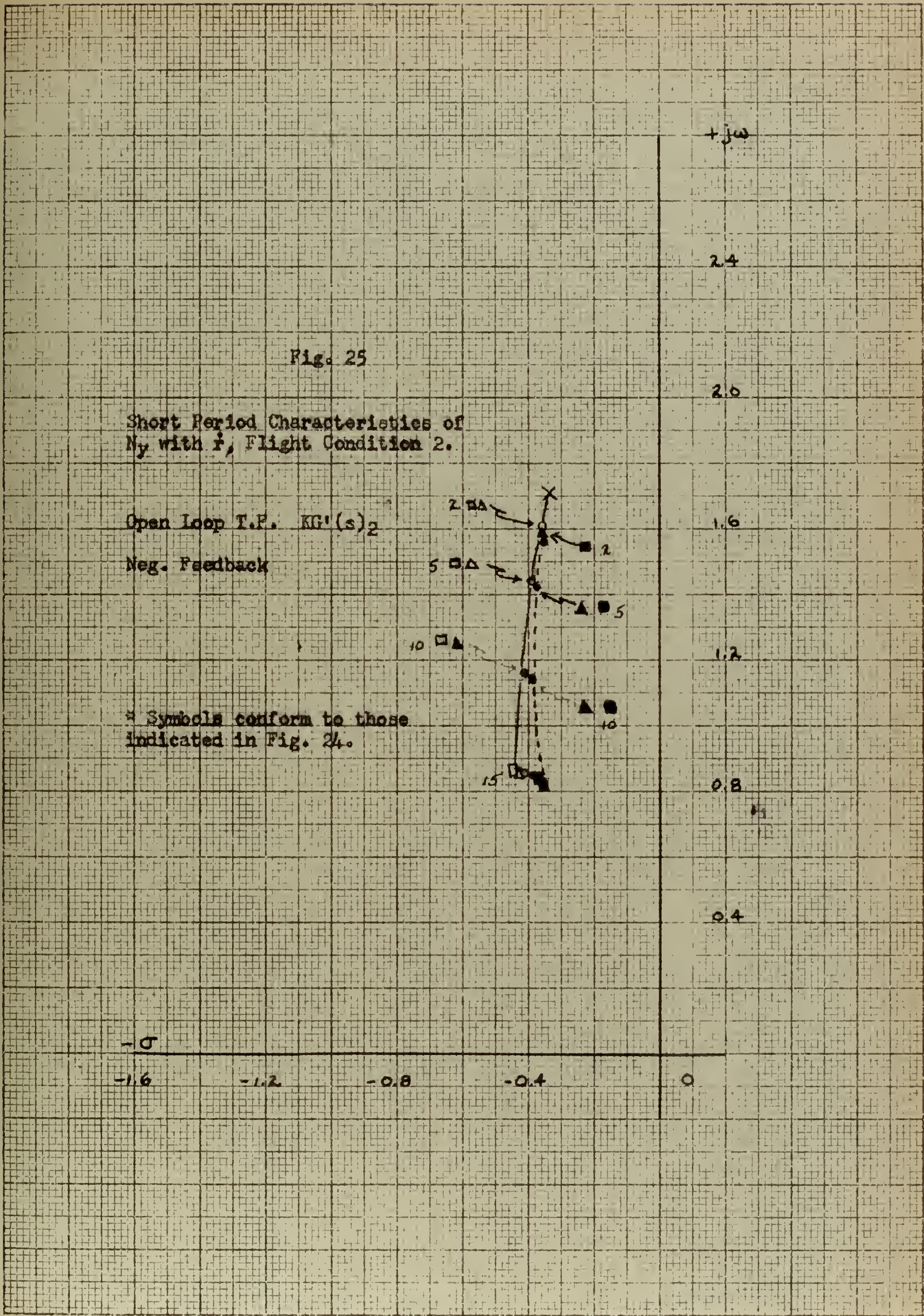
Fig. 25
Short Period Characteristics of N_y with $\dot{r}$, Flight Condition 2.
Open Loop T.F. $KG'(s)_2$
Neg. Feedback
* Symbols conform to those indicated in Fig. 24.
$+j\omega$
2.4
2.0
1.6
1.2
0.8
0.4
$-\sigma$
-1.6
-1.2
-0.8
-0.4
0
2
5
10
15

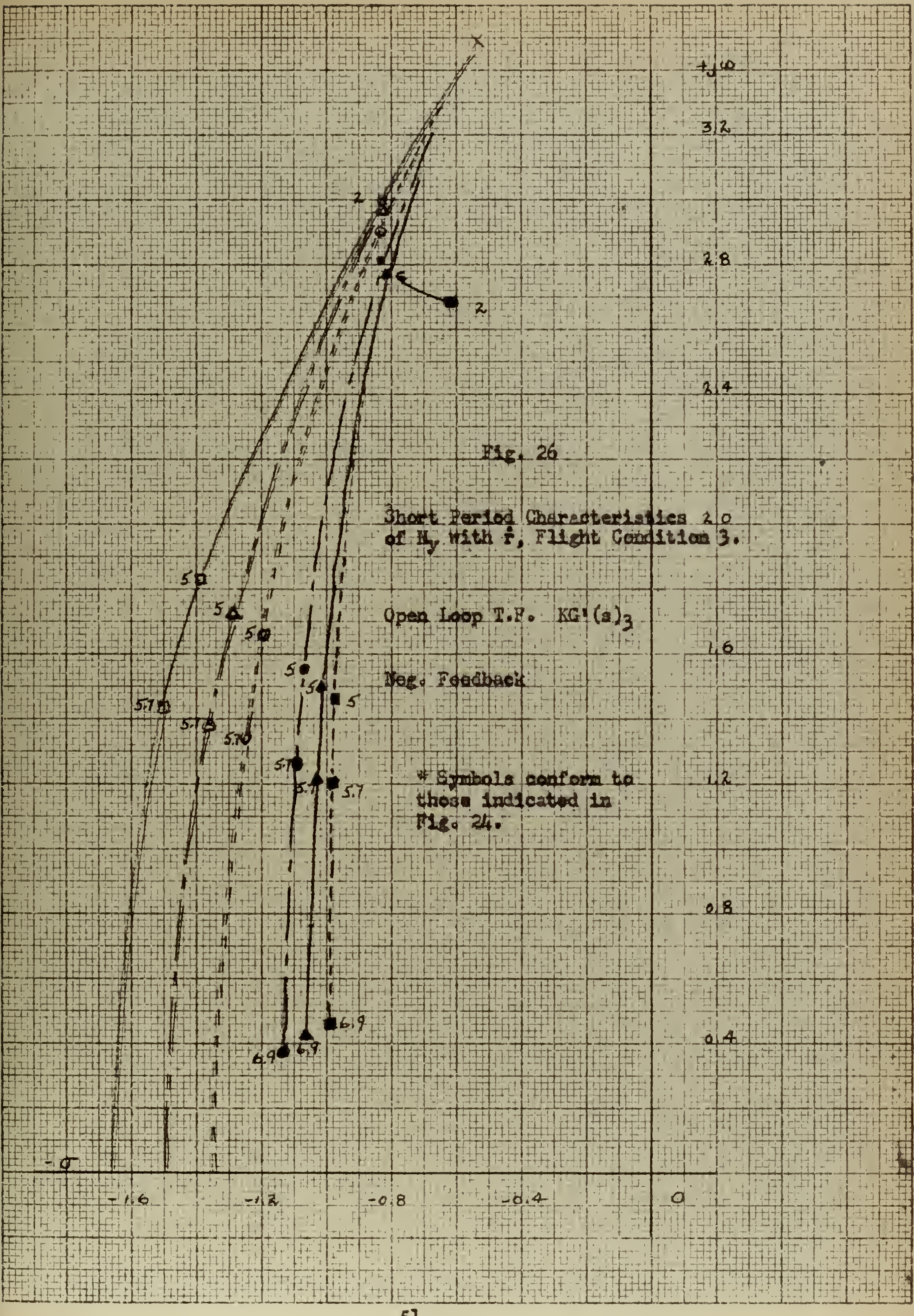

Fig. 26

Short Period Characteristics of M_y with $\dot{r}$, Flight Condition 3.

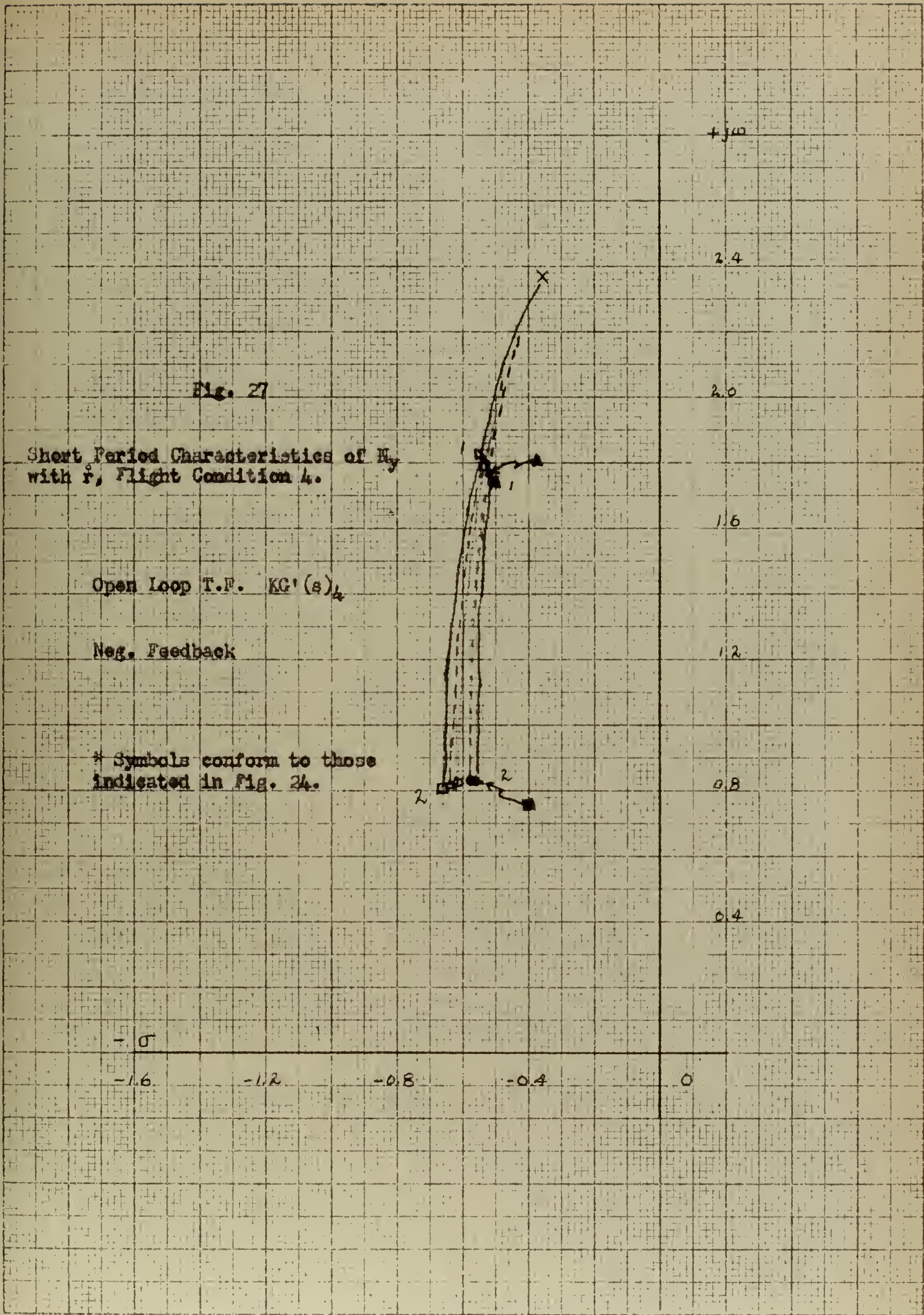

Fig. 27

Short Period Characteristics of N_y with r, Flight Condition 4.

Open Loop T.F. $KG'(s)_4$

Neg. Feedback

* Symbols conform to those indicated in Fig. 24.

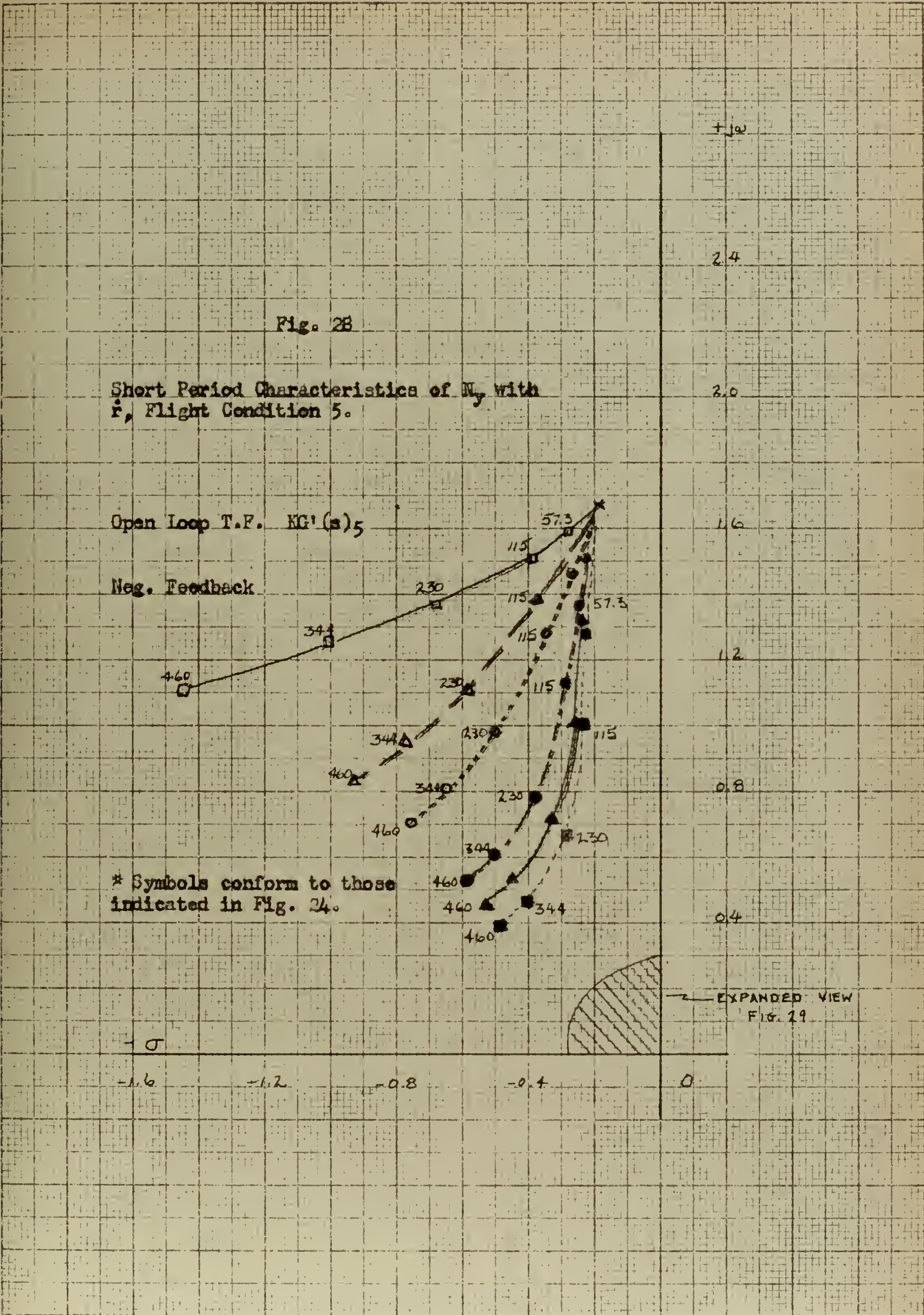

Fig. 28

Short Period Characteristics of N_y with $\dot{r}$, Flight Condition 5.

Open Loop T.F. $KG'(s)_5$

Neg. Feedback

* Symbols conform to those indicated in Fig. 24.

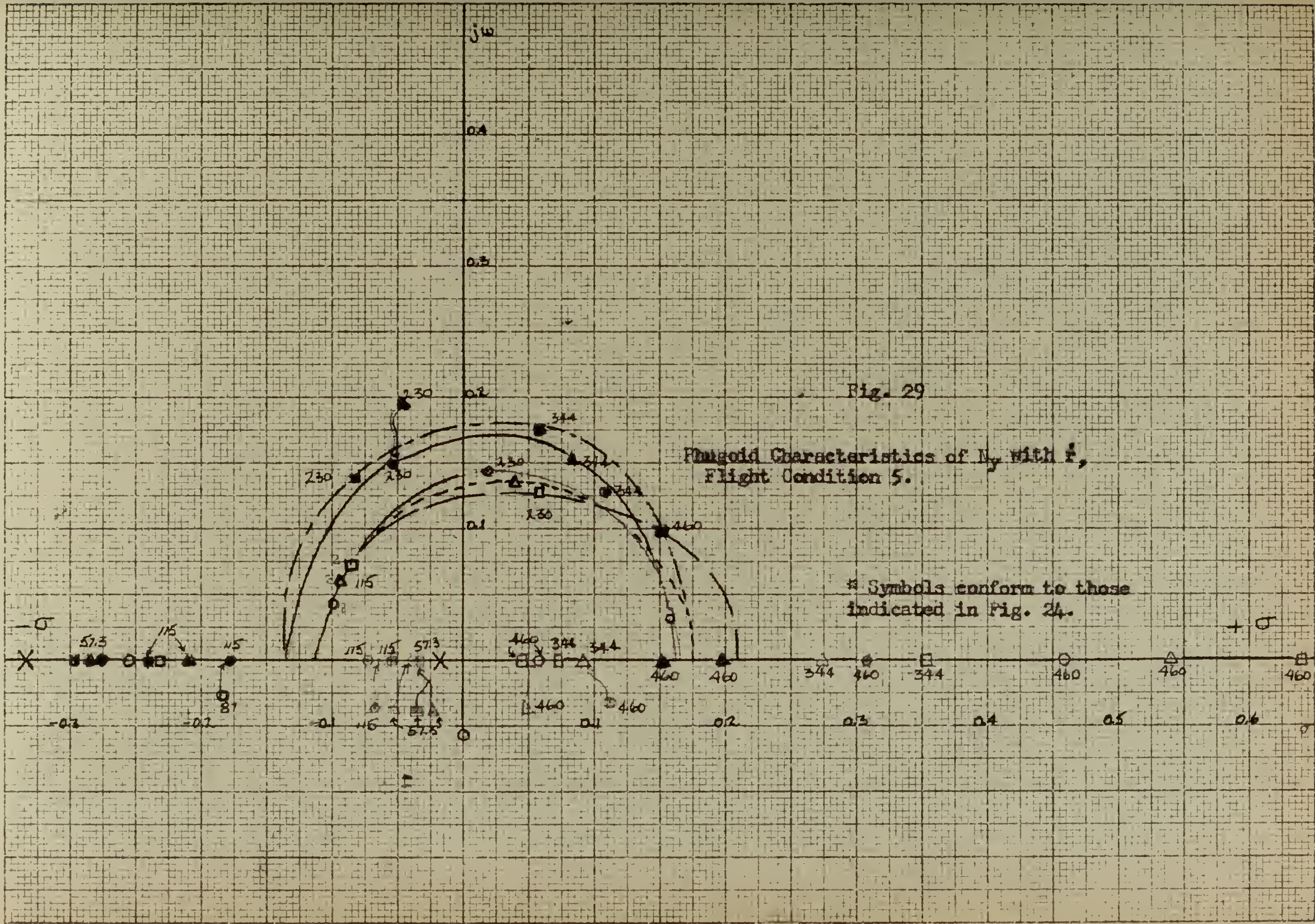

Fig. 29

Phugoid Characteristics of N_y with $\dot{r}$,
Flight Condition 5.

* Symbols conform to those indicated in Fig. 24.

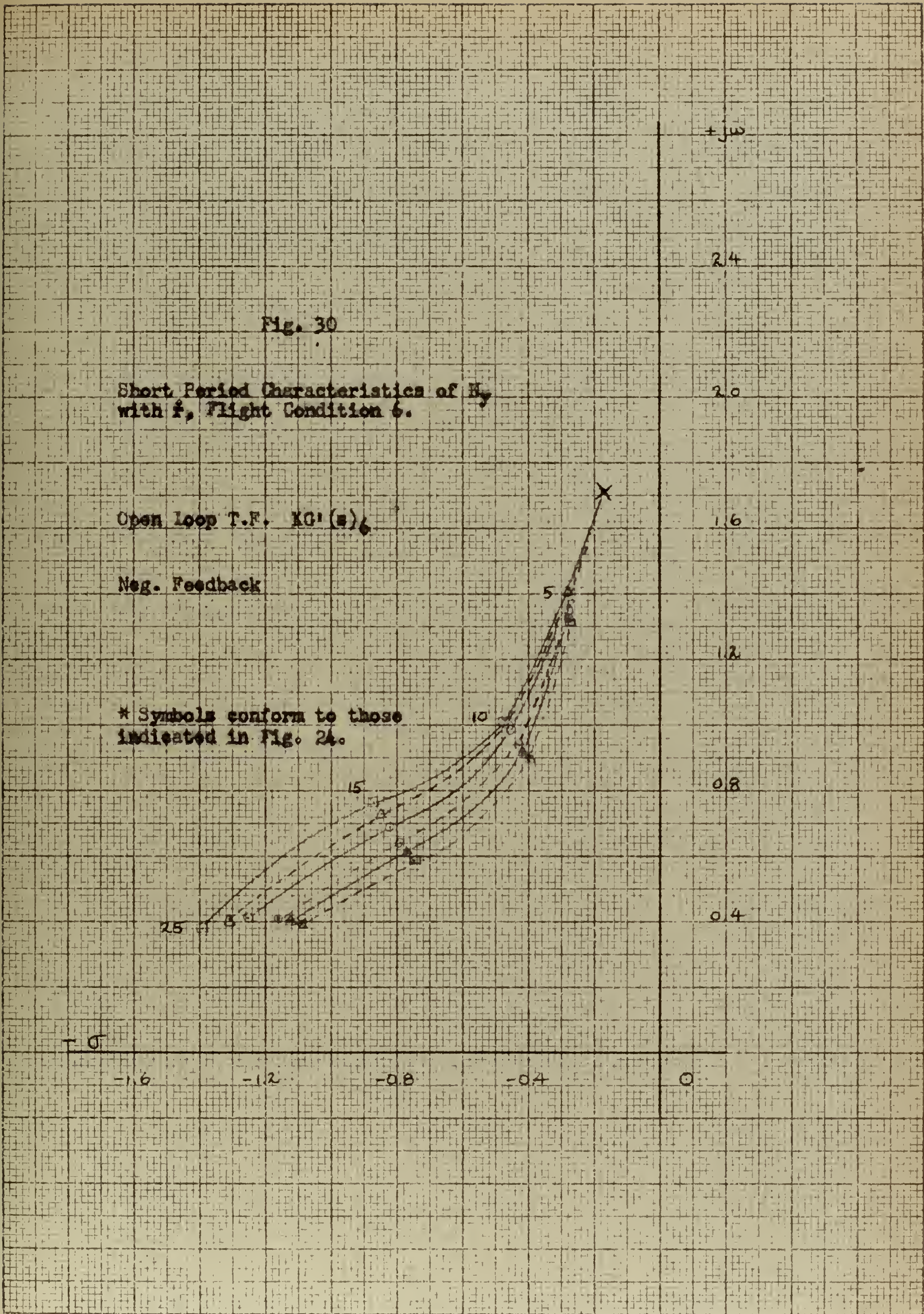

Fig. 30

Short Period Characteristics of H_y with f, Flight Condition 6.

Open Loop T.F. $KG'(s)_6$

Neg. Feedback

* Symbols conform to those indicated in Fig. 24.

In order to corroborate the information obtained from the root locus plots of N_y and compensating filters, analog computer simulation of the airframe and control loop was carried out as detailed in Appendix B. The data obtained from the analog study is developed and discussed in Chapters on the system analysis.

Chapter V

Scope of This Investigation

Yaw Rate, r, as a Lateral Response

Referring again to Fig. 2, the lateral airframe response yaw rate, 4, may be inserted into the control loop. The lateral transfer functions then become r/δ_R where r and δ_R may be expressed in deg./sec or radians/sec and degrees or radians respectively. The airframe equations for each flight condition are contained in Table IV.

Combination of these transfer functions with the instruments and the variable gain parameter, K_r, expressed in the units deg/deg/sec or rad/rad/sec are contained in Table V and are the open loop transfer functions where $\Delta(s)_n$ has been previously defined.

Root locus plots as a function of variable gain, K_r, were obtained as in previous examples and are plotted as such in Figs. 31 through 36.

As in the preceding investigations, it was hoped from the analysis to determine whether this lateral response offers the desirable characteristics upon which the adaptive scheme is to be based.

Simulation of the aircraft and control loop were again made on the analog computer to confirm the information derived from the root locus investigation as well as establish definite transient characteristics.

TABLE IV

Three Degree Lateral Transfer Functions for the Response r/δ_R for Each Specified Flight Condition

Condition 1:

$$r/\delta_R = \frac{-0.6075(s-0.18705 \pm j0.7062)(s+1.2189)}{(s+0.0657)(s+0.7322)(s+0.4715 \pm j1.5798)}$$

Condition 2:

$$r/\delta_R = \frac{-1.6807(s+0.0061 \pm j0.5116)(s+2.2549)}{(s+0.0189)(s+2.3972)(s+0.3376 \pm j1.7172)}$$

Condition 3:

$$r/\delta_R = \frac{-8.8853(s-0.1834)(s+0.4983)(s+5.176)}{(s-0.0007)(s+5.209)(s+0.532 \pm j3.4933)}$$

Condition 4:

$$r/\delta_R = \frac{-8.7821(s+0.0898 \pm j0.7098)(s+4.8061)}{(s+0.044)(s+4.7792)(s+0.3571 \pm j2.3784)}$$

Condition 5:

$$r/\delta_R = \frac{-0.7948(s-0.1928 \pm j0.5343)(s+0.8006)}{(s+0.0194)(s+0.3334)(s+0.187 \pm j1.6679)}$$

Condition 6:

$$r/\delta_R = \frac{-2.4175(s-0.0685 \pm j0.4221)(s+1.0343)}{(s+0.0079)(s+0.7404)(s+0.1706 \pm j1.706)}$$

TABLE V

Open Loop Transfer Functions for the Lateral Response

r/δ_R at Specified Flight Conditions

Condition 1:

$$KG''(s)_1 = \frac{-0.7676\times10^8 K_r(s-0.1871\pm j0.7062)(s+1.2189)}{\Delta(s)_1}$$

Condition 2:

$$KG''(s)_2 = \frac{-2.1237\times10^8 K_r(s+0.0061\pm j0.5116)(s+2.2549)}{\Delta(s)_2}$$

Condition 3:

$$KG''(s)_3 = \frac{-11.2275\times10^8 K_r(s-0.1834)(s+0.4983)(s+5.176)}{\Delta(s)_3}$$

Condition 4:

$$KG''(s)_4 = \frac{-11.0971\times10^8 K_r(s+0.0898\pm j0.7098)(s+4.8061)}{\Delta(s)_4}$$

Condition 5:

$$KG''(s)_5 = \frac{-1.0043\times10^8 K_r(s-0.1928\pm j0.5343)(s+0.8006)}{\Delta(s)_5}$$

Condition 6:

$$KG''(s)_6 = \frac{-3.0548\times10^8 K_r(s-0.0685\pm j0.4221)(s+1.0343)}{\Delta(s)_6}$$

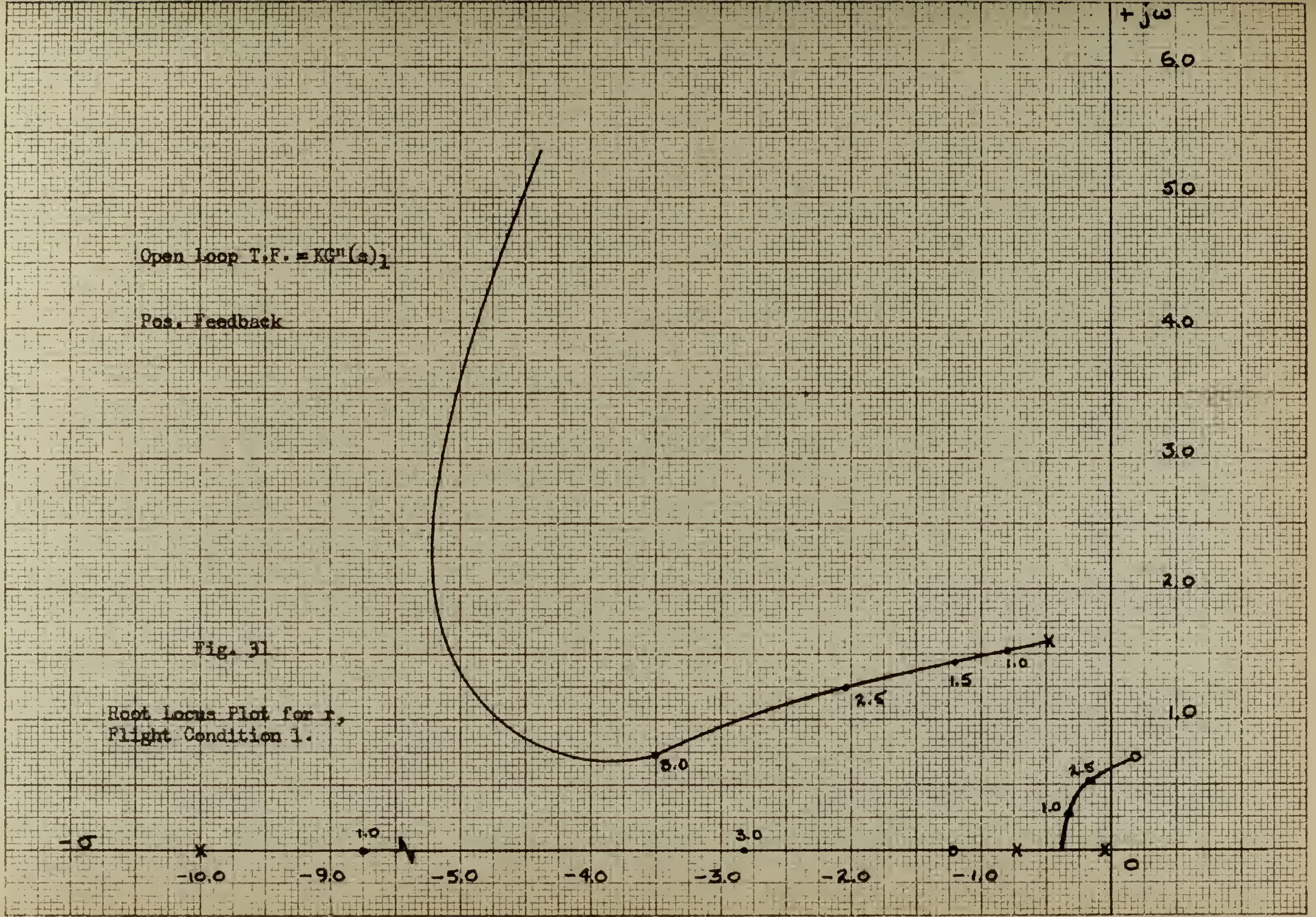

Fig. 31

Root Locus Plot for r,
Flight Condition 1.

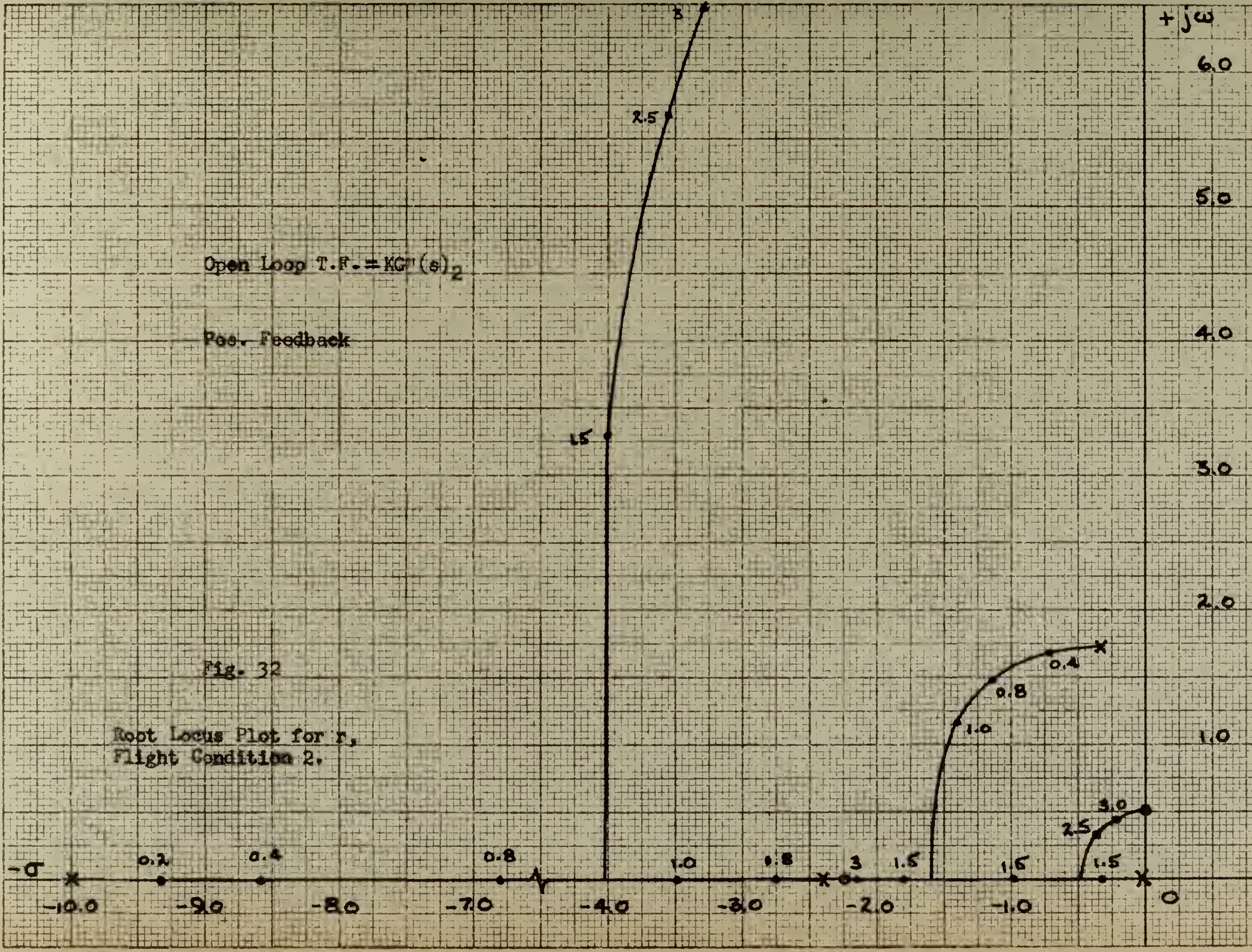

Open Loop T.F. = KG''(s)$_2$

Pos. Feedback

Fig. 32

Root Locus Plot for r,
Flight Condition 2.

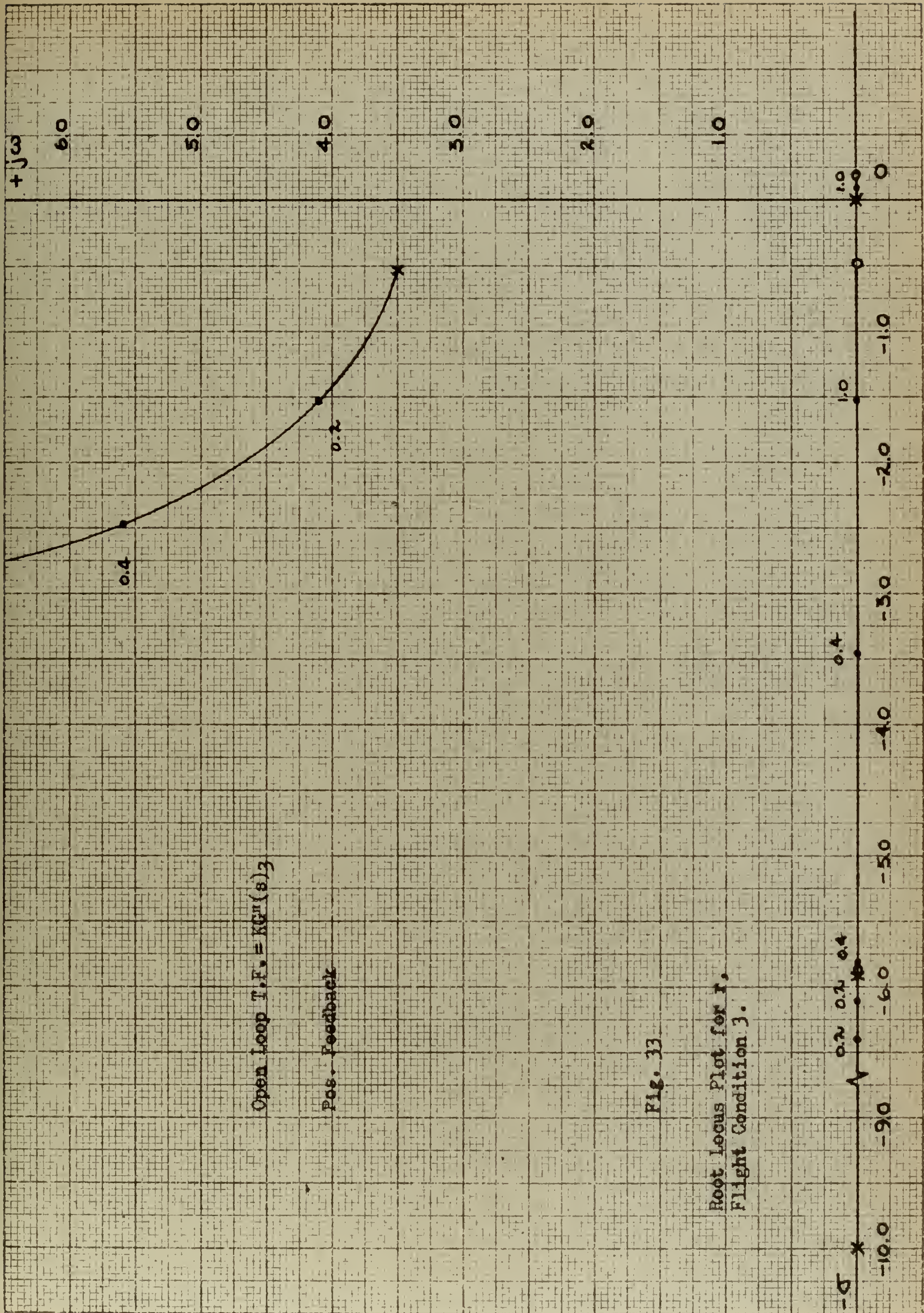

Fig. 33

Root Locus Plot for r,
Flight Condition 3.

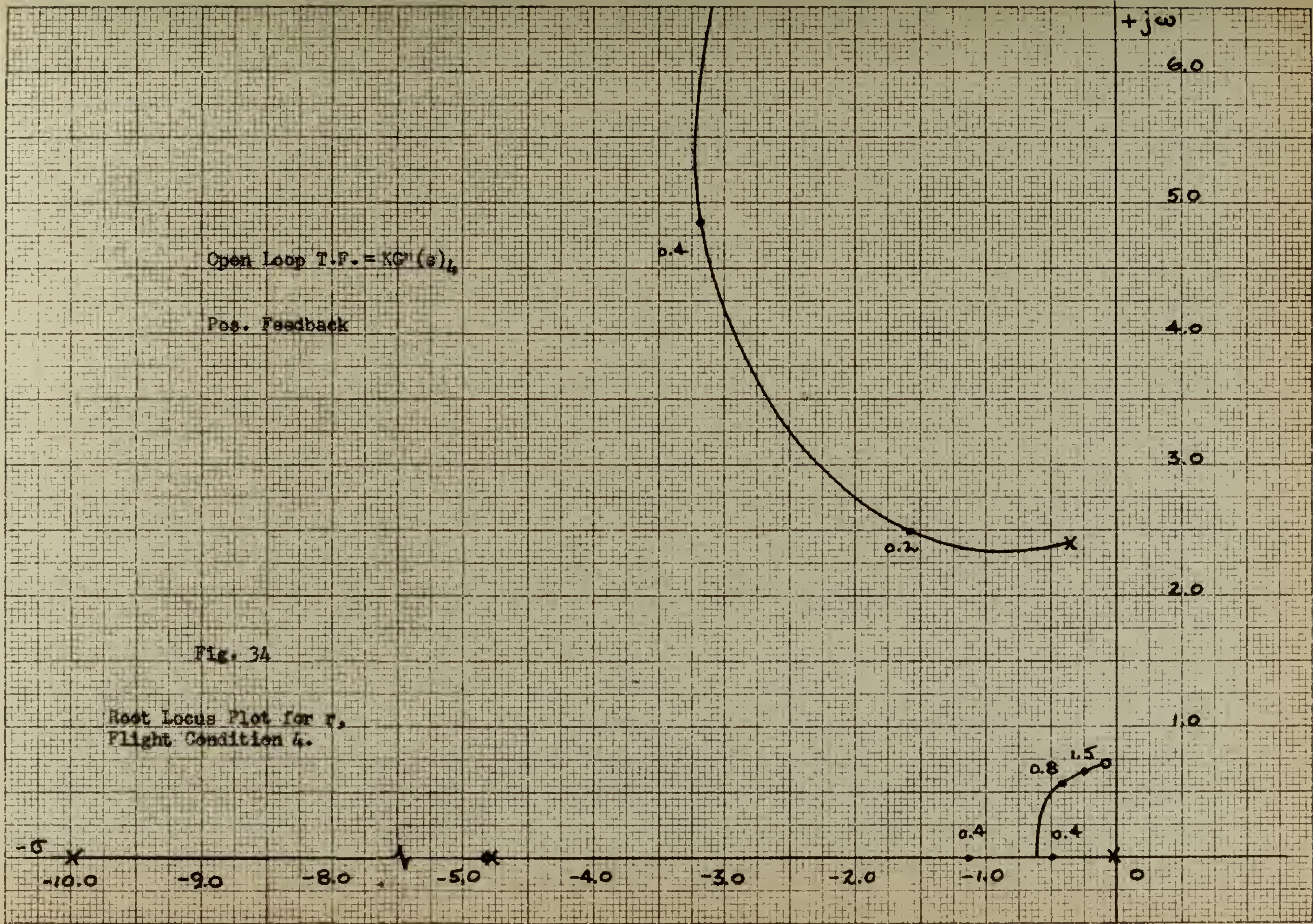

Open Loop T.F. = $KG'(s)_4$

Pos. Feedback

Fig. 34

Root Locus Plot for r,
Flight Condition 4.

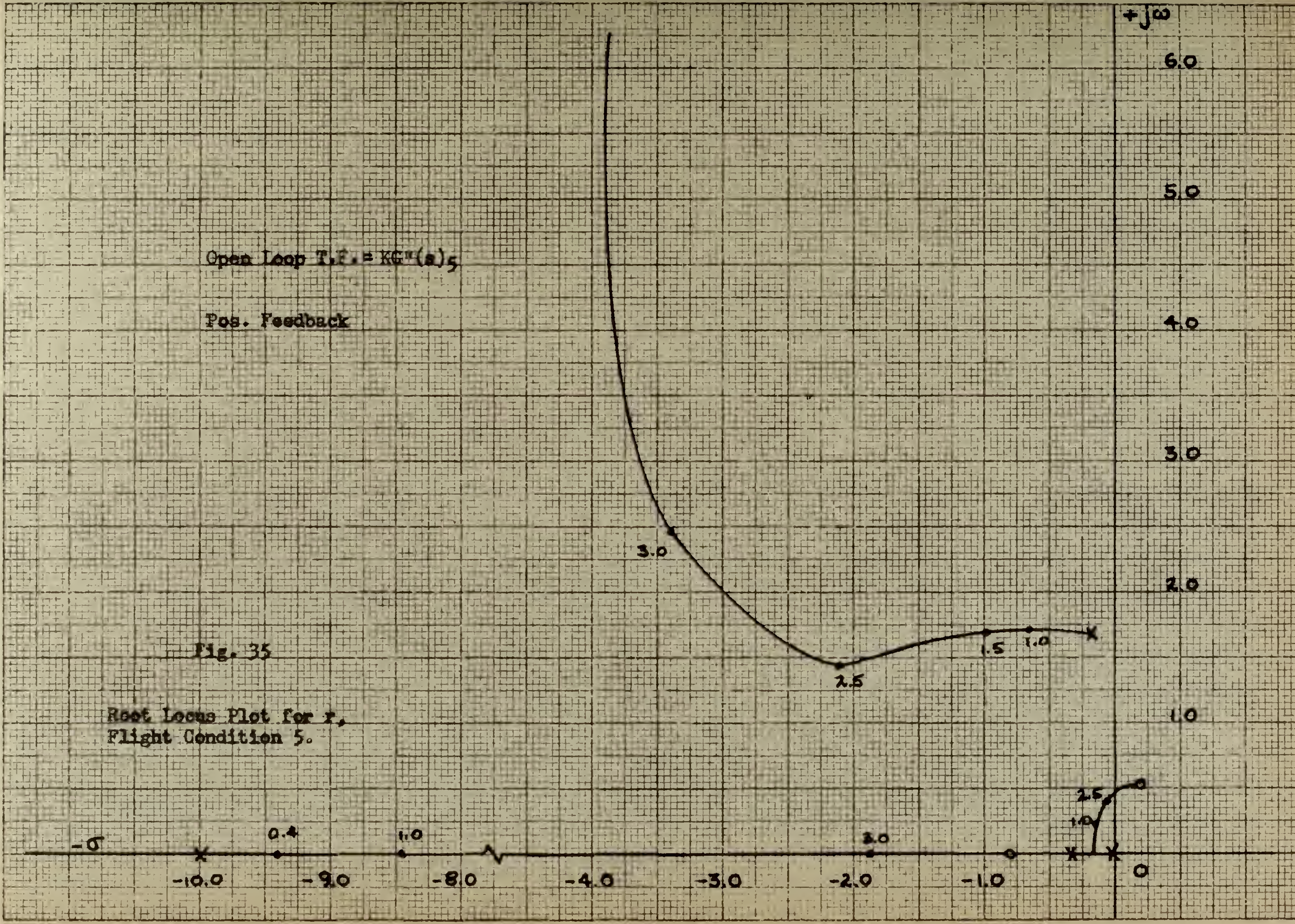

Fig. 35

Root Locus Plot for r,
Flight Condition 5.

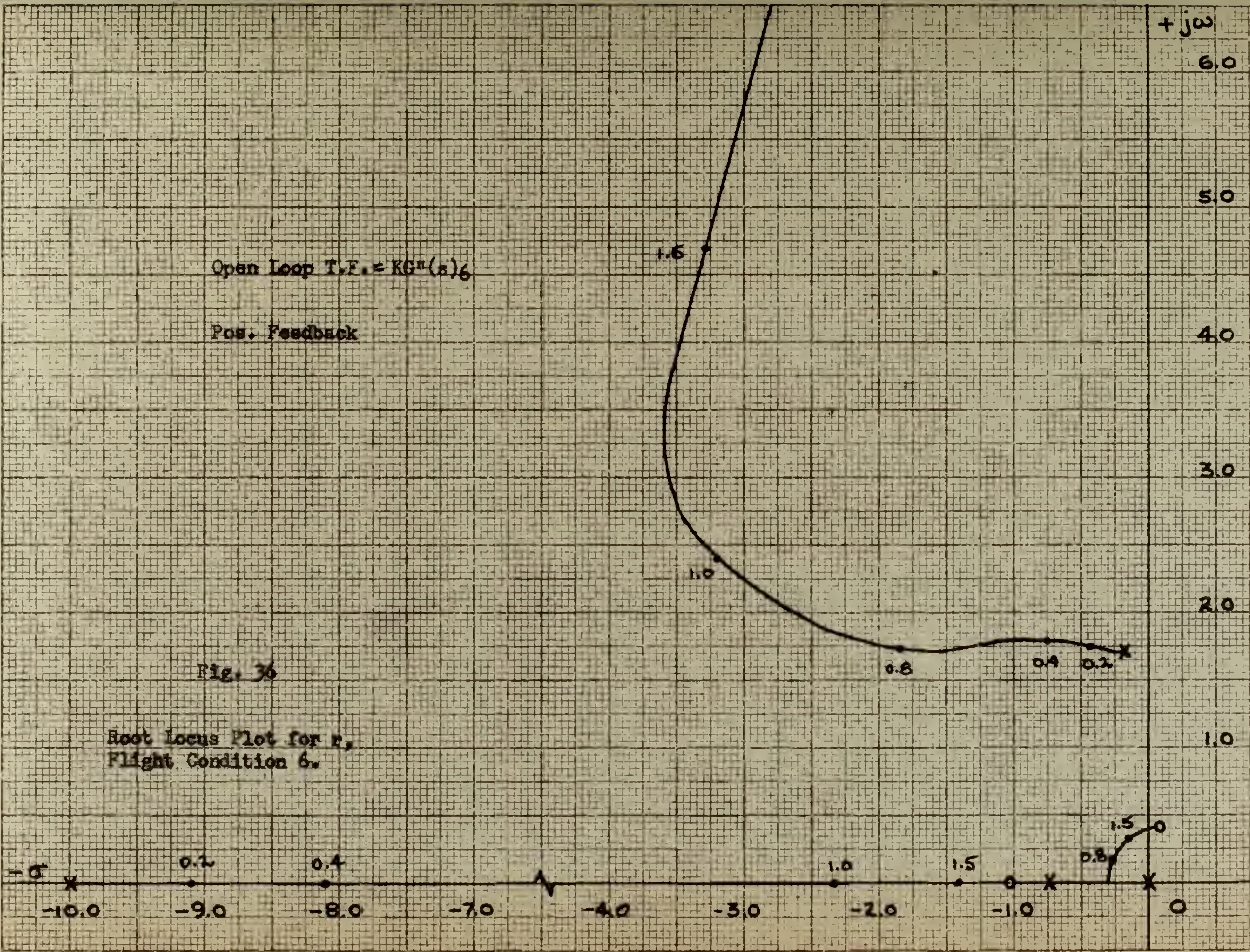

Open Loop T.F. = KG"(s)$_6$
Pos. Feedback
Fig. 36
Root Locus Plot for r,
Flight Condition 6.
+jω
6.0
5.0
4.0
3.0
2.0
1.0
-σ
-10.0
-9.0
-8.0
-7.0
-4.0
-3.0
-2.0
-1.0
0
1.6
1.0
0.8
0.4
0.2
0.2
0.4
1.0
1.5
1.5
0.8

Chapter VI

Scope of This Investigation: The Adaptive Scheme

The adaptive scheme used to vary the loop gain and achieve the desired damping ratio is indicated in block diagram form in Fig. 37. The scheme is designed to select, according to an error criterion, the characteristic damping ratio at the criterion minimum by furnishing through logic circuitry a voltage proportional to the error incurred which in turn drives a servo positioned potentiometer. Design of the logic circuitry was accomplished in conjunction with R. K. Smyth, Senior Research Engineer and Supervisor of the Advanced Analysis Unit, Autonetics Division, North American Aviation Corporation.*

The error criterion selected as the basis of the adaptive scheme was

$$E = \int_0^T |A| \, dt$$

where A represents the signal chosen to represent the particular airframe variable which it is desired to control. With lateral transfer functions based on the measurement and control of N_y this variable would become the quantity to be minimized. Furthermore, since it would be ideal as concerns aircraft control to maintain zero lateral acceleration or zero angle of yaw with respect to the aircraft's course, a minimization of these quantities would serve to approach ideal conditions with respect to lateral motion.

* Patent application filed

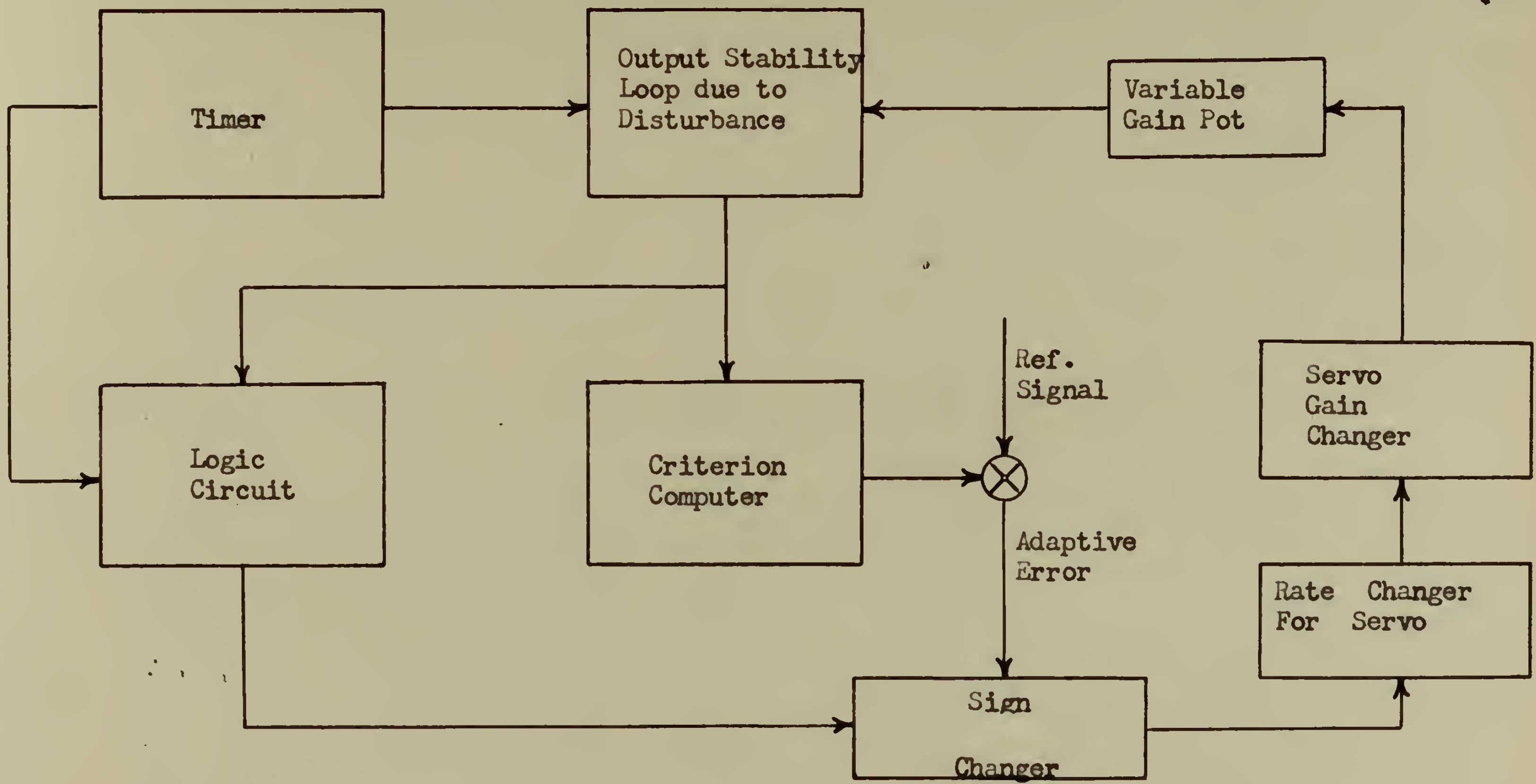

Fig. 37

Block Diagram of the Adaptive Scheme

Reference 5 examines the behavior of the integral

$$\int_0^T |A|\, dt$$

as a function of damping ratio for a second order servomechanism. Fig. 38 illustrates this graphically. While the integral certainly minimizes at a damping ratio of 0.7 for the second order servomechanism, there was no reason to suppose that for a higher order servomechanism, where dominant complex roots occurred, that the criterion did not minimize at the complex root location resulting in the least oscillatory or the most damped condition. Root locus studies detailed in preceding chapters indicated that at no time would damping ratios greater than 0.7 be attained.

Therefore, for these reasons and the additional fact that the lateral response was to be minimized, the error criterion stated above was adopted.

The adaptive scheme was designed to operate by supplying periodically to the airframe a disturbance in the form of a short duration rudder pulse. The response variable to be minimized was measured by conventional instrumentation. The instrument output then formed the basic signal operated upon by the adaptive logic circuits.

The logic circuitry is schematically illustrated in Fig. 39 and consists of three memory storage elements or intergrators I_1, I_2 and I_3, relay switches and summation devices which finally provide the output or drive voltage to the servo driven potentiometer.

The time sequencing of the logic circuit was accomplished by relay control of a stepping switch. The optimizing period, or, the period during which the logic circuit computes its output and the control loop gain is

Fig. 38

Criterion Value, $\int |E|\,dt$ as a Function of Damping Ratio and therefore Loop Gain.

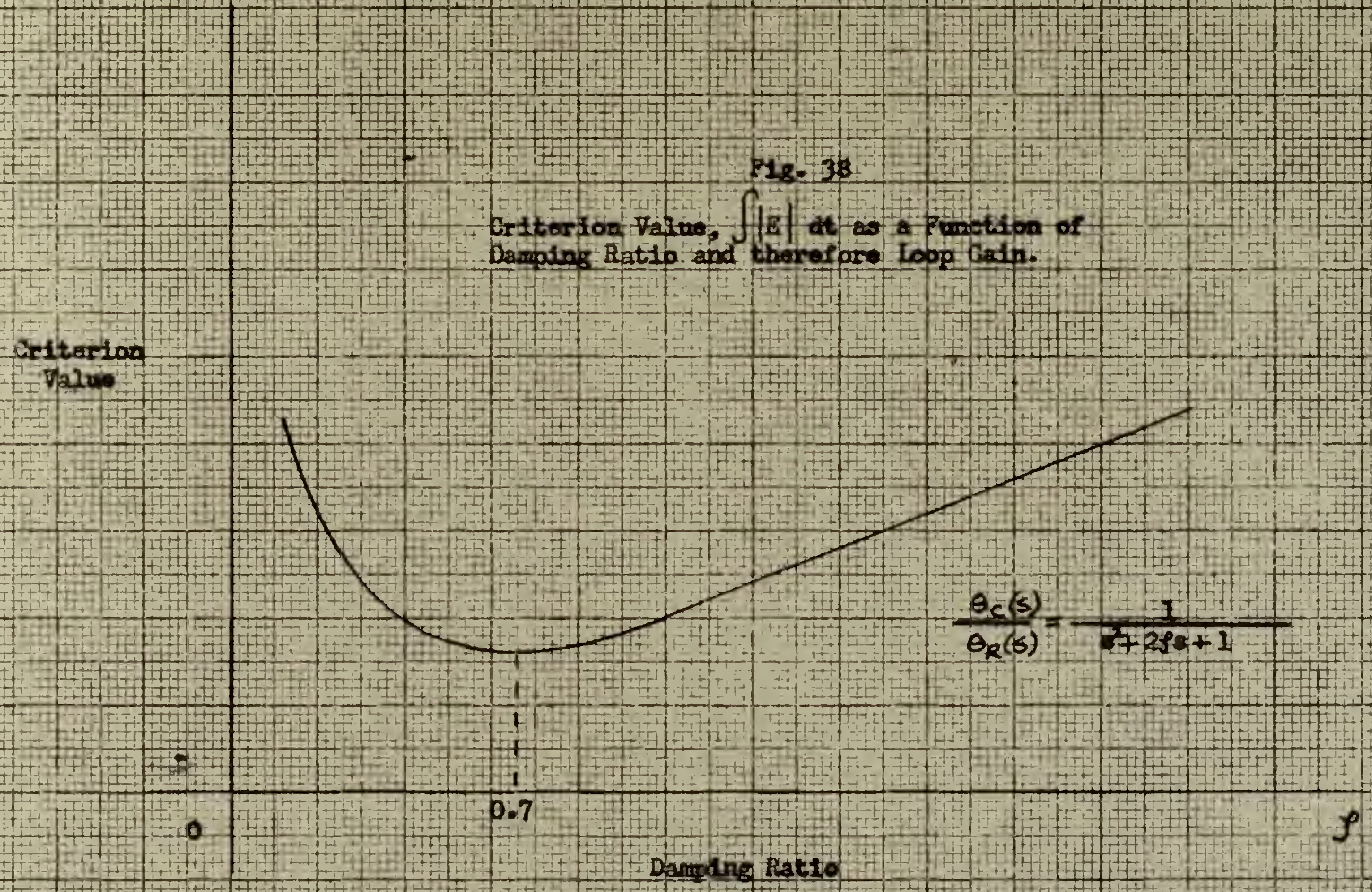

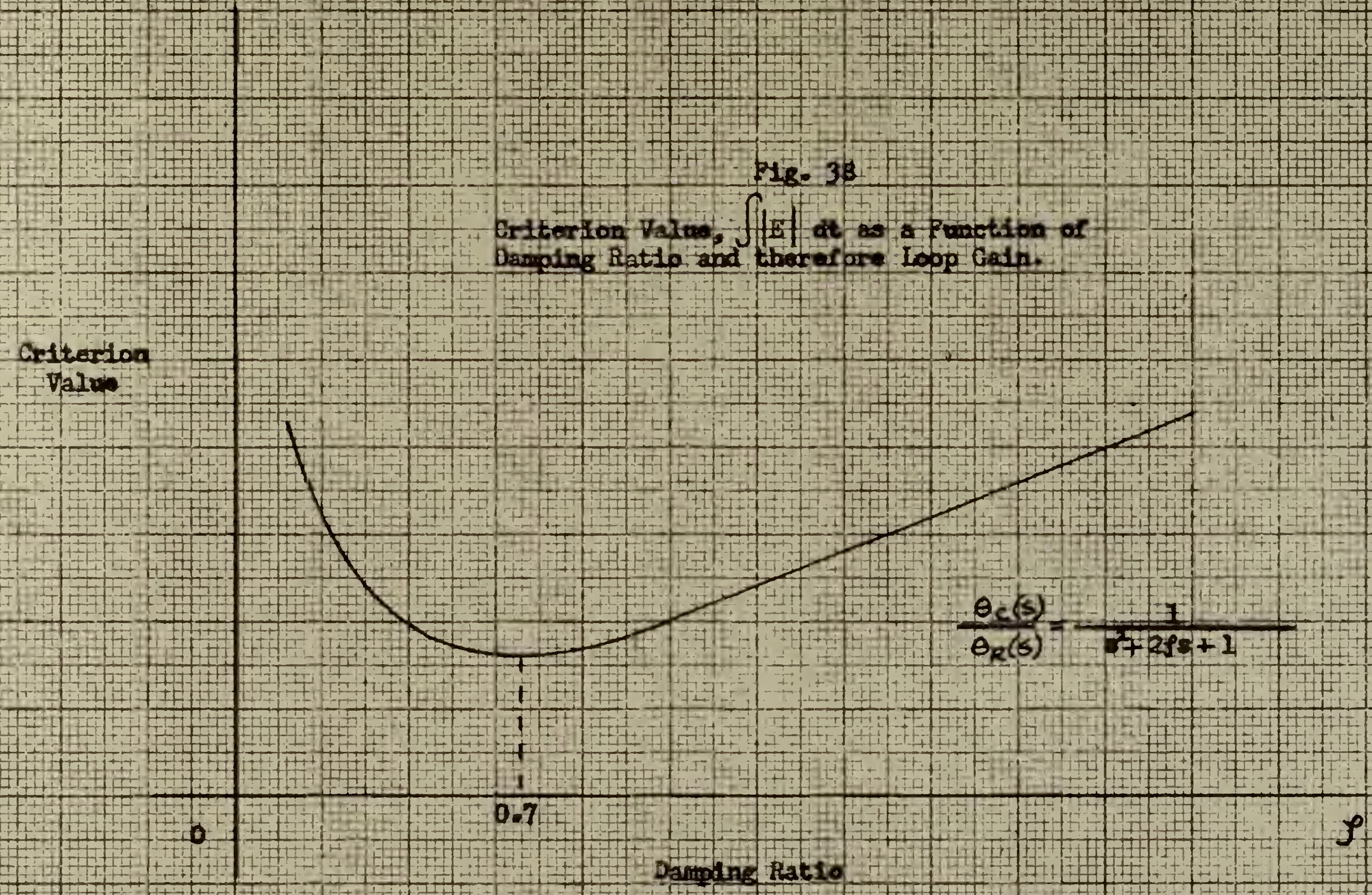

Fig. 38

Criterion Value, $\int |E|\, dt$ as a Function of Damping Ratio and therefore Loop Gain.

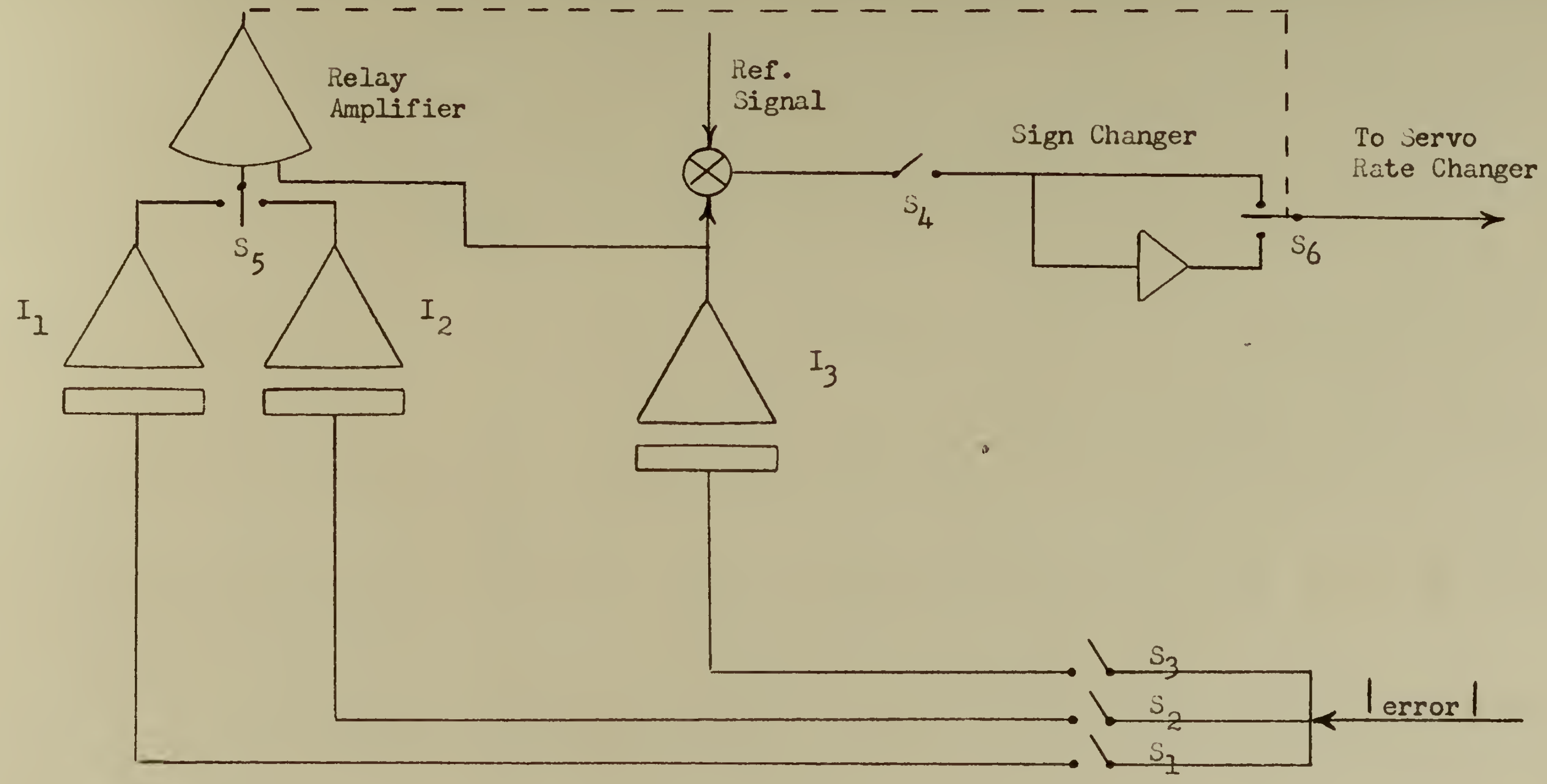

Fig. 39

Schematic Diagram of Adaptive Logic

Circuitry

adjusted, is shown in Fig. 40. The period is divided into distinct intervals during which the various components perform the indicated tasks. At time t_{11}, integrators I_1 and I_3 might integrate the value of the criterion over the period t_{11} to t_{12}. I_2 does not integrate at this time but contains the stored value of the criterion from the previous interval. This occurs since I_1 and I_2 alternate, or, reset and integrate every other period. During period 1, I_1 and I_3 are the working integrators while I_2 retains a stored value from period 0. During period 2, I_2 has been reset to zero and integrates with I_3 while I_1 retains its integrated value from period 1.

The criterion value as obtained by I_3 is combined with some reference value of the criterion to form the adaptive error which is fed to the positioning servo. I_1 and I_2 compare values by applying their voltages to a relay switch. If $|I_1| > |I_2|$, during t_{11} to t_{12} mentioned above, the sign switch reverses since the value of error is increasing and the sign of the adaptive error applied to the pot servo is reversed. Thus the gain will be increased by an increment proportional to the adaptive error in the opposite direction. Should $|I_1| < |I_2|$, the sign will not reverse and the gain will vary in the same direction as in the previous period. Fig. 41 indicates the operation of these integrators within several typical optimizing periods.

In order to insure good response from the servo driven potentiometer, the servo gain was made a function of the value of the adaptive error. A threshold value was incorporated below which the servo gain was a fraction of its gain with an above threshold value of adaptive error. This was intended to reduce the sensitivity of the gain adjuster when the minimum value of the criterion was approached and thus reduce hunting of the mechanism. A non-linear potentiometer was included also to permit more sensitivity in gain selections. The pot characteristics are presented

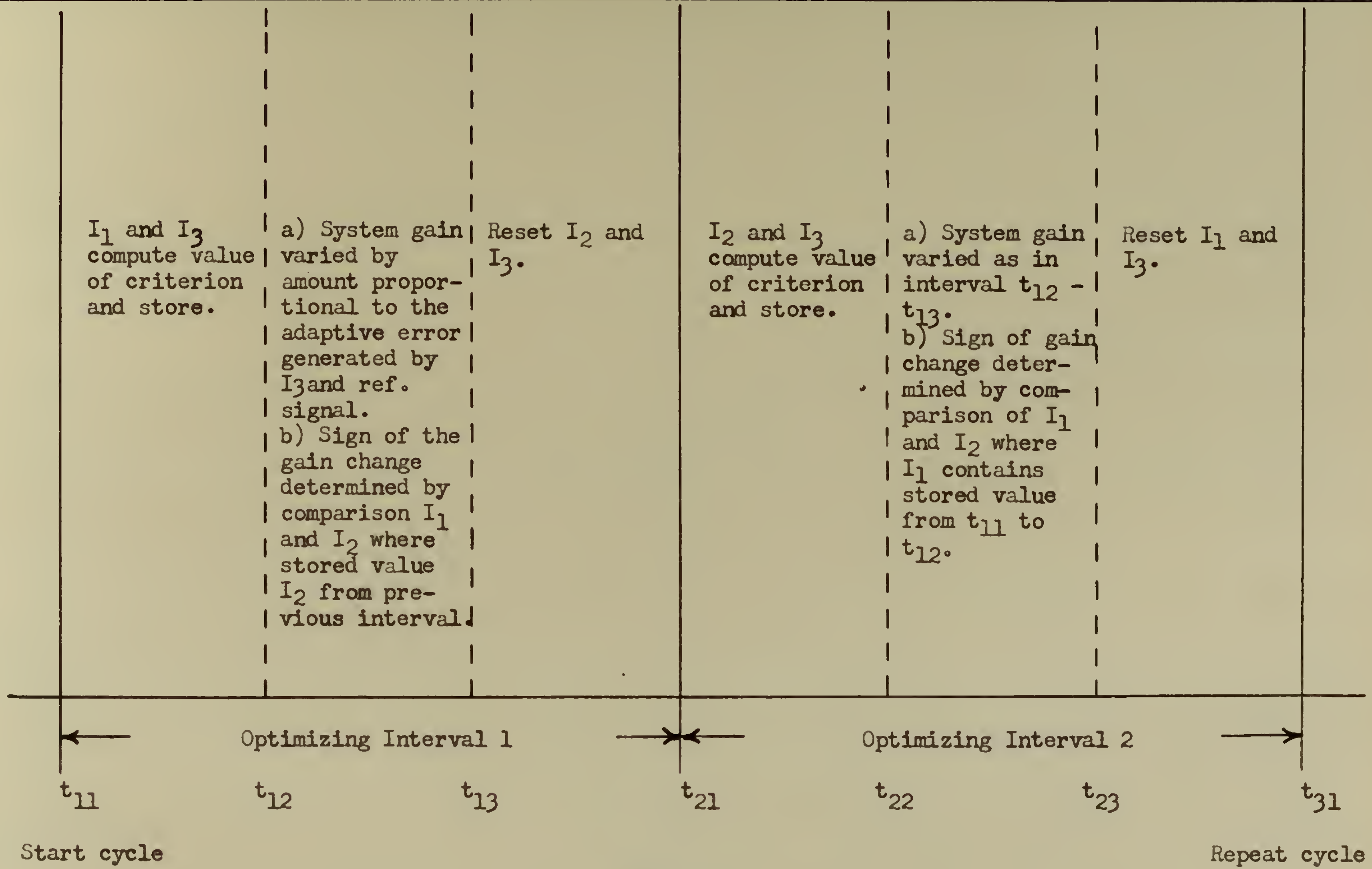

Fig. 40

Time Sequence of the Logic Circuitry

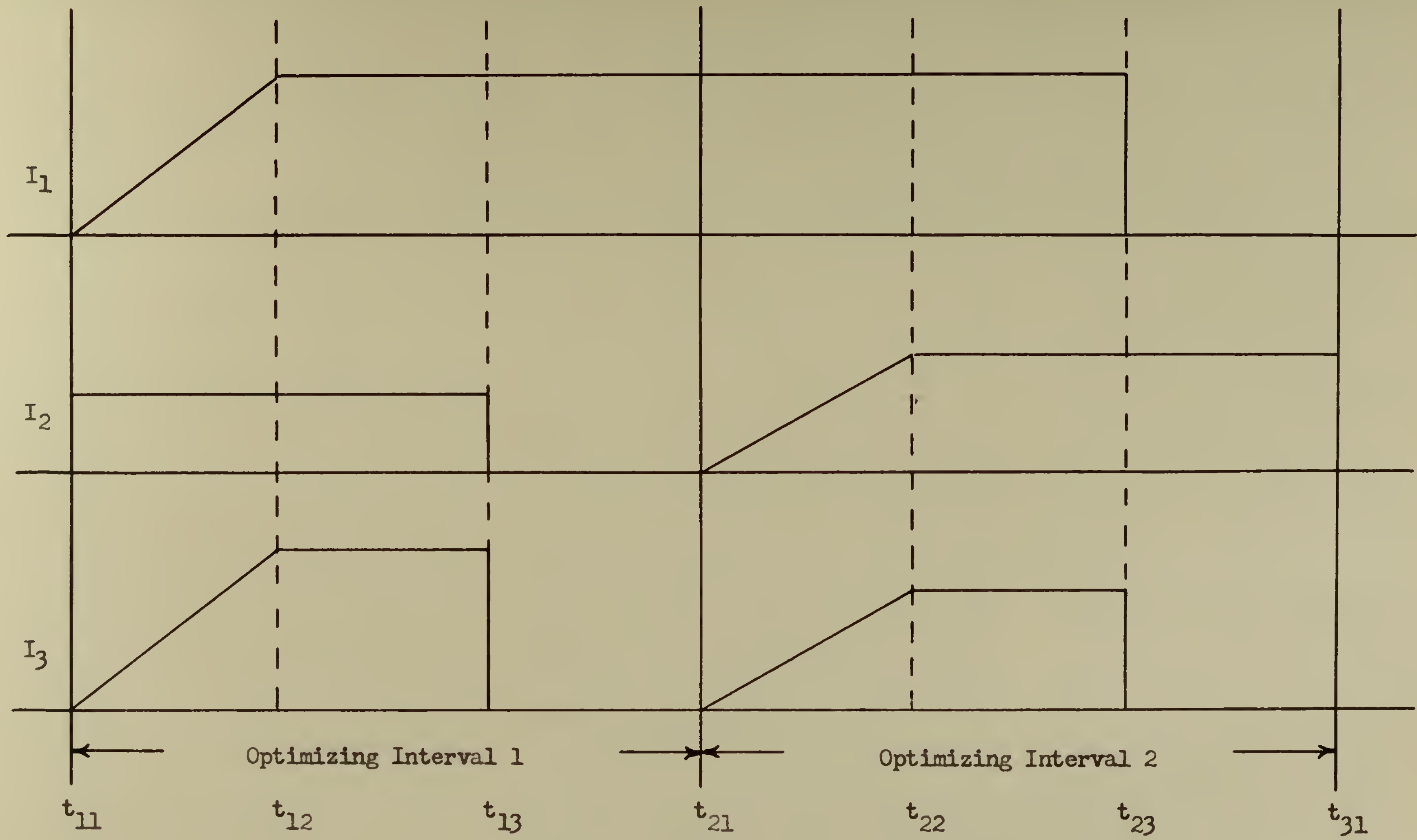

Fig. 41

Typical Integral Sequence of I_1, I_2 and I_3 within an Optimizing Period

in Fig. 42 and as indicated provided a lower rate of gain change in the lower gain regions as a function of angular positioning.

The criterion reference signal was available as a predetermined DC signal of desired polarity or was capable of being generated as some proportional increment of the measured criterion value during the optimizing period. The latter method was desirable, in case it was necessary, to offset noise effects in the system by error derivations from signals which included the same noise effects thereby tending to cancel undesirable inputs.

The selection of the time interval durations within the optimizing period was made on the basis of the stability analysis conducted on the control loop parameters. The primary requirements were that the intervals allow integration over the maximum rate of error change and that sufficient time be allowed for comparison and reset of integrators in the desired sequence. It was determined from root locus plots of desirable lateral responses that a choice of 2 second time interval durations would be adequate since in this period of time all responses had achieved one overshoot and essentially one undershoot. Thus the most sizeable variations in response were measured.

The analysis and basic testing of the adaptive scheme was carried out by analog computer simulation of the three degree of freedom aircraft and integrating units of the adaptive controller. Timer functions were performed by a mechanical stepping switch which actuated portions of the adaptive controller according to the previous discussion in this chapter. In order to provide a certain amount of testing flexibility, provision was made at the computer console to provide a means of altering the magnitude of the rudder pulse disturbance to the control loop and to

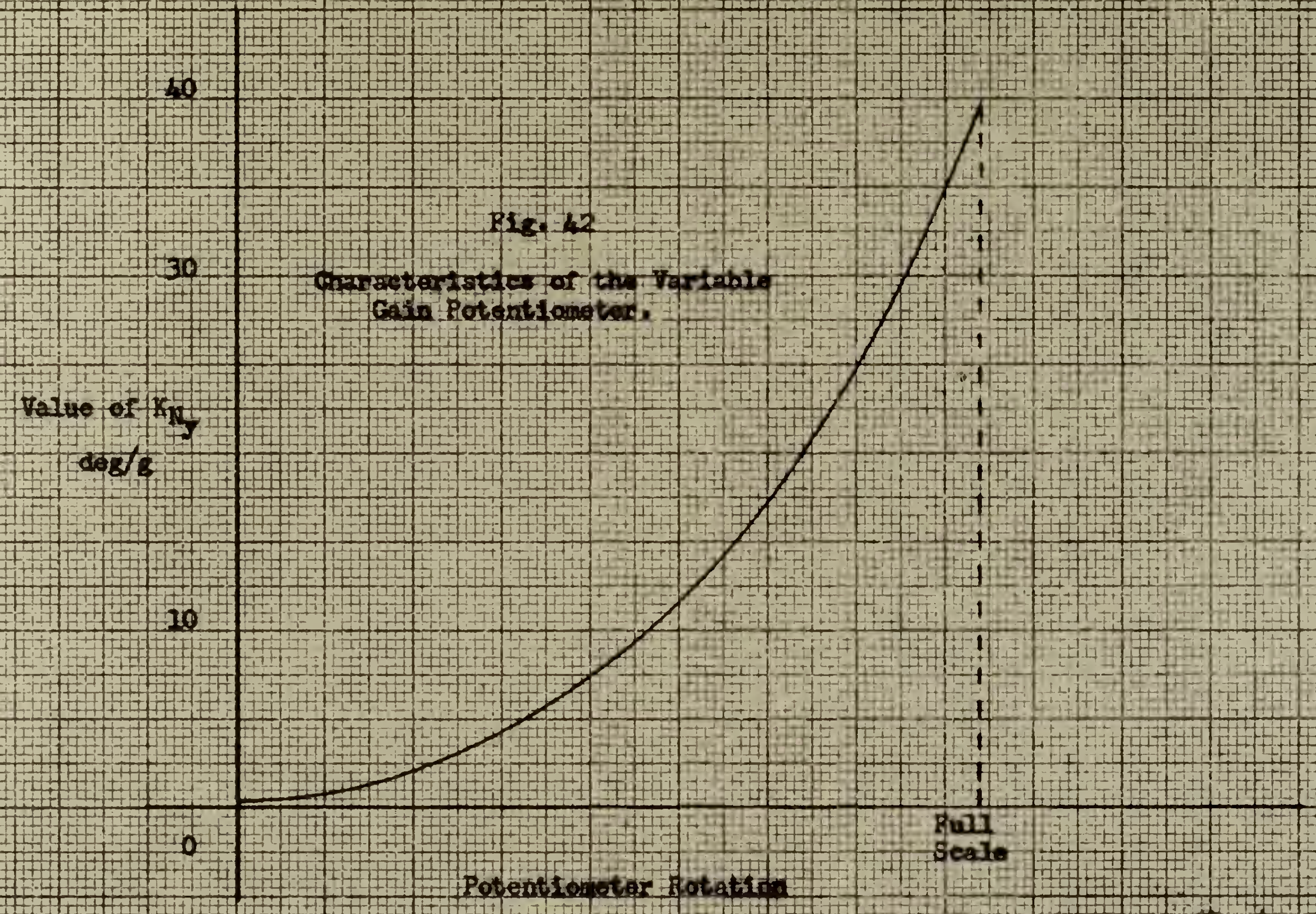

Fig. 42

Characteristics of the Variable Gain Potentiometer.

permit an unrealistic instantaneous switch from one flight condition to another. While unrealistic, this enabled a maximum test of the adaptive controller's ability.

A limited investigation of the adaptive scheme was performed on the analog computer by applying the controller to a simulated second order servomechanism whose maximum damping ratio was adjustable. The sole purpose of this investigation was to permit some check on the characteristics of the adaptive controller as applied to a basic system prior to its application to the more complex aircraft. It was determined that the adaptive logic was correct and that whenever the maximum damping ratio was 0.7 or less, the logic was capable of adjusting the servomechanism gain so that this maximum damping ratio was achieved.

CHAPTER VII

The Analysis of Ny Plus Lead Filter System

As stated previously in Chapter IV, the case of negative feedback using filter 1 was entirely unsatisfactory. Using negative feedback a damping ratio greater than that for K_{Ny} equal to zero could not be obtained. Therefore, negative feedback will be discussed no further for this case.

The case of positive feedback, however, shows satisfactory results possible in several ways. First, it permits adaptive control of the feedback gain. By this it is meant that an improvement in damping ratio can be obtained by varying K_{Ny}. Secondly, the period of the high frequency pair is acceptable, and finally, the range of values for K_{Ny} is reasonable. Table VI contains the estimated optimum values of K_{Ny}, damping ratio, and natural frequency, ω_n, for this scheme. To obtain these values the system was considered to approximate a second order system. The value of K_{Ny} was chosen from the root locus plots such as to give the best damping ratio and still have stable roots of the characteristic equation. From these values one can see that a mean ζ of 0.3 is achievable, excepting condition 3. In other flight conditions, 2 and 6, greater damping ratios can be obtained. The period of the short period response varies from 3.5 seconds to 1.36 seconds.

In figure 6 through 11, and in all subsequent root locus plots, no attempt was made to show the loci emanating from the autopilot actuator and measuring instrument poles. This was possible since the IBM studies showed that these roots moved only a short distance for the range of loop gain employed and the roots could be considered as essentially constant.

Table VII contains a tabulation of several of the significant root loci characteristics for all six flight conditions of this case. Note

TABLE VI

Root Locus Second Order Approximations of Transient Characteristics

N_y Plus Filter 1

Flight Cond.	K_{Ny} deg/g	ζ	ω_n rad/sec
1	20	0.312	1.8
2	5	0.45	2.2
3	0.6	0.22	4.6
4	0.7	0.29	3.8
5	20	0.25	2.0
6	5	0.42	2.4

TABLE VII

Compiled Root Locus Characteristics for

N_y with Filter 1

Flight Cond.	Ref. Fig.	Phugoid Characteristics	Short Period Characteristics	Real Root Characteristics	Unstable Mode	Remarks
1	6	None	Possibly at higher gains short period roots modified by H.F. locus at s= -10.0. Otherwise form dominant osc. pair	H.F. due loci from double pole	H.F. due loci from double pole	Short period locus entered neg. real axis, remained in stable plane
2	7	None	Formed dominant osc. pair. Possible modification by H. F. Locus	None in rt. half plane	H.F. due loci from double pole	Same as for flight cond. 1
3	8	None	Short period roots curve into rt. half plane. Dominance distorted by real root divergence.	System always contains unstable root	Divergent real root	Severe divergent instability prior short period pair entering rt. half plane. Locus from double pole remains in stable plane.
4	9	None	Dominant but curve into rt. half plane at increased gains.	None in rt. half plane	Short period pair	Same general pattern as cond. 3, however, no real root instability. Locus from double pole remains in stable plane, low ζ and high osc. freq.

TABLE VII (Cont.)

Flight Cond.	Ref. Fig.	Phugoid Characteristics	Short Period Characteristics	Real Root Characteristics	Unstable Mode	
5	10	None	Possibly at higher gains short period pair modified by H.F. roots from double pole, otherwise dominant pair.	None in rt. half plane	H.F. due loci from double pole	Same as for cond. 1. The same pattern of loci existed as for cond. 1.
6	11	None	Same as for cond. 5	None in rt. half plane	H.F. locus from double pole	Same as for cond. 5.

that no phugoid oscillations will occur, and only condition 3 has a spiral divergency condition. The system exhibits the possibility in conditions 1, 2, 5, and 6 of a higher frequency mode going unstable first if K_{Ny} is set at too high a value. These are also the conditions which are relatively insensitive to gain changes, especially with regard to the movement of the short period pair of roots. Flight conditions 3 and 4 represent the most sensitive conditions of the system. Here the value of K_{Ny} must be low and closely regulated for stability. The varying degrees of sensitivity to gain changes are due to the airframe transfer functions and must be tolerated.

It may be noted that from these root loci studies an acceptable basis for the proposed adaptive system may be found. A variation of K_{Ny} as flight conditions vary will produce a system which will have a more acceptable response than a fixed gain system. This fact is substantiated by the variance in K_{Ny} necessary to produce acceptable response over the region of flight. If the relative degrees of sensitivity to gain changes does not prove to be a prohibitive factor, this scheme is suitable for adaptive control using only gain changes.

CHAPTER VIII

The Analysis of Ny Plus Lag-Lead Filter System

Negative feedback was used in this scheme with the most success. With positive feedback the short period pair went directly into the right half plane, and therefore will be discussed no further for this case.

The scheme of using negative feedback with filter 2 will be discussed first. This scheme also showed desirable characteristics since it was possible to vary the location of the dominant complex pair by a variation of K_{Ny}. However the frequency associated with this pair of roots was in general lower than those experienced with filter 1 and the gain variation range was considerably larger. At the same time, the damping ratios were generally greater and showed less variation from one flight condition to another at the optimum values of K_{Ny}. The most desirable values of K_{Ny}, ζ, and ω_n are tabulated in Table VIII. These values were obtained by overall stability considerations and the use of a second order approximation as in the case of filter 1. The value of K_{Ny} was again chosen for the best damping ratio consistant with stability. The values for this scheme using filter 3 are not included in Table VIII.

Table VIII shows that a damping ratio of 0.4 or better is a capability at each flight condition, with 0.54 being the maximum. The period of the high frequency pair varies from 4.8 seconds to 2.1 seconds. However, in this scheme, the period is more consistent than with filter 1. In addition there is a capability of providing a constant damping ratio.

Several of the significant characteristics of the root loci for the six flight conditions have been tabulated in Table IX. This tabulation is the case of filter 2 only. The pugoid pair of roots, if oscillatory,

TABLE VIII

Root Locus Second Order Approximations of Transient Characteristics

N_y Plus Filter 2

Flight Cond.	K_{Ny} deg/g	ζ	ω_n rad/sec
1	115	0.44	1.4
2	23	0.54	1.4
3	5	0.515	3.0
4	1.4	0.44	2.3
5	130	0.44	1.3
6	23	0.54	1.5

TABLE IX

Compiled Root Locus Characteristics for

N_y With Filter 2

Flight Cond.	Ref. Fig.	Phugoid Characteristics	Short Period Characteristics	Real Root Characteristics	Unstable Mode	Remarks
1	12	Becomes osc. at high gain, then only briefly at very low freq.	Dominant pair. Moving towards neg. real axis	At high enough gains the phugoid pair moves to positive real axis, otherwise none in rt. half plane	Phugoid pair	Phugoid pair moves quickly through osc. phase and into rt. half plane. H.F. pair from double pole no trouble
2	13	Osc. at very low freq.	Dominant pair, move down to neg. real axis	With high gains possible that phugoid pair move to pos. real axis, otherwise none in rt. half plane	Phugoid pair	Same as for cond. 1
3	14	Osc. at very low freq.	Dominant pair, move to complex pair of zeros well into left half plane	Same as for cond. 2	Phugoid pair	Same as for cond. 1
4	15	Same as for cond. 3	Same as for cond. 2	Same as for cond. 2	Phugoid pair	Same as for cond. 1
5	16	Same as for cond. 3	Same as for cond. 2	Same as for cond. 2	Phugoid pair	Same as for cond. 1
6	17	Same as for cond. 3	Same as for cond. 2	Same as for cond. 2	Phugoid pair	Same as for cond. 1

have a very low frequency and move rapidly into the right half plane once they break out of the negative real axis. This results in these roots generally dictating the limiting values of K_{Ny} for stability. The pair of roots on the loci from the double pole at s equals -10.0 do threaten, in several flight conditions, to go unstable at about the same values of K_{Ny} .

The root loci study using filter 3 to compensate the lateral characteristic Ny was conducted primarily as an investigation of filter perturbations. Again, as with filter 2, positive feedback was unsatisfactory. It failed to allow an increase of damping ratio for an increase in K_{Ny} due to the fact that the short period loci moved immediately into the unstable right half plane. Referring to Figs. 18 through 23, note that the loci followed very closely the characteristic loci for filter 2 at each condition of flight. There are, however, two major differences. First, the loci from the two real poles (at s equal to -8.0 and -10.0) emerges at a value of s between -8.9 and -9.0. Secondly, the roots move along the locus segments very slowly and consequently a change in K_{Ny} produces less movement with filter 3 than it did with filter 2. These loci show that an adaptive control might be feasible but this filter was not considered further in the study because of the following reasons: (1) Higher values of gain could be used to get an acceptable damping ratio but this in itself is not an advantage over filter 2. (2) The higher gains which are necessary to obtain comparable values of damping ratio and natural frequency cause the phugoid pair to become unstable.

Therefore, the scheme using filter 3 showed no great improvement over the advantages of filter 2.

The study of filter 2 and 3 indicates that system characteristics desirous for adaptive control are present. As previously stated, filter

2 is preferable to filter 3. While greater damping ratios are obtainable with filter 2 than those obtained in the scheme using filter 1 the corresponding frequency is lower. The range of K_{Ny} necessary for adaptive control using this scheme is large and might be difficult to obtain satisfactorily by adaptive control. This range extends from a K_{Ny} of 1.4 to 130 deg/g to insure provision for the most acceptable response. Great accuracy and sensitivity in the change of gain by the adaptive controller would be required since the stability limit of several of the flight conditions is close to the most acceptable gain for short period root location. The gain change, from one flight condition to another, must be quickly achieved in order to prevent large gain change requirements from causing temporary instability.

CHAPTER IX

The Analysis of Ny Plus $\dot{r}$ System

The root locus study of this scheme was performed in the manner indicated in Appendix A. Although both positive and negative feedback were developed, the use of positive feedback was found to be unsatisfactory in comparison with the loci using negative feedback. This again was due to the short period pair moving directly into the right half plane. Consequently damping ratios could not be obtained which were greater than those achieved with K_{Ny} equal to zero. Therefore, the case of positive feedback is not further developed.

Since the nature of this particular study was merely to establish feasibility, only the loci of the short period pair was plotted. However, the phugoid pair loci was plotted for one flight condition as a general indication of performance. Compensation was not used, and in general the root loci allow a satisfactory placement of the short period pair of roots without compensation. These root loci plots are a family of loci in the sense that they show the effect of a variation of $K_{\dot{r}}$. For the other flight conditions the phugoid pair either did not become complex or, for the range of gains used, did not become unstable.

By considering that the system could be approximated as a second order system, and choosing a value of $K_{\dot{r}}$ equal to + 0.2 as representative, the values of damping ratio, natural frequency, and K_{Ny} used to position the roots are tabulated in Table X. These values are again chosen so as to give a good damping ratio and still have a stable system. The range of K_{Ny} is about 115 to 1 which might prove difficult to provide by adaptive means. Another complication is that the flight conditions which require the smaller values of K_{Ny} are the most sensitive and cannot tolerate large gains without severe instability. The available frequency associated with

TABLE X

Root Locus Second Order Approximations of Transient Characteristics

N_y with $K_{\dot{r}}$ $\mathring{r}$; $K_{\dot{r}}$ = + 0.2

Flight Cond.	K_{N_y} deg/g	ζ	ω_n rad/sec
1	230	0.63	1.42
2	15	0.465	0.96
3	5.2	0.575	2.18
4	1.7	0.62	1.06
5	230	0.476	1.26
6	11.5	0.656	1.08

the short period roots is low and not too consistent. This short period varies over a range of 6.5 to 2.9 seconds.

Perhaps a brief look at the root locus plots of the individual flight conditions would be in order. In Fig. 24, for flight condition 1, the short period pair displays a varying behavior. With larger negative values of $K_{\dot{r}}$ the loci parallels the imaginary axis toward the origin. However with smaller values of positive $K_{\dot{r}}$ the loci approximately parallels the negative real axis. Finally with $K_{\dot{r}}$ equal to 0.3 the loci starts to curve up quickly. The effect of varying $K_{\dot{r}}$ is quite pronounced in this flight condition.

For flight condition 2, as shown in Fig. 25, the effect of $K_{\dot{r}}$ is much less pronounced. While the loci does show some shift due to varying the value of $K_{\dot{r}}$, in general they proceed downward and nearly parallel to the imaginary axis. Ultimately they proceed down to the negative real axis and become real roots.

Fig. 26, that of condition 3, the same pattern is shown as for condition 2. However, the loci bow out more from the imaginary axis and the effect of $K_{\dot{r}}$ is more pronounced. This flight condition, as always, exhibits sensitiveness of K_{N_y} changes. None of the loci curve away, rather all of them proceed down to the negative real axis.

Flight condition 4, shown in Fig. 27, follows closely the general pattern found in the condition 2 loci. The flight condition is sensitive to gain changes as was to be expected. The effect of $K_{\dot{r}}$ was noticeable but again produced no marked effect.

Flight condition 5, normally a well behaved condition, was again so. This is noted in Fig. 28, where the loci return to the same general pattern as that found for condition 1. The effect of $K_{\dot{r}}$ is shown by the tendency of negative values to pull the loci close to the imaginary axis. Positive

values tended to move the loci out into the left half plane and more closely parallel with the negative real axis. Fig. 29 is a plot of the phugoid pair for flight condition 5, to an expanded scale. This is included to show the general pattern of this pair of roots in all flight conditions as well as its pattern for condition 5. The effect of $K_{\dot{r}}$ is not very large. The roots follow pretty much the same path, or at least form a very narrow pencil. The phugoid pair, if K_{Ny} is large enough to permit it to develop, contribute a very low frequency. It is also seen that the value of gain chosen in Table X must be reduced with positive values of $K_{\dot{r}}$ to have a stable phugoid pair. This reduction would be less than 10% of the tabulated value.

Finally, flight condition 6 is portrayed in Fig. 30. The loci pattern here is somewhere between that of conditions 2, 3, and 4 and that of conditions 1 and 5. The effect of $K_{\dot{r}}$ is noticeable but not pronounced. This loci family is not very sensitive to gain changes and for a range of K_{Ny} values from 10 to 15 exhibits almost constant frequency and only varies damping ratio. The variation of damping ratio is quite small.

In summary it may be noted that from the standpoint of placement of the short period pair and stability, this scheme could provide some basis for self adaptive control. It, of the schemes previously analyzed, provides for the most consistent damping ratio which is closest to 0.7. However, achievement of this damping ratio for all flight conditions requires a wider variation of K_{Ny} than the scheme analyzed in Chapter VII. Also the frequency of the system is low and speed of response would consequently suffer.

Perhaps the most interesting thing about this scheme is the effect of $K_{\dot{r}}$. The value of $K_{\dot{r}}$ has practically no effect on damping ratio for a

fixed value of K_{Ny}. Of course, one must restrict this statement to the more well behaved regions of the loci. The sole effect of $K_{\dot{r}}$ seems to be to vary the frequency of the short period pair. The dominant frequency increases with increasing values of $K_{\dot{r}}$. While it affects the other roots its effect is most marked on the short period pair. This particular characteristic may be noted in flight condition 5, Fig. 28. Here for a fixed value of K_{Ny}, the short period roots for various values of $K_{\dot{r}}$ lie very close to a constant damping locus.

There are two more noticeable characteristics of this scheme. First, the lines of constant K_{Ny} have a negative slope for K_{Ny} values low in the stability range. As K_{Ny} increases toward the maximum stable gain, this slope of the constant K_{Ny} lines becomes positive. This can be most readily seen in Fig. 26. This shows that for higher values of $K_{\dot{r}}$ the movement of the root for a change in K_{Ny} is increased. Second, the effect of varying $K_{\dot{r}}$ has the opposite effect on the phugoid pair as compared to the short period pair. It may be noted in Fig. 29 that, as $K_{\dot{r}}$ increases, the loci tends to collapse on the origin. Thus, the frequency of this pair of roots decreases with increasing $K_{\dot{r}}$.

CHAPTER X

The Analysis of the Yaw Rate System

The origin of the root loci plots for this scheme were obtained using the procedures of Appendix A. While the loci for both negative and positive feedback were computed, the negative case was unsatisfactory. For this case the short period pair did not possess the desired characteristics and there was a real root at all times on the positive real axis which moved rapidly away from the origin with increasing gain. Further discussion of this feedback case is considered unnecessary.

The loci of the control loop with positive feedback are plotted in Fig. 31 through 36 for each of the six flight conditions. The values of damping ratio, natural frequency, and variable loop gain, K_r, are listed in Table XI. This again assumes that the transient oscillation characteristics can be approximated by the second order short period pair. These values were selected for the damping ratio closest to 0.7 with the loop still stable.

Noting the values in Table XI it can be seen that this scheme, as far as the root loci is concerned, is capable of providing desirable oscillating characteristics throughout the region of flight by a variation in K_r . The range of gain is of an order of magnitude readily attainable. A damping ratio of 0.7 is possible with the exception of conditions 3 and 4. For these conditions, the most acceptable damping ratio is lower. For most flight conditions the frequency is low but practically uniform, while the frequency for conditions 3 and 4 is high. An ω_n of 2.0 rad/sec is slow and one of 4.4 rad/sec, as in condition 3, is slightly high. It was noted that the flight condition with higher short period frequencies also exhibited smaller damping ratios. This results in a marked difference in responses over the flight region.

TABLE XI

Root Locus Second Order Approximations of Transient Characteristics

Yaw Rate

Flight Cond.	K_r deg/g	ζ	ω_n rad/sec
1	1.8	0.7	2.0
2	0.9	0.7	1.9
3	0.2	0.35	4.4
4	0.3	0.61	4.1
5	2.0	0.7	2.25
6	0.75	0.7	2.4

Table XII contains the more significant characteristics of the root loci for this case. Here again the stability limit for K_r is set by the phugoid pair of roots, except for condition 3. This condition has a spiral divergency condition at higher gains and this root thus limits the value of K_r which can be accepted.

In summary, this scheme indicates that a variation in control loop gain could provide desirable damping ratios and frequencies from the short period pair. The range of K_r is small and capable of provision by a self adjusting system. However, the frequency of the short period pair is too low in general based on human pilot preferences previously indicated and varies by a factor of 2 within the six flight conditions.

The fixed gain performance of this scheme is quite acceptable. However, the response could be improved with self adjusting control.

The phugoid pair was not troublesome, but as previously stated, one flight condition did exhibit spiral divergence. Further discussion of this scheme and its acceptability is contained in Chapter XI.

TABLE XII

Compiled Root Locus Characteristics for Yaw Rate

Flight Cond.	Ref. Fig.	Phugoid Characteristics	Short Period Characteristics	Real Root Characteristics	Unstable Mode	
1	31	Good damping at 0.5 rad/sec	Dominant pair, osc. for all gains	None in rt. half plane	Phugoid pair	Very good damping on short period pair, and with acceptable phugoid pair
2	32	Will not develop as osc. in this case	Dominant pair, move to neg. real axis. At higher gains broke out of real axis	None in rt. half plane	Phugoid pair	At gain values for desired short period pair phugoid pair has not broken out of real axis
3	33	None	Dominant pair, moved rapidly up to excessively high freq. while not achieving good damping	Root moved into rt. half plane	Real root	Spiral divergence condition existed
4	34	Can develop as osc., low freq.	Dominant pair, moved rapidly up to higher freq. but good damping	None in rt. half plane	Short period pair	Phugoid pair does not break out of real axis for gain values desired Damping on short period pair better than cond. 3
5	35	Develop as osc. Very low freq. and well damped	Same as for cond. 1, very good damping achievable	None in rt. half plane	Phugoid pair	Same pattern as for cond. 1
6	36	Osc., extremely well damped, low freq.	Same as for cond. 1, good damping achievable	None in rt. half plane	Phugoid pair	Same pattern as for cond. 1

CHAPTER XI

Summary of Analysis and Analog Computer Verification

As mentioned in the previous chapters the analysis of the system was specifically directed toward noting the characteristics of damping ratio and frequency associated with the dominant complex roots. The existence of a phugoid pair of roots and, or, real roots close to the origin will certainly modify the transient response. However, in that phase of the analysis it was feasible to consider only the phugoid pair and any real roots from a qualitative standpoint. This allowed the various schemes to be compared from the standpoint of root locations, since the primary desire was to place the short period pair at a desirable location for oscillatory dominance.

The root loci in the analysis took into account, computation, all poles and zeros. However, only one quadrant and the loci most important to the analysis were shown in the figures. Thus the analysis was based on very accurate root loci configurations which enabled good qualitative comparison.

In this analysis, which of course was to outline the requirements and feasibility of self adapting control by gain variation only, the values of gain considered best for each flight condition have been chosen and tabulated in Tables VI, VIII, X, and XI. These were determined on the basis of a damping ratio, closest to 0.7, with the system still stable, and a frequency as close to 3 rad/sec as possible. These were considered to be the ideal response characteristics for the dominant short period pair. A reasonable contribution from a phugoid pair could be tolerated, as could a spirally divergent condition, as long as they were within the control capabilities of the pilot or autopilot.

From basic research and previous experience, there exists the definite possibility that the small value real roots, very close to the origin, will in effect vanigh when the entire autopilot and all its loops are closed.

As previously stated the purpose of this analysis was to choose a scheme which would be the best for self adaptive control. The scheme chosen was N_y with filter 1 compensation. This scheme was chosen since it offered the best combinations of aerodynamic suitability and root location possibilities.

As this rudder control loop normally functions independent of the maneuvering section of the autopilot, this loop plays a dominant role in insuring a coordinated turn for the aircraft. This coordination is mandatory for acceptable maneuvering performance. Since lateral acceleration of the c.g. is one of the best indications of coordinated turning there are no aerodynamic reasons for rejection. With N_y equal to zero the longitudinal axis of the aircraft is parallel to the airstream at all times.

The root locations possible under the adopted scheme were not exactly as desired but represented the most acceptable in overall considerations. The short period pair are not well damped but the damping ratios obtainable are fairly consistent. For flight conditions 1, 2, 5, and 6 the frequency is lower than that desired but this was characteristic of these conditions for all schemes. Also quite important is the fact that no real roots were unstable for the range of desirable K_{Ny} with the exception of condition 3. This condition possesses a real root segment in the right half plane, but short period root location could be effected with the unstable root still close to the origin. For the range of gain necessary for adaptive control the phugoid pair does not become oscillatory in any flight condition.

In flight conditions 1 and 5 the system exhibits relative degrees of insensitivity to gain changes. This is characteristic of these conditions mainly because of the low q involved, while for conditions 3 and 4 the system is very sensitive to gain changes. These are the conditions with a high q. However, N_y plus filter 1, with the mentioned drawbacks, still represents the best scheme and as such was selected for the Adaptive Controller phase of the study.

The next scheme was that of N_y with filters 2 and 3. This scheme was capable of providing a system for self adaptive control. However, in comparison with the N_y plus filter 1 scheme it was less desirable. The range of gain values required was greater, and, even though achievable damping ratios were better, the frequency of the short period pair was lower resulting in a slower response. The phugoid pair held their positions on the negative real axis and then became unstable very quickly with increasing K_{Ny}. Thus the phugoid pair was oscillatory for just a very small range of gains and obviously at a very low frequency. In fact this pair, in general, were the roots which provided the stability limit.

As in the case of the other investigations, flight conditions 3 and 4 were the most sensitive to gain changes. The gains could be kept low enough in each of these conditions to prevent any spiral divergence condition from arising, and while the damping on these short period pair was acceptable their companion frequency was too high.

The perturbation scheme, using filter 3, proved to be even more unsatisfactory. It contributed loci essentially the same as those with filter 2 but they were much more insensitive to gain changes. The response was slower and in general filter 3 was no improvement on filter 2.

The next scheme used in the analysis was N_y with $\dot{r}$. This scheme was also acceptable for self adapting control and required no compensation

filters. The damping ratios are good, the frequency is low, and the range of gains required is large. However, the principal drawback might be the presence of aerodynamic roll cross-coupling effects which enter because of the $\dot{r}$ term, and make coordinated maneuvers somewhat difficult. Since only the feasibility of this control was investigated, no attempt to apply it to the adaptive controller was forthcoming.

The investigation of this scheme does give some information in rather an indirect manner. While the lateral accelerometer is to be placed at or displaced from the aircraft center of gravity, the c.g. may move. The analysis of this scheme shows that such movement affects principally the frequency of the short period pair and not their damping ratio. This may provide some limits on the amount of c.g. shift a system using this scheme can tolerate.

The last response analyzed was that of yaw rate feedback. This scheme gave good damping ratios and a reasonable range of gain required. The frequency of the short period pair, while low, is acceptable. However, the scheme is essentially unacceptable, with an integrated autopilot, from an aerodynamic standpoint. The roll coupling could prevent coordinated turns. As the aircraft banked into a turn the yaw rate introduced might oppose the change in heading. Considering a three degree of freedom aircraft this scheme is quite satisfactory but with a five degree of freedom aircraft it may be unacceptable.

As an integral portion of the study the analog computer was used to verify the predicted performance obtained from the root locus analysis. The three degree aircraft equations of motion as well as all loop transfer equations were mechanized for the analog computer as indicated in Appendix B. Transient characteristics were investigated for all lateral response schemes with the exception of N_y plus $K_r \dot{r}$.

The major reasons for this portion of the analysis were to determine response characteristics not discernible from the root locus analysis. The inputs were 1 deg. rudder deflections (δ_R) and 1 deg. β , or sideslip angle, gusts. The loop gain was varied, as in the root locus approach, to establish the optimum gain for each flight conditions. In addition the value of gain at the stability limit was obtained. These values agreed rather well with those obtained in the root locus study.

The transient characteristics, as determined from the analog study, are tabulated in Tables XIII, XIV, and XV. Comparing Table XI with Table XIII for the case of r feedback it may be noted that for flight condition 3 the second order approximation is quite good. However, for the other flight conditions particularly damping ratio correlation is poor. This is due, mainly, to distortion of the transient response due to real root influence. This fact can be illustrated by referring to Fig. 43 which illustrates the most acceptable r responses obtained at each flight condition. Since the real root distortion of the basic second order response was present in every flight condition, the existence of errors in determination of damping ratios is probable. Therefore, the characteristic response is not approximated by a second order system for the flight conditions.

For the N_y with filter 2 scheme the second order approximation was not totally free of distortion. The transient response data, for the most acceptable N_y response as shown in Fig. 44, did not conform to the estimated values of damping ratio and frequency. Again this was the result of real root influence on the transient characteristics. Resultant distortion of the oscillatory response of the short period roots made data correlation impossible or inadequate.

TABLE XIII

Analog Computer Second Order Approximations of Transient Characteristics

Yaw Rate Feedback (No Filter)

Inputs 1 deg δ_R or 1 deg β Gust

Flight	K_r	ζ		f(cps)		T(sec)	
Cond.	deg/deg/sec	Est.	Actual	Est.	Actual	Est.	Actual
1	0.2		0.27		0.244		4.1
	0.4		0.44		0.244		4.1
	0.6		0.17		0.263		3.8
	0.8		0.18		0.25		4.0
	1.0		0.18		0.263		3.8
	1.5	0.62	0.23	0.302	0.25	3.32	4.0
	2.0		0.25		0.228		4.4
2	0.5		0.42		0.278		3.6
	0.75		0.44		0.286		3.5
	1.0	0.7	0.5	0.286	0.27	3.48	3.7
	1.25		0.6		0.27		3.7
	1.5		.42		---		---
	2.0		0.4		---		---
3	0.1		0.47		0.588		1.7
	0.15		0.31		0.588		1.7
	0.2	0.35	0.42	0.7	0.625	1.43	1.6
	0.25		0.405		0.588		1.7
	0.3		0.42		0.588		1.7
	0.35		0.5		0.588		1.7

TABLE XIII (Cont.)

Flight Cond.	K_r deg/deg/sec	ζ Est.	ζ Actual	f(cps) Est.	f(cps) Actual	T(sec) Est.	T(sec) Actual
4	0.2	0.515	0.6	0.475	0.77	2.1	1.3
	0.5		0.6		---		---
	0.8		---		H.F. osc @ 2 cps		---
5	0.5		0.28		0.27		3.7
	1.0		0.21		0.278		3.6
	1.5	0.52	0.28	0.318	0.278	3.14	3.6
6	0-1	Response too distorted to provide good estimate on ζ and f. Damping comparable to 1 overshoot and low undershoot.					

TABLE XIV

Analog Computer Second Order Approximations of Transient Characteristics

N_y Plus Filter 2

Inputs 1 deg δ_R or 1 deg β Gusts

Flight Cond.	K_{Ny} deg/g	ζ Est.	ζ Actual	f (cps) Est.	f (cps) Actual	T (sec) Est.	T (sec) Actual
1	10		0.32		0.256		3.9
	20		0.32		0.25		4.0
	30		0.42		0.25		4.0
	40		0.475		0.244		4.1
	50		0.475		0.244		4.1
	60		0.54		0.227		4.4
	70		0.54		0.222		4.5
	80		0.7		0.22		4.5
	90	0.4	0.7	0.222	0.22	4.5	4.5
2	1.5		0.2		0.286		3.5
	2.0		0.2		0.286		3.5
	2.5		0.18		0.286		3.5
	3.0		0.2		0.294		3.4
	4.0		0.195		0.294		3.4
	8.0		0.21		0.303		3.3
	12		0.22		0.333		3.0
	15		0.25		0.303		3.3
	20		0.24		0.303		3.3
	23	0.44	---	0.222	---	4.5	---

TABLE XIV (Cont.)

Flight Cond.	K_{Ny} deg/g	ζ Est.	ζ Actual	f (cps) Est.	f (cps) Actual	T (sec) Est.	T (sec) Actual
3	1.5		0.23		0.5		2.0
	1.75		0.27		0.526		1.9
	2.0		0.285		0.541		1.85
	2.25		0.285		0.541		1.85
	2.5	0.31	0.32	0.51	0.5	1.96	2.0
4	0.3		0.185		0.345		2.9
	0.5		0.23		0.357		2.8
	0.7		0.32		0.333		3.0
	0.9		0.34		0.313		3.2
	1.4	0.44		0.365		2.74	
	1.5	Diverges					
5	15		0.1		0.266		3.9
	20		0.09		0.25		4.0
	25		0.14		0.25		4.0
	30		0.12		0.25		4.0
	35		0.14		0.25		4.0
	40		0.12		0.25		4.0
	45		0.14		0.238		4.2
	50	0.154	0.12	0.27	0.238	3.7	4.2
6	0.3		0.02		0.27		3.7
	0.5		0.06		0.263		3.8
	0.7		0.02		0.27		3.7
	0.9		0.02		0.27		3.7
	1.1		0.02		0.27		3.7
	1.3	0.11	0.02	0.27	0.278	3.7	3.6

TABLE XV

Analog Computer Second Order Approximations of Transients Characteristics

N_y Plus Filter 1

Inputs 1 deg δ_R or 1 deg β Gust (High Freq. Values in Parens)

Flight Cond.	K_{Ny} deg/g	ζ Est.	ζ Actual	f (cps) Est.	f (cps) Actual	T (sec) Est.	T (sec) Actual
1	10		0.23		0.25		4.0
	15		0.27		0.278		3.6
	20	0.312	0.37	0.288	0.263	3.48	3.8
	25		0.5		0.286 (1.67)		3.5 (0.6)
	30		0.5		0.2 (1.43)		5.0 (0.7)
	37		0.6 (0.3)		0.278 (1.43)		3.6 (0.7)
	40		0.6 (0.3)		0.333 (1.43)		3.0 (0.7)
	45		--- (0.2)		--- (1.33)		--- (0.75)
	50		--- (0.14)		--- (1.43)		--- (0.7)
	55		--- (0.1)		--- (1.33)		--- (0.75)
	60		--- (0.085)		--- (1.33)		--- (0.75)
	65		--- (0.02)		--- (1.25)		--- (0.8)

TABLE XV (Cont.)

Flight Cond.	K_{N_y} deg/g	ζ Est.	ζ Actual	f (cps) Est.	f (cps) Actual	T (sec) Est.	T (sec) Actual
2	1.6		0.17		0.286		3.5
	2.0		0.185		0.286		3.5
	2.5		0.18		0.286		3.5
	3.0		0.21		0.29		3.45
	3.5		0.215		0.294		3.4
	4.0		0.21		0.303		3.3
	4.5		0.22		0.294		3.4
	5.0	0.45	0.24	0.35	0.294	2.85	3.4
	5.5		0.24		0.294		3.4
3	0.5	0.22	0.265	0.73	0.625	1.37	1.6
	0.75		0.33		0.77		1.3
	1.0		0.35		0.91		1.1
	1.25		0.225		1.11		0.9
	1.5		0.0		1.25		0.8
4	0.3		0.275		0.385		2.6
	0.5		0.295		0.435		2.3
	0.6		0.4		0.455		2.25
	0.7	0.29	0.4	0.605	0.476	1.65	2.1
	0.8		0.4		0.5		2.0
	0.9		0.47		0.526		1.9
	1.0		0.62		0.466		2.15
	1.72		0.0		1.22		0.82

TABLE XV (Cont.)

Flight Cond.	K_{Ny} deg/g	ζ Est.	ζ Actual	f (cps) Est.	f (cps) Actual	T (sec) Est.	T (sec) Actual
5	10		0.13		0.278		3.6
	15		0.14		0.278		3.6
	20	0.25	0.14	0.32	0.278	3.12	3.6
	25		0.17		0.286		3.5
	30		0.21		0.286		3.5
	35		0.3		0.278 (1.33)		3.6 (0.75)
	40		0.3		--- (1.33)		--- (0.75)
	45		(0.05)		(1.33)		(0.75)
6	2.0		0.17		0.308		3.25
	3.0		0.185		0.333		3.0
	4.0		0.24		0.333		3.0
	5.0	0.42	0.29	0.382	0.345	2.62	2.9
	6.0		0.29		0.364		2.75
	7.0		0.4		0.4		2.5
	8.0		0.5 (0.15)		--- (1.33)		--- (0.75)
	9.0		--- (0.05)		--- (1.25)		--- (0.8)

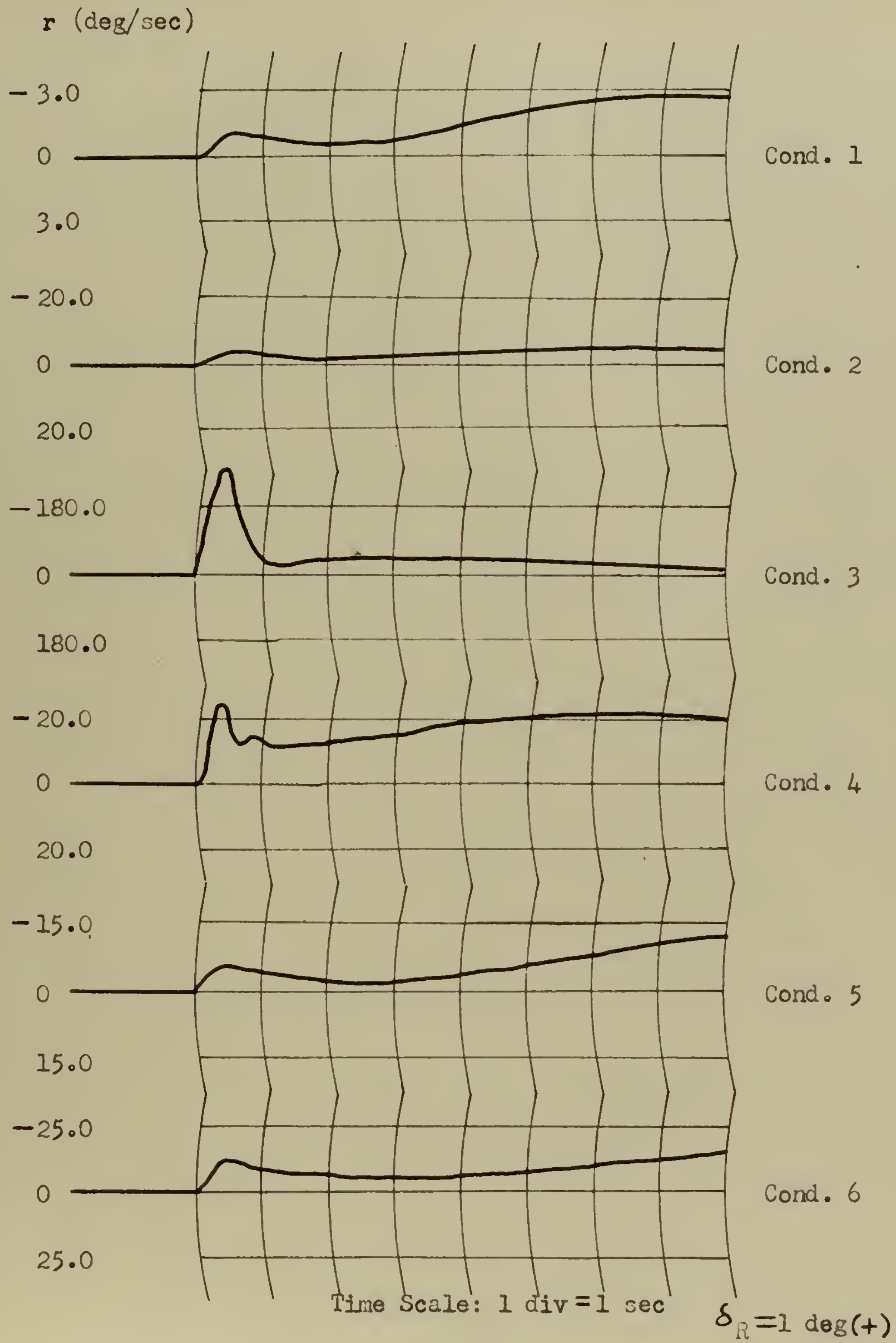

Fig. 43

Airframe Response, r, to Command Rudder Input at Optimum Loop Gain for Each Flight Condition.

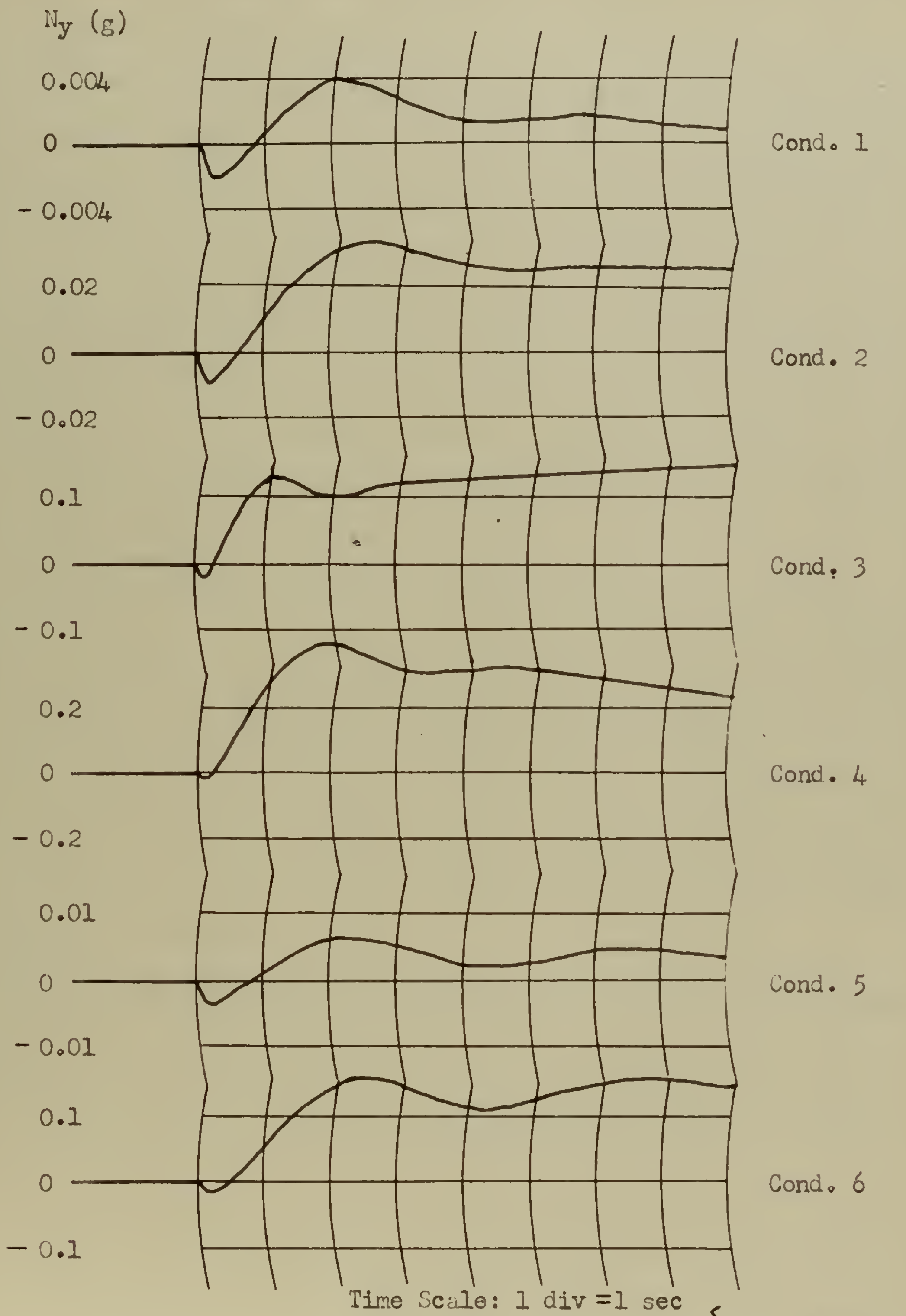

Fig. 44

Airframe Response, N_y, to Command Rudder Input with Filter 2 Compensation and at Optimum Loop Gain for Each Flight Condition.

In the final scheme, N_y with filter 1, studied on the analog computer the N_y response obtained was closer to that predicted from the root locus. While the second order approximation was not exact it was quite close for all six flight conditions. This may be noted from a comparison of the data in Tables VI and XV. Fig. 45 contains the characteristic response of N_y, at the most acceptable values of K_{Ny}, for each flight condition. In general, the damping was less and the frequency lower than the second order root locus predictions. However, the higher frequency oscillation discussed in Chapter VII does make itself evident. This data is included in Table VII. The lower damping ratio and frequency represent the contributions from roots in regions adjacent to the origin.

It must be concluded that the analog study definitely verified the choice of the N_y with filter 1 scheme for adaptive control. The oscillatory nature of the response essentially permitted a more rapid control of damping ratio as a function of variable loop gain. The real root distortion of the dominant complex roots in the case of filter 2 and in the use of r as a lateral response were detrimental in provision of a rapid indication of varying $\mathcal{S}$.

Furthermore, this analysis demonstrated the feasibility of Adaptive Control of this system over its flight regime, using gain changes only, and indicated that this was possible with several schemes of feedback.

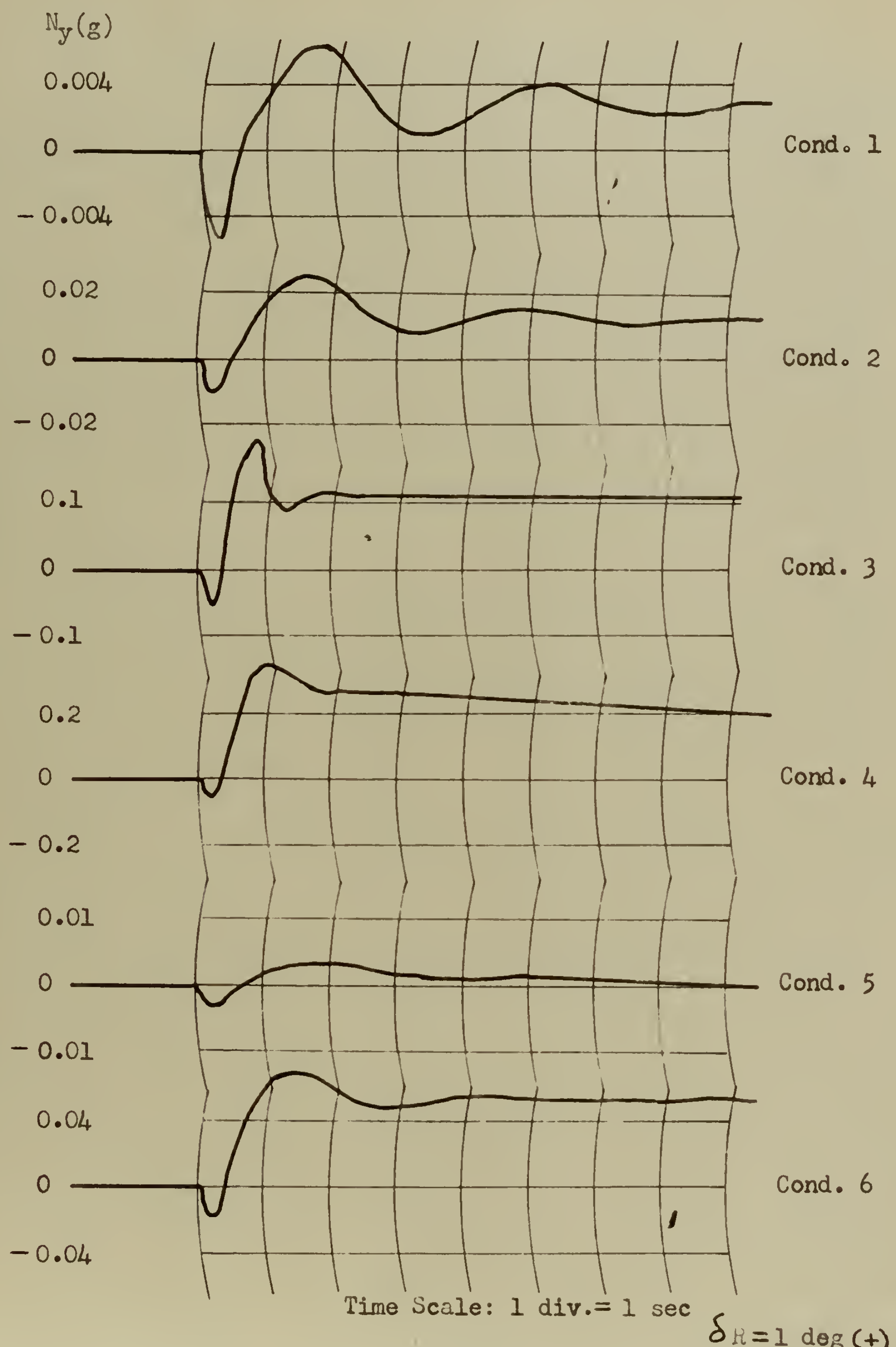

Fig. 45

Airframe Response, N_y, to Command Rudder Input with Filter 1 Compensation and at Optimum Loop Gain for Each Flight Condition.

Chapter XII

Analysis of the Self Adaptive Scheme

On the basis of the stability analysis conducted on the aircraft, the lateral airframe response corresponding to N_y with lead filter compensation, filter 1, was selected as the response to be controlled. Values of K_{Ny} were chosen as those variable gain values which permitted the criterion value to minimize. In terms of damping ratios, this corresponds to a ζ equal to 0.7 or if not obtainable, ζ equal to a maximum value. Table XVI contains the values of K_{Ny} optimum and ζ corresponding to K_{Ny} optimum determined by results of the analog computer stability study.

Input disturbance to the airframe was supplied by a short duration pulse input inserted by signal generator into the loop at the input side of the variable gain pot. The pulse was below the pilot's threshold value of 0.05 g lateral acceleration.

Results of the adaptive scheme as applied to the selected lateral response are contained in Table XVII. These data are basically arranged with regard to flight condition and may be discussed in this manner.

The landing condition, condition 1, was tested and found to be extremely sluggish in adaptive corrective response. While the optimum gain selected from the analysis should have been K_{Ny} equal to 25.0 deg/g, the system barely corrected from the initial K_{Ny} of 0.5 in a period of two minutes. More success was obtained by letting K_{Ny} equal 10 initially. In this case, the adaptation was more satisfactory but a K_{Ny} equal to 30.0 deg/g was selected by the scheme. Finally, an initial K_{Ny} of 40.0 deg/g was incorporated and adaptation served to produce no change in the variable loop

TABLE XVI

Values of K_{N_y} for Desired Optimum and Corresponding ζ

Flight Cond.	K_{N_y} (optimum) deg/g	ζ
1	25.0	0.5
2	5.5	0.24
3	1.0	0.35
4	0.9	0.47
5	30.0	0.21
6	7.0	0.4

TABLE XVII

Compiled Data on Test of Adaptive Controller, N_y Plus Filter 1

Flight Cond.	Most Adequate Reference Signal	K_{Ny} Sought	Max. N_y By Airframe	Remarks
1	Appeared to be insensitive to polarity of reference signal.	Barely moved from 0.5 for 0.5 as initial value. With initial value of 10.0 adapted to 30.0. For initial value of 40.0 no gain correction.	Less than 0.05g	System very sluggish and adaptation, when occurring was too slow. Was able to recover from initial unstable K_{Ny}.
2	Positive	Always sought value of K_{Ny} between 3.0 and 6.0.	About 0.02 g	Adaptation, while faster than in cond. 1, was still slow. Was able to recover from initial unstable K_{Ny}.
3	Positive	Always sought 0.5 to 0.6 with initial K_{Ny} of 0.5. Sought 1.0 with return from divergent instability.	About 0.02g with N_y(avg) of about 0.01g.	Capable of recovering from real root instability in 5 sec. Adaptation faster than in previous flight conditions.

TABLE XVII (Cont.)

Flight Cond.	Most Adequate Reference Signal	K_{Ny} Sought	Max. N_y by Airframe	Remarks
4	Positive and zero	Sought to remain at K_{Ny} of 0.5 when imposed as initial value. After some time hunted about range of K_{Ny} from 0.5 to 0.9.	About 0.05g	Adaptation rapid accompanied by hunting about value sought Attempts made to inspect ability to recover from unstable K_{Ny} were not valid. Computer overloads were an almost instantaneous result with therefore no chance for the system to recover.
5	Positive and zero	Appeared to correct only slightly from initial values of K_{Ny}	About 0.02g	System slow and appeared sluggish in adapting. Did not test ability to recover from initial unstable K_{Ny}.
6	Positive and zero	Sought 1.0 to 2.0 with initial value of 0.5. With initial value of 3.0, sought 6.0. With increased disturbance signal sought 3.0 from an initial value of 0.5 and 6.0 from an initial value of 5.0	About 0.02g	Adaptation faster than conditions 1, 2, and 5. Instability tests were not made for the reasons explained under condition 4.

gain. This testing was carried out with zero reference signal. Testing at $\pm$ 0.4 volt reference signal indicated that the flight condition was essentially insensitive to the polerity of the reference but did tend to adapt very slowly for the + 0.4 volt reference. In all cases tested, the maximum lateral acceleration was well within the threshold of the pilot. The system recovered when purposely given an unstable loop gain as an initial value. The final K_{Ny} sought by the mechanism was varied about the optimum value selected from the root locus plots.

Flight condition 2 exhibited satisfactory tendencies while using a + 0.4 volt reference signal. Adaptation for zero or negative referencing was either prohibitively slow or unsatisfactory. Under the positive reference signal, the K_{Ny} sought by the system was at all times between the values of 3.0 to 6.0 deg/g. This compares with an optimum K_{Ny} of 5.5 deg/g. At K_{Ny} equal to 0.5 initially, adaptation was slow. The system was able to seek the optimum gain region with conditions of stable and unstable loop gains initially imposed. An investigation of the behavior under increased pulse disturbance resulted in the system seeking the 3.0 value. The maximum lateral acceleration experienced in the stable testing above was 0.02 g.

Flight condition 3 as with the previous flight conditions performed most satisfactorily with a positive reference value. With negative reference applied, the loop gain correction tended to be applied in the wrong direction while, with a zero reference, corrective action approached that of the positive reference. The maximum stable N_y experienced was 0.02 g with an increased disturbance amplitude. The average N_y was 0.01 g. Since this flight condition was the only one which was divergently unstable, it

furnishes the only information on stable recovery from this condition. The system was capable of adjusting from divergent instability to a K_{Ny} equal to 1.0 deg/g in 5 sec. With the positive reference signal, the system sought to adapt the variable loop gain to a value of K_{Ny} from 0.5 to 0.6 deg/g.

The most sensitive flight condition, condition 4, adapted quickly, usually after a maximum of two optimizing periods. In this case the maximum N_y observed during adaption was the pilot threshold, 0.05 g. Both positive and zero reference signals provided the most satisfactory response. The system, with K_{Ny} initially 0.5 deg/g, tended to remain at this value. After an excessive amount of time the selected gain sought to increase to a greater value. This caused a decrease in ζ and the resultant immediate adaptation to a K_{Ny} of 0.5 to 0.9 deg/g as compared to the optimum of 0.9 deg/g. Since this lower end value also constitutes the residual loop variable gain there is no data to support the tendency of the adaptive scheme to remain at this value rather than decrease further. As a result of the airframe sensitivity at this flight condition, there was a noticeable tendency for the system to attempt to hunt or drift about values of K_{Ny} to which it adapted. This tendency was actually noticed to produce a more positive adapting action since the system tried to continuously correct rather than sluggishly allow considerable error to accumulate.

Flight condition 5, a sluggish flight condition, exhibited satisfactory tendencies with positive or zero reference signals applied. Divergent or unstable tendencies were not present. The system was capable of recovering from near unstable or very low ζ and high frequency conditions. Since the

maximum gain possible with the variable pot was 40.5 deg/g it was not possible to drive the aircraft unstable and inspect recovery tendencies. For K_{Ny} initially equal to 0.5 deg/g the system should have adapted to the optimum value of 30.0 deg/g. Due to the relative insensitive aircraft response to the input disturbance however, very little corrective tendency was noted. After a period of 7 minutes the variable gain had adjusted from 0.5 to only 0.7 deg/g. An initial K_{Ny} of 20.0, which coincided with the optimum gain value, was imposed upon the system. The controller did not attempt to adapt from this position. Data is not conclusive enough to conclude that the scheme sensed the optimum condition since in the sluggish condition of flight the value of $\mathcal{J}$ varies imperceptibly with a small variance in K_{Ny} . Under the stable conditions of test and maximum N_y achieved was 0.02g.

Finally, condition 6 with an optimum K_{Ny} of 5.0 deg/g exhibited fairly satisfactory tendencies at reference signals equal to zero and positive 0.4 volts. However, the K_{Ny} sought was in the region 1.0 to 2.0 deg/g. With an initial K_{Ny} of 3.0 the tendency of the system was to select a variable gain value of 6.0 deg/g. Increasing the disturbance magnitude with the same initial conditions tended to cause a selection of variable gain in the region of 3.0 deg/g with hunting about this value. Imposing an initial condition of 5.0 deg/g with the increased disturbance resulted in hunting about the value K_{Ny} equal to 6.0 deg/g. The maximum Ny achieved was no greater than 0.02g during this testing. As in condition 4 tests, it was noticed that adaption was relatively faster since airframe response was generally more sensitive to a disturbance.

Figs. 46 through 51 contain the plots of $\int_{0}^{2\ \text{sec.}} |\text{error}|\ dt$ for 1 deg. δ_R versus variable gain K_{Ny}, for each flight condition tested where $|\text{error}|$ equals $|N_y$ plus filter 1$|$ and is measured at the output of filter 1 to take advantage of a larger signal. Comparison of these figures to Fig. 38 indicate that the second order variance was not reasonably attained. The most resemblance was attained in those cases where the real root contributions were less distorting to the short period characteristics. It may be noted that minimums occur in each error function in the general vicinity of the predicted optimum K_{Ny}. Furthermore, several of the error integrals display minimums at values other than at the predicted optimum K_{Ny} indicated in Table XIII. Fig. 46 indicates a minimum in the vicinity of K_{Ny} equal to 22.5 deg/g while there are also exhibited "flats" or negligible change in the error integral on either side of the minimum. Fig. 47 for flight condition 2 indicates a minimum at about K_{Ny} equal to 5.0 deg/g. This coincides with the predicted minimum. Condition 3 shown in Fig. 48 indicates a definite minimum at K_{Ny} equal to 1.25 deg/g but a region of maximum error at K_{Ny} equal to 0.7 deg/g the predicted optimum value. For all intents and purposes the function exhibits a minimum at K_{Ny} equal to 0.5 deg/g, the residual pot gain, should the system attempt to initially adapt from this value. Fig. 49, the most critical flight condition, exhibited a satisfactory variance of the error function with varying loop gain. The curve, at all gain values, slopes so that increases or decreases of gain from the minimum serve to always increase the criterion value. Fig. 50, condition 5, indicates that the error exhibits flat regions from 0.5 to 35.0 deg/g. This flat region coincides with the minimum values of the integral. The

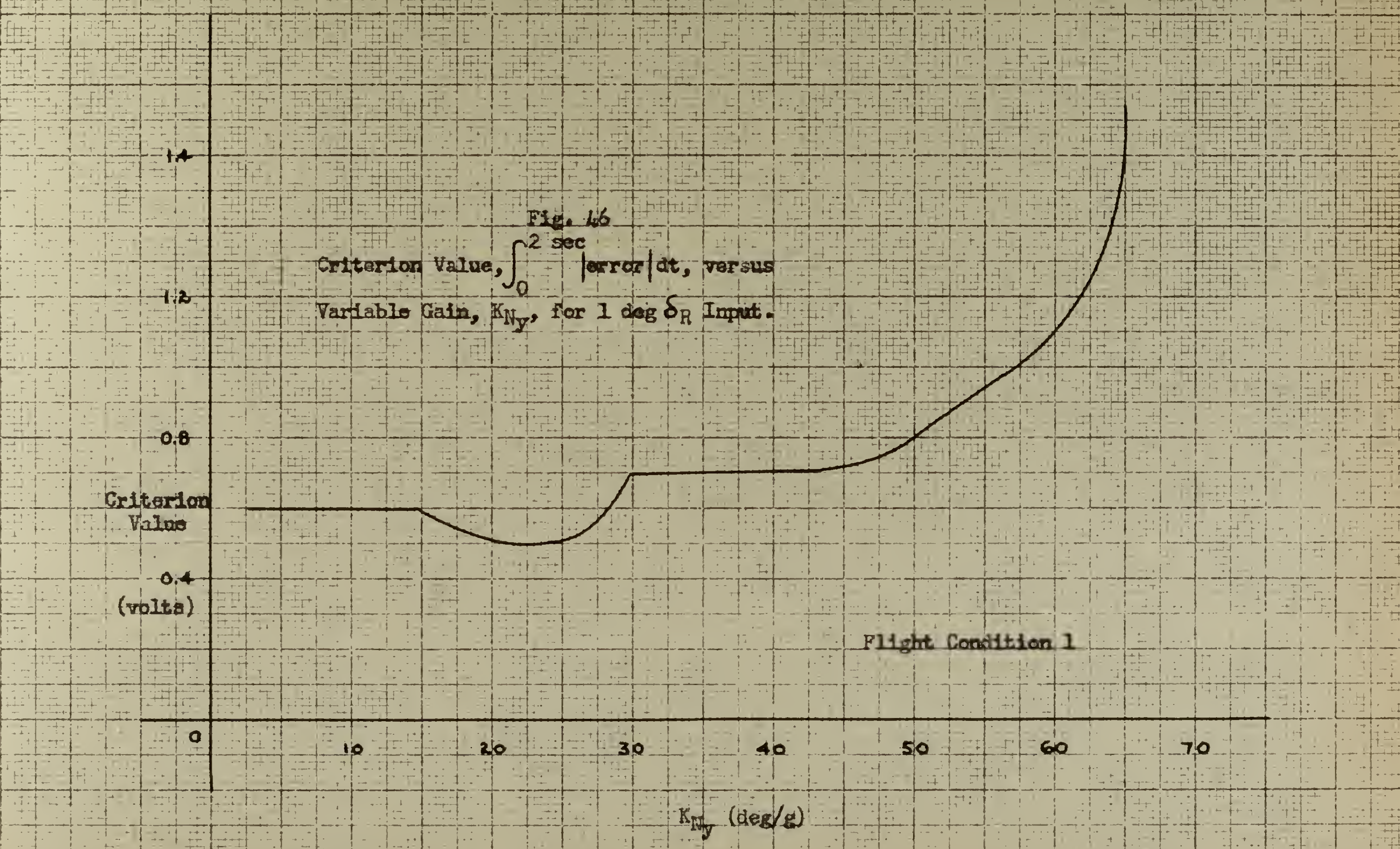

Fig. 46

Criterion Value, $\int_0^{2\,\text{sec}} |\text{error}|\,dt$, versus Variable Gain, K_{N_y}, for 1 deg δ_R Input.

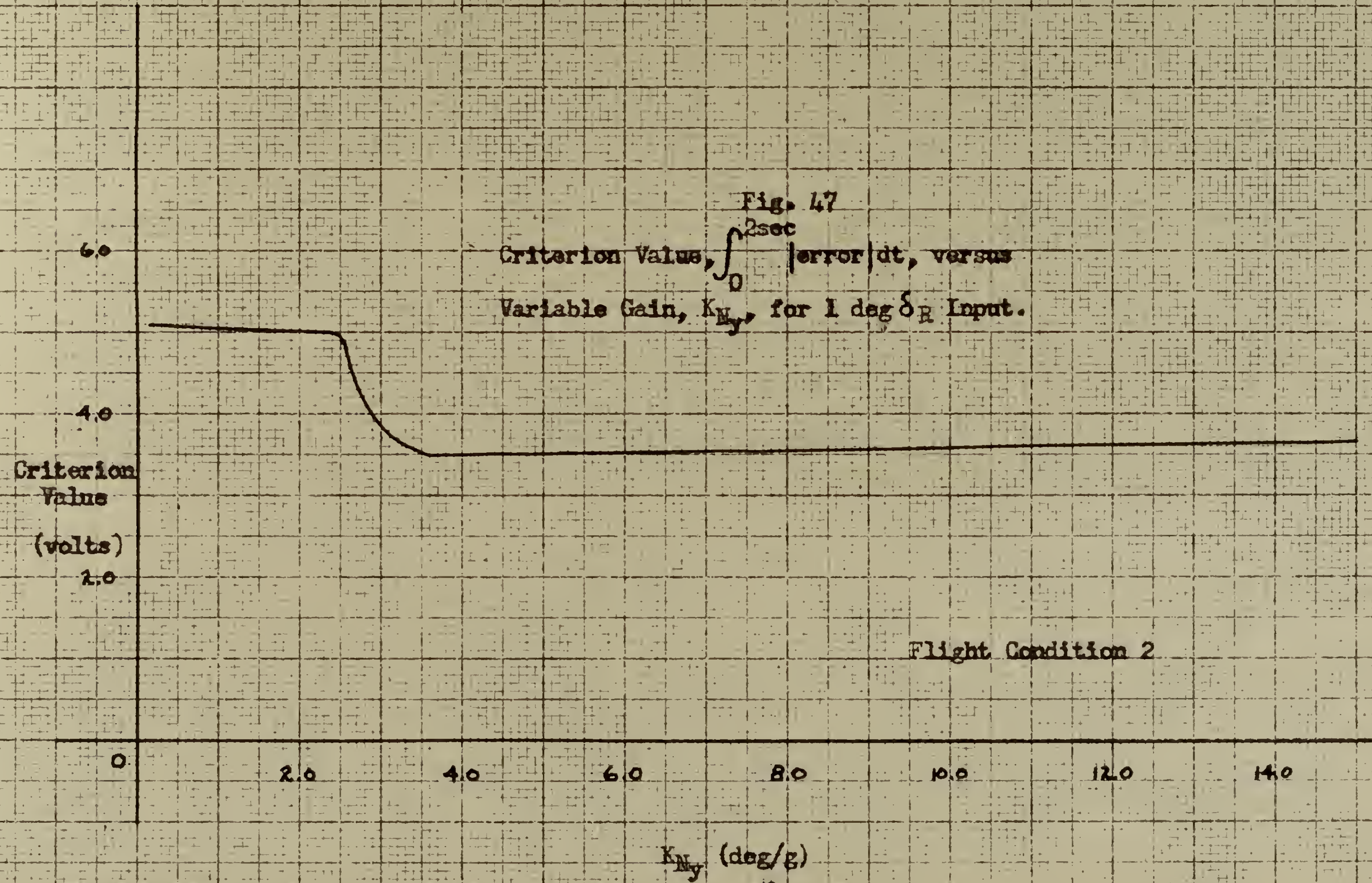

Fig. 47

Criterion Value, $\int_0^{2sec} |error|\,dt$, versus Variable Gain, K_{N_y}, for 1 deg δ_R Input.

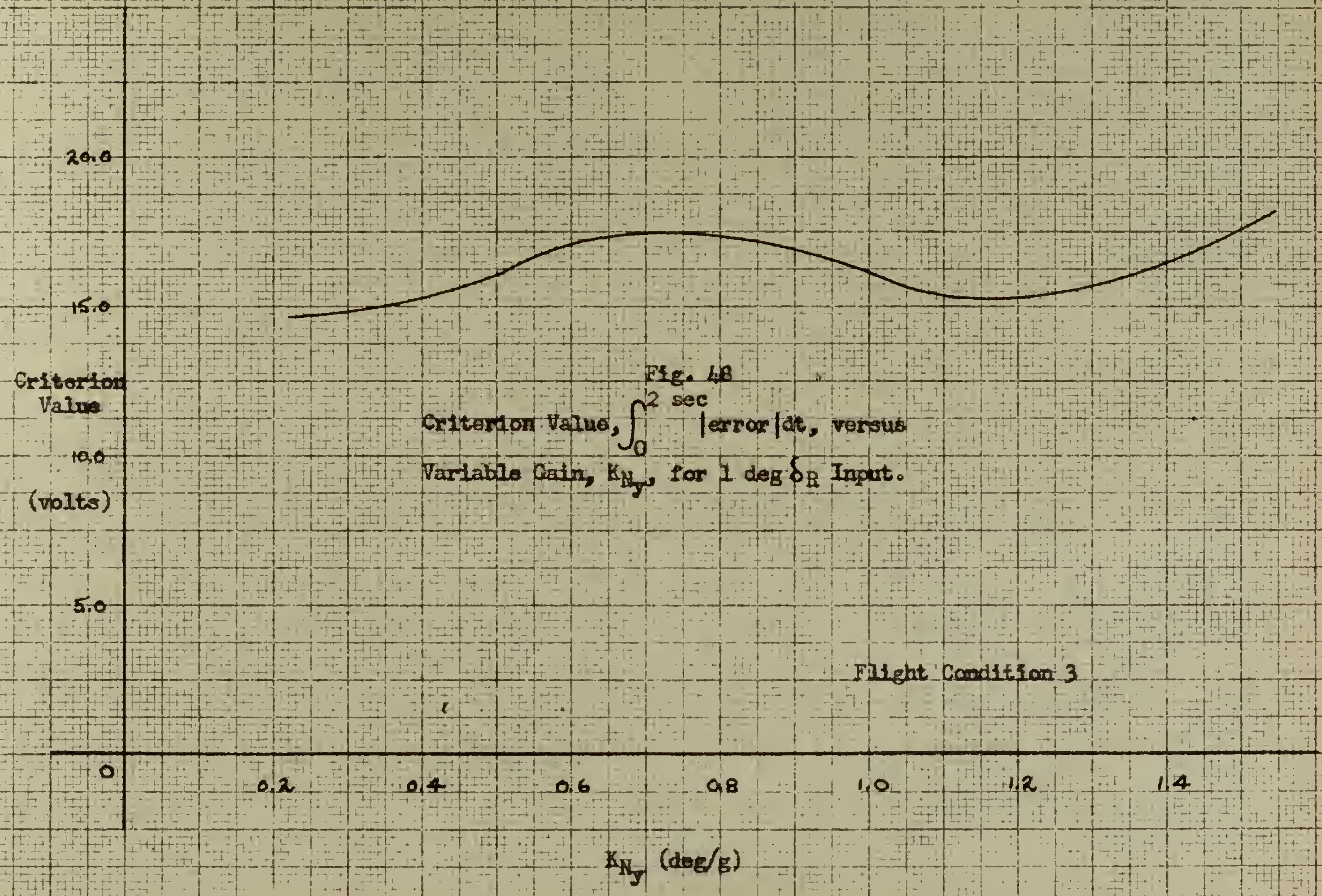

Fig. 48

Criterion Value, $\int_0^{2\ \text{sec}} |\text{error}|\, dt$, versus Variable Gain, K_{N_y}, for 1 deg δ_R Input.

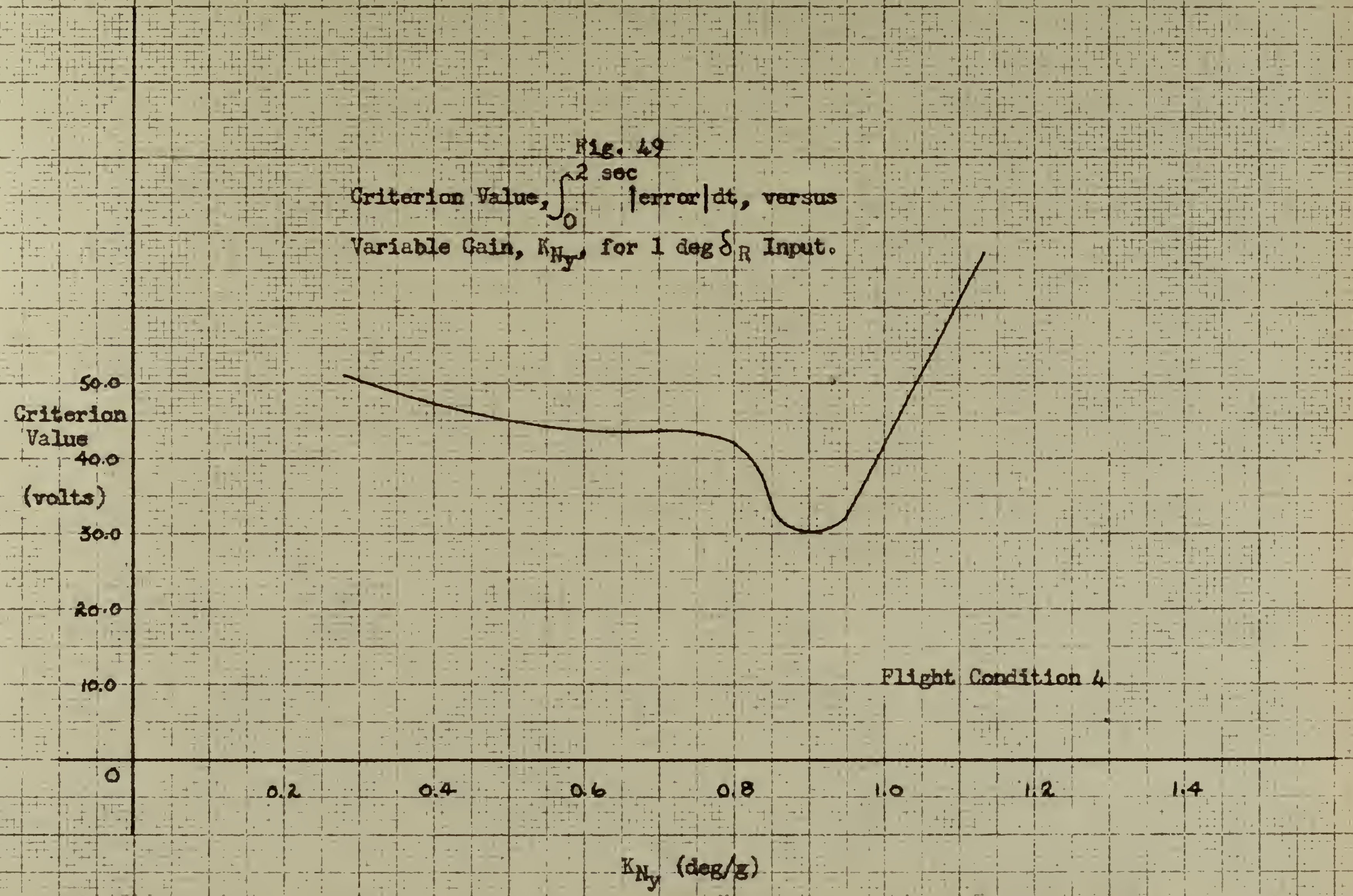

Fig. 49

Criterion Value, $\int_0^{2\,\mathrm{sec}} |\mathrm{error}|\,dt$, versus Variable Gain, K_{N_y}, for 1 deg δ_R Input.

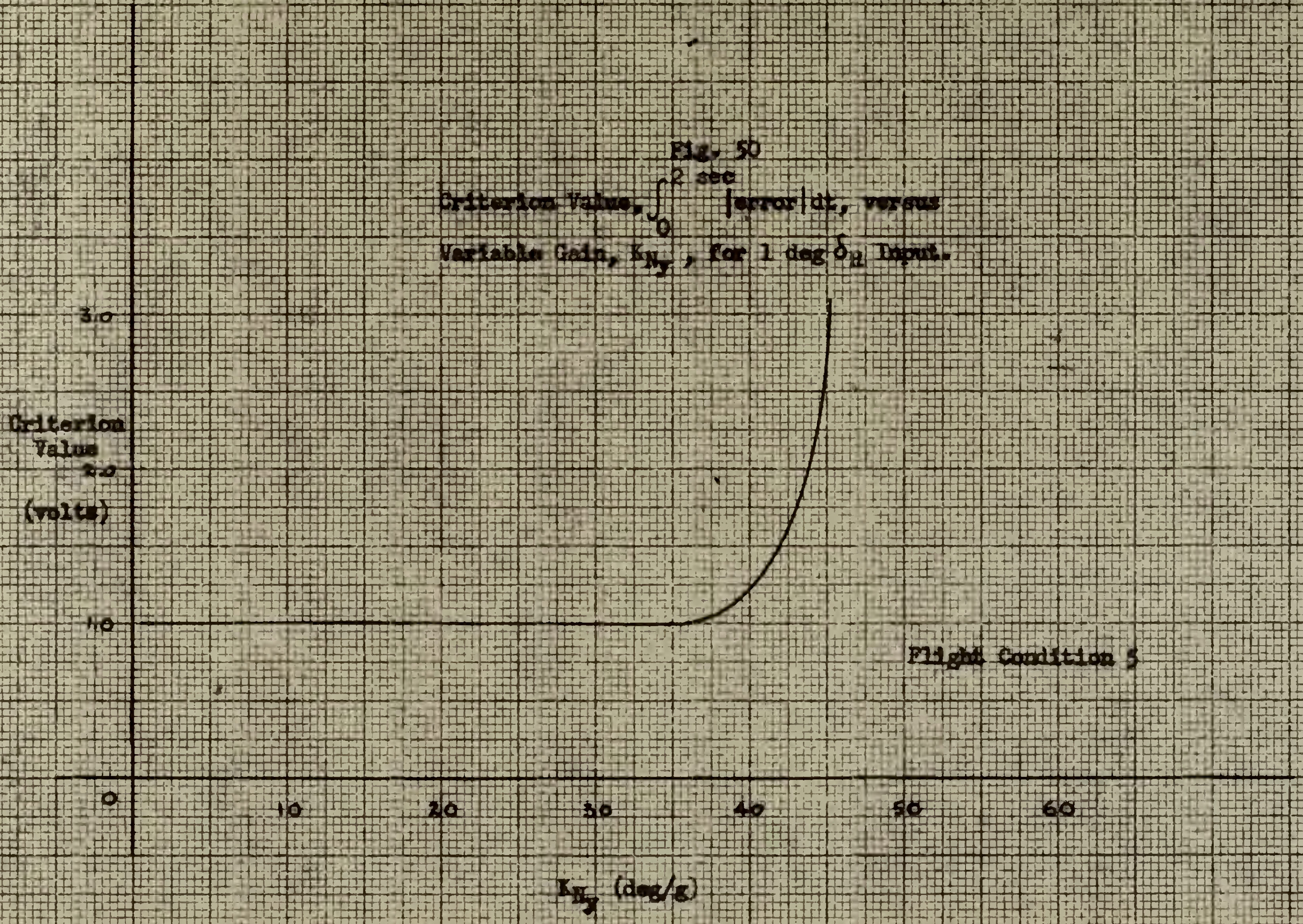

Fig. 50

Criterion Value, $\int_0^{2\,sec} |error|\,dt$, versus Variable Gain, K_{N_y}, for 1 deg δ_H Input.

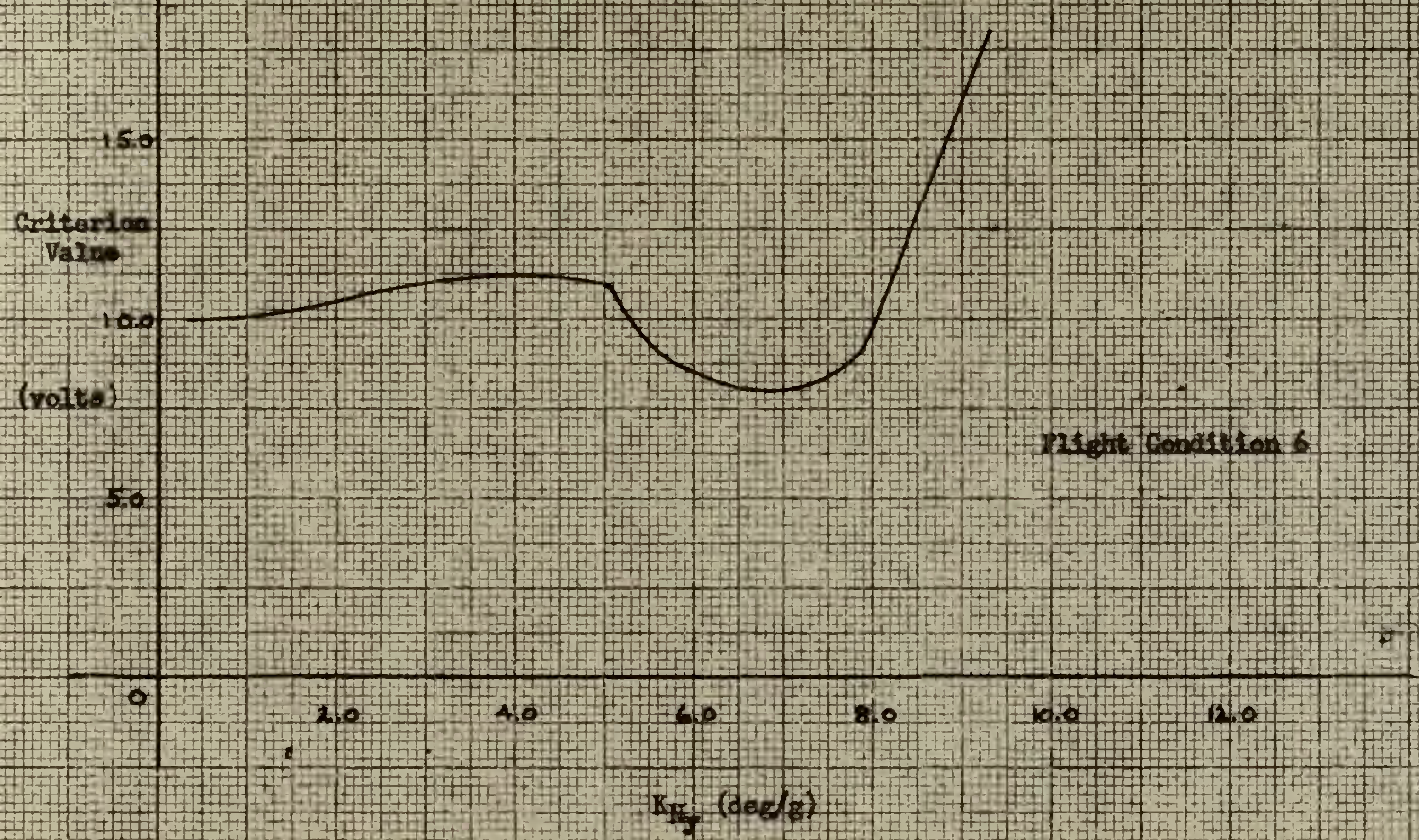

Fig. 51

Criterion Value, $\int_0^{2\ \mathrm{sec}} |\mathrm{error}|\,dt$, versus Variable Gain, K_{N_y}, for 1 deg δ_R Input.

final flight condition indicated in Fig. 51 exhibited an essentially flat region from the residual gain K_{Ny} equal to 0.5 deg/g to approximately K_{Ny} equal to 2.0 deg/g. The error integral then achieved a maximum and thereafter a minimum value of K_{Ny} equal to 6.0 deg/g. Again, in this flight condition, there were, as far as the corrective logic could discern, two seekable minimums which depended upon the initial value of K_{Ny} imposed, or, the value of variable gain with relation to the criterion maximum mentioned above.

Therefore, in the case of flight condition 1, the landing condition and one in which maximum stability is desired from a control standpoint, it was ascertained that adaptation was sluggish and slow due to relatively small values of the error criterion as a result of the input disturbance. Furthermore, the flat regions of criterion value caused little or no variation with gain and therefore the criterion was actually insensitive to gain in these regions. These tendencies will result in the adaptive controller remaining in the region or perhaps slightly drifting in variable gain value until either an increase or decrease in criterion value causes further adjustment. Admittedly, the change is oscillating damping ratio between these regions is small and this may be noted from the root locus plot in Fig. 6. Since, as seen from the figure, the movement of the short period root from the complex pole is slight over the gain region 0.5 deg/g to 45 deg/g.

Therefore, it may be concluded that the ability of the system to seek the flat or minimum regions of the criterion was considered adequate while its ability to seek and remain at the minimum value of the criterion was inadequate. Furthermore, it may be concluded that relatively small values

of criterion signal resulted in a small adaptive error or drive signal to the servo gain changes which made corrective action sluggish even at high servo gains. The positive reference signal was adequate for adaptation and maximum Ny was acceptable. Finally, the system exhibited the ability to recover from oscillatory instability and adapt to an acceptable response.

Flight condition 2 effectively adapted in the regions of K_{Ny} equal to 3.0 to 6.0 deg/g. This agrees with the region of minimum values of the error criterion. Due to the flat region exhibited by the low gain region of the error criterion, adaptation from the residual K_{Ny} of 0.5 deg/g was unacceptably slow. This can be attributed to the fact that the adaptive error or criterion value remained essentially constant. The slope of the criterion curve for values of K_{Ny} greater than the optimum value of 5.0 deg/g was adequate to determine quickly an increase in the criterion and apply the necessary correction. The performance under increased pulse disturbance was satisfactory and desirable under the existing conditions since the increased pulse would supply more positive directional information at the gain region, K_{Ny} equal to 0.5 to 2.5 deg/g. The system was also capable of recovering from unstable initial conditions and did so adequately. The maximum Ny achieved during stable adaptation was acceptable and well below the pilot's sensing threshold.

Therefore, it may be concluded, that for flight condition 2 the positive reference signal was satisfactory; adaptation at all initial values of K_{Ny} greater than or equal to 3.0 deg/g was satisfactory; and, maximum airframe stresses were tolerable. Furthermore, it may be stated that performance of the system at initial values of K_{Ny} less than 3.0 deg/g was slow and essentially ineffective.

In the case of flight condition 3 the positive reference signal of 0.4 was again found to be the most effective and acceptable. The system showed the ability to recover adequately from divergent instability in approximately one optimizing interval. This particular flight condition indicated compatibility with the maximum and minimum values of the error criterion. When forced to adapt from an initial K_{Ny} of 0.5 deg/g the system sensed a minimum and was unable to attain the desirable minimum at approximately a K_{Ny} of 1.2 deg/g. On the other hand, when recovering from divergent instability, the system sought to minimize in the preferred location. In the other requirements the flight condition appeared to be adequately handled by the adaptive logic.

It may be concluded then that the system was satisfactory in adapting speed, recovery from divergent instability and operation with positive reference signal. The data also conclusively shows that when approaching the flight condition from higher gains than K_{Ny} equal to 1.2 deg/g the system will adequately adapt to this minimum.

Flight condition 4 contains the most satisfactory performance data with regard to operation of the adaptive controller. The system sought a minimum between the values of K_{Ny} equal to 0.5 deg/g and 0.9 deg/g. The error criterion variance with gain indicates that the minimum Ny should occur at a K_{Ny} of 0.9 deg/g. The minimum, however, is critical since the value of the error rapidly increases on either side. The hunting between the values stated above can be most intelligently reasoned by noting that the adaptive error would be large and the necessary gain variance is small. Slight overdriving of the adaptive positioner could result in the system sensing an error increase and overdriving the minimum which again results

in an error increase which results in overdriving the minimum in the opposite direction. Admittedly non-linear variance of the potentiometer at these lower gain values increases the system sensitivity but apparently not enough to allow the system to remain at the minimum error position. As previously stated, this action was not detrimental to the stability of the aircraft but served to eliminate the sluggish nature of response encountered in conditions 1 and 2.

It may be concluded that with regard to condition 4 the adaptive system operated satisfactorily with regard to corrective tendencies. The system never was capable of settling to the minimum value of the error criterion due to large drive voltages to the positioning servo causing overshoot not completely compensated for. The system was obviously capable of recovering from situations approaching instability as evidenced by its tendency to never exceed a K_{Ny} of approximately 0.9 deg/g. The value of the criterion increased so rapidly beyond this point that corrective action was always in the stabilizing direction. Conclusions about recovery from unstable conditions at this flight condition are meaningless since the aircraft could not possibly withstand the structural stresses.

Condition 5 performed adequately with the positive reference signal but conformed to the relatively insensitive variance of the error criterion with variable gain by adapting in a sluggish manner at all imposed initial conditions. Since the variable gain has very little effect upon the detectable response in the region of K_{Ny} from 0.5 deg/g to 40.0 deg/g, the location of the gain within this region is significantly unimportant. The major requirement in this instance is that the departure of the aircraft from this flight condition create suitable changes in the error criterion

variance with gain to permit selection of corrective information for the flight condition being approached which may, and probably does, require more exacting placement or positioning of the gain pot controlling K_{Ny}.

Therefore, it may be concluded that the tests at flight condition 5 are inconclusive since practically any gain within the region of the adjustable gain pot results in an undetectable variation in the error criterion.

Finally, in flight condition 6, the positive reference signal proved acceptable with regard to performance tendencies. The variance of the error criterion with variable K_{Ny} exhibited two minimum values separated by a maximum. The effect of this maximum was undesirable since it conceivably could result in performance at the flight condition at some non-optimum point determined by the minimum sought at values of low K_{Ny}. This is borne out by the actual results of testing which indicated the tendency of the controller to minimize at two separate values of gain. These K_{Ny} values coincide approximately with the observed minimums in Fig. 51.

Therefore, it may be concluded that adaptation of flight condition 6, while being satisfactory with respect to adapting speed and positive reference signal, was unsatisfactory in being able to seek the minimum value of the error criterion under all imposed initial conditions. The controller did conclusively prove, however, that it was capable of seeking a minimum which, though not the minimum value of the error criterion, was the only minimum the system could discern.

In summary, the analysis of the adaptive controller unit must be considered to establish the fact that the basic logic and principles of

controller design are satisfactory. It is concluded that the designed sequence and logic of the controller is acceptable for application to any control process whose parameter or parameters may be altered as the direct result of the minimization of some measurable variable. Since the adaptive controller is definitely limited by the necessary time sequencing, the period of control that must be exhibited by the adaptive scheme is of considerable importance and must be studied and proved acceptable before application. There was insufficient mechanization available on the computer to enable test of the adaptive system over some characteristic flight profile to establish that the controller was capable of continuously modifying the loop gain to insure the most acceptable, minimum error response. Study of the variation in the value of the absolute integral of error indicated that the system would most probably exhibit no difficulty in adapting from large gain values to the smaller values of K_{Ny} required for the more sensitive flight conditions. However, these same curves indicated that in some instances of low gain, false minima occurred because of real root incluence and these may result in the adaptive system being subjected to minimum values which were stable but certainly did not produce the most acceptable response.

Therefore, it is considered that there is inadequate data to enable prediction of whether or not the adaptive system will successfully handle a particular flight profile.

The information obtained on the behavior of the error criterion during the variation of gain for each particular flight condition indicates that for the aircraft the selection of the integral of the absolute error was unsatisfactory. The principal reasons for its inadequacy were the fact that

in several instances gain variations produced little or no effect upon the value of the criterion and the fact that false minima occurred in several flight cases. The former was attributed to the slow movement of the roots from the short period poles causing very little change in the value of the resulting error. The latter inadequacy was directly attributable to the influence of the real roots over the complex dominant roots at low values of K_{Ny} .

Therefore, it is concluded that the error criterion was inadequate in the majority of flight conditions for the reasons given above. Since the adaptive controller depends entirely upon the establishment of adequate, constantly minimizing error criteria, it must be furthermore concluded that establishment of the system for the particular aircraft tested was not achieved.

Finally, it must be concluded that the investigation of all possible methods of compensation and establishment of appropriate error criteria which do properly behave has by no means been exhausted. Therefore, it is recommended that additional testing and analysis in these particular areas be conducted. Detailed recommendations with these thoughts in mind are included in the following chapter.

CHAPTER XIII

Conclusions and Recommendations

The stability analysis conducted using the various suggested lateral responses as methods of providing a means for stable adaptive control resulted in the following conclusions:

1. Yaw rate and N_y with filters 2 and 3 were undesirable as control variables since the second order dominance of the short period pair of roots were greatly distorted by the real roots. Due to this fact, the system tended to be less oscillatory and therefore less sensitive to a variation in ζ as a result of varying loop gain.
2. The aerodynamic inadequacies of yaw rate as a response precluded its use in an integrated control loop of a flight control system.
3. The feasibility of the combined response N_y with $\dot{r}$ was established with regard to provision of a system whose characteristics more closely resembled those desired for adaptive control by the methods contained in the report.
4. N_y with filter 1 compensation was the most desirous of the responses analyzed, however, in several insensitive flight conditions variation of ζ with varying K_{Ny} was inadequate.

With regard to the analysis, design, and performance of the adaptive controller the following conclusions are advanced:

1. Operation and performance of the logic and sequencing of the adaptive controller was satisfactory and design was adequate.
2. The error criterion, $\int |E|\, dt$, chosen as the vehicle by which the controlled response was to be minimized was inadequate in many flight conditions since it failed to produce directional, corrective

information to the controller. In the case of flight conditions 3 and 6 it exhibited minimum values which were in addition to the désired minimum occurring at the optimum response.

3. Performance indicated that provision of the proper minimizing criterion, as might be indicated by application of the tested error criterion to a second order servomechanism, would result in adaptation to the specified minimum criterion value.

The recommendations shall be primarily concerned with the further analysis of the lateral loop response and refinements or variations of the Self Adaptive Controller. The ramifications of some of the problems concerned with a five degree of airframe will also be pointed out as paths for further study to proceed upon.

Certainly the study of additional compensation devices should be pursued. The effect on the root loci family for N_y with perturbations of the lead filter pole and zero should be investigated. The use of more complex compensation to place complex conjugate zeros at a location to aid in forcing the short period pair of roots into a desirable domain by high gains may be possible and worthy of study. Study should be conducted upon the effect of lead compensation on the N_y plus $\dot{r}$ scheme.

Concerning the adaptive controller, the greatest area for study is in the selection of a suitable error criterion. A criterion must have a distinguishable minimum at the optimum value. Preferrably it should be concave in shape with a single, well defined minimum. To be able to establish this characteristic for an error criterion for any complex servo would make this Adaptive Controller very effective. The time sequence of the controller

should be studied further. The relative length of the operating portions of the optimizing period as well as the overall length of the period need investigation to choose their optimum. Studies to develop systems to establish procedures for choosing of optimum times would be of value.

Further study should be made of the methods available for introducing disturbance signals to the airframe. Studies should provide for investigation of the most suitable type of disturbance. Certainly the use of random noise to actuate the controller instead of pulsing the rudder would be of an advantage. However, the effect of this would have to be determined with regard to adequacy, magnitude and sensitivity.

Another area for study would be the gain changing servo loop itself. The use of rate limiting on this loop was proposed to enable it to adapt faster yet be less sensitive to a gusting environment. Further study is necessary to pick the best value for the threshold which changes the gain of this loop.

Considering a five degree of freedom airframe many problems arise. The solution of these problems, or at least a feel for their effect, would be necessary before design is considered final. The effect of δ_A inputs must be further investigated. The analysis and testing of the effect of roll cross coupling would be of great interest. The effect of this coupling would be of great interest. The effect of this coupling when using schemes like N_y plus $\dot{r}$ should be analyzed. The effect of residual vibrations or environmental vibrations on instrumentation should be investigated. The analysis of the airframe considered as flexible, with the consequent involvement of bending modes, would complete any study of this control loop.

APPENDIX A

Computation Methods for Determination of Root Locus Plots

In order to conveniently compute the numerous root locus plots required during the analysis, the stability matrix associated with the control loop, or its characteristic determinant, was derived for solution by digital computer. Thus the small but present contribution from distant poles and zeros were taken into account.

The characteristic determinant of the stability loop was formed by the coefficients of the variables defined by all loop transfer functions. Referring to Fig. 2, it may be noted that these variables are:

N_y or r	Airframe lateral response
N_{y1} or r_1	Lateral response measured by instruments
δ_{R_2}	Output of variable gain pot and compensation network, if included
δ_{R_1}	Output of autopilot actuators
δ_R	Output of main rudder actuators

Because of the inability of the IBM 704 computer to accept, in determinant solution, a coefficient of higher order than a quadratic the airframe lateral transfer functions were not used as such. The basic equations of motion, for three degree lateral response, from which the lateral transfer functions were derived, were substituted. In this method all coefficients were second order or lower. The three equations of motion are developed in Chapter II of Reference 10. Assuming rudder deflections as the only forcing function and after application of perturbation techniques and the LaPlace transform for each flight condition the equations take the form:

$$(a_1 s^2 + a_2 s + a_3)\ \beta + (b_1 s^2 + b_2 s + b_3) r + (c_1 s^2\ c_2 s\ c_3)\ \phi = A\ \delta_R$$

where the coefficients of the variables take on values assigned by aerodynamic constants and derivatives. Any of the constants may take the value of zero with the exception of the constant A.

In the cases where N_y is the lateral response being plotted, or some portion of it such as $N_y + \dot{r}$, a supplementary equation is needed to establish the relation between the motion equation variable and N_y. This equation is established by a force equation in the lateral direction which results in;

$$F_y = Y \dotplus mg \sin\phi = mV(\dot{\beta} + r) + m\dot{V}\beta$$

In magnitude comparison, the last comparison, the last term, $m\mathring{V}\beta$, is negligible and is dropped. Therefore, the lateral force, F_y, becomes $mV(\dot{\beta} + r)$. Then it follows that N_y is expressed in g's by;

$$N_y = \frac{F_y}{mg} = \frac{V}{g}(\dot{\beta} + r) = \frac{V}{g}(x\beta + y\delta_R)$$

where it conveniently is true that one of the equations of motion contains $\dot{\beta}$ and r with coefficients of 1.0 and a substitution to terms of β and δ_R may be made.

The remaining loop variables are then defined and interrelated by the transfer functions of loop components. In the case of N_y as the airframe response and filter 1 as a compensation network, these equations become;

$$N_{y1}(s^2 + 175.9s + 15795) - 15795N_y = 0$$

$$\delta_{R_2}(0.1s - 1) - N_{y_1} K_{Ny}(s + 1) = 0$$

$$\delta_{R_1}(s^2 + 40s + 800) \pm \delta_{R_2}(800) = 0$$

where $\pm$ determines feedback sign employed, and finally;

$$\delta_R(s + 10) - 10\delta_{R_1} = 0$$

Therefore the coefficients may be arranged in matrix form as shown in Fig. A-1. Thus by varying the value of K_{Ny} and solving the determinant, the characteristic equation is produced and may be factored to produce the roots coincident with the particular value of K_{Ny} and flight condition.

In a similar manner the matrices for the other responses chosen in the analysis can be derived. The number of loop variables present then determining the number of simultaneous equations necessary to solve the matrix determinant. The control equations for each flight condition will not vary as various responses are tested. However the response N_y does require an extra equation to relate this force to the control variable.

In summary it may be noted that the characteristic determinant is actually a set of simultaneous equations whose coefficients determine the characteristic equation of the loop and hence its roots. It is emphasized again that due only to computer characteristics were the basic equations of motion substituted for the airframe transfer functions previously given. The control equations are not furnished in this report but in continuing work, where more extensive root locus investigation is necessary, the transfer functions are adequate as a basis.

β	r	ϕ	δ_R	$N_{y'}$	$N_{y'}$	δ_{R1}	δ_{R2}		
$(a_{11}s^2+a_{12}s+a_{13})$	$(b_{11}s^2+b_{12}s+b_{13})$	$(c_{11}s^2+c_{12}s+c_{13})$	A_1	0	0	0	0	=	0
$(a_{21}s^2+a_{22}s+a_{23})$	$(b_{21}s^2+b_{22}s+b_{23})$	$(c_{21}s^2+c_{22}s+c_{23})$	A_2	0	0	0	0	=	0
$(a_{31}s^2+a_{32}s+a_{33})$	$(b_{31}s^2+b_{32}s+b_{33})$	$(c_{31}s^2+c_{32}s+c_{33})$	A_3	0	0	0	0	=	0
$(a_{41}s^2+a_{42}s+a_{43})$	0	$(c_{41}s^2+c_{42}s+c_{43})$	A_4	-1.0	0	0	0	=	0
0	0	0	0	-15795	$(s^2+175.9s+15795)$	0	0	=	0
0	0	0	0	0	$-K_{Ny}(s+1)$	0	$(0.1s+1)$	=	0
0	0	0	0	0	0	$(s+40s+800)$	(± 800)	=	0
0	0	0	$(s+10)$	0	0	-10	0	=	0

Fig. A-1

Stability Matrix for Determination of Root Locus Plots

APPENDIX B

Analog Computer Implementation and Techniques

As a part of this study analog simulation of the aircraft and control loop was made and computer solutions obtained. This study was carried out for two basic purposes. First, in order to amplify or verify the root locus characteristics of the various schemes and thereby enable the choice of the most acceptable lateral response. Secondly, in order to provide the capacity for proving or disproving the Adaptive Controller's capabilities. This was the most practical way to test the adaptive controller in the allotted time.

To accomplish the first part of the analog study the aircraft control equations and equations of the various other parts of the system were mechanized on Electronic Associates Analog Computers. This mechanization was done in accordance with the diagram in Fig. 52. The lateral, three degree aircraft control equations used were as follows;

$$\dot{\beta} = \frac{1}{1 - \dfrac{\bar{q}_0 S b}{2 m V_0^2}} \Bigg[\frac{\bar{q}_0 S b}{2 m V_0^2} C_{Y_p} p + \left(\frac{\bar{q}_0 S b}{2 m V_0^2} C_{Y_r} - 1 \right) r + \frac{\bar{q}_0 S b}{m V_0} C_{Y_\beta} \beta + \frac{\bar{q}_0}{V_0} \cos\phi \cdot \phi + \frac{\bar{q}_0 S}{m V_0} C_{Y_{\delta_A}} \delta_A + \frac{\bar{q}_0 S}{m V_0} C_{Y_{\delta_R}} \delta_R \Bigg]$$

ROLL RATE GYRO
CONTROL STICK
BANK LIMITER
ROLL RATE LIMITER
TRIM INT.
ROLL AFCS ACTUATOR
CADS
AILERON ACTUATOR
LATERAL ACCELEROMETER
LEAD NETWORK
YAW AFCS ACTUATOR
RUDDER ACTUATOR
TO SELF-ADAPTIVE COMPUTER

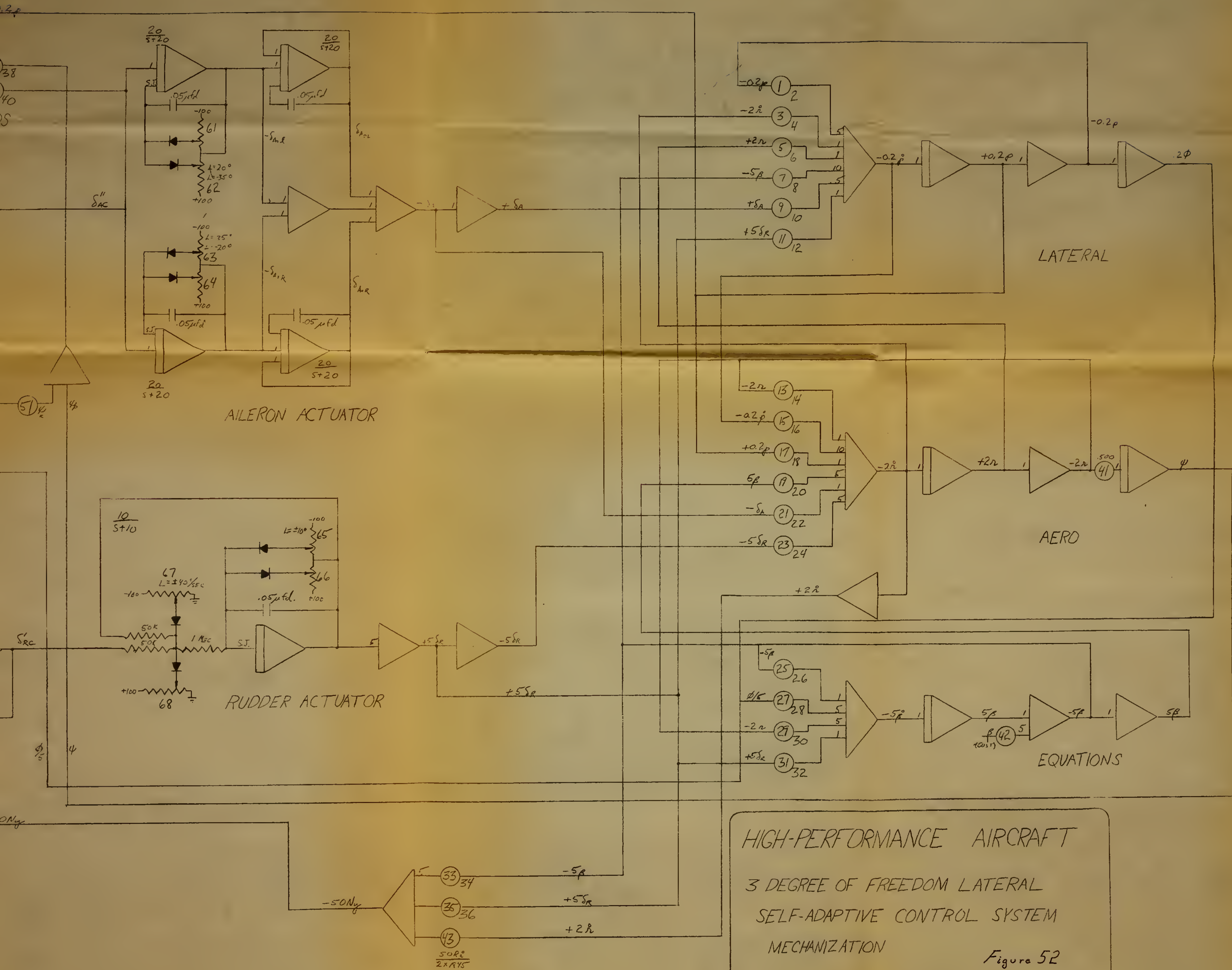

HIGH-PERFORMANCE AIRCRAFT

3 DEGREE OF FREEDOM LATERAL SELF-ADAPTIVE CONTROL SYSTEM MECHANIZATION

Figure 52

7-21-59 TEM

$$\dot{p} = \frac{\bar{q}_0 S b^2}{2 I_x V_0} C_{L_{\dot{\beta}}} \dot{\beta} + \frac{\bar{q}_0 S b}{I_x} C_{L_\beta} \beta + \frac{\bar{q}_0 S b^2}{2 I_x V_0} C_{L_p} p + \frac{I_{xz}}{I_x} \dot{r}$$

$$+ \frac{\bar{q}_0 S b^2}{2 I_x V_0} C_{L_r} r + \frac{\bar{q}_0 S b}{I_x} C_{L_{\delta_A}} \delta_A + \frac{\bar{q}_0 S b}{I_x} C_{L_{\delta_R}} \delta_R$$

$$\dot{r} = \frac{\bar{q}_0 S b^2}{2 I_z V_0} C_{N_{\dot{\beta}}} \dot{\beta} + \frac{\bar{q}_0 S b}{I_z} C_{N_\beta} \beta + \frac{I_{xz}}{I_z} \dot{p} + \frac{\bar{q}_0 S b^2}{2 I_z V_0} C_{N_p} p$$

$$+ \frac{\bar{q}_0 S b^2}{2 I_z V_0} C_{N_r} r + \frac{\bar{q}_0 S b}{I_z} C_{N_{\delta_A}} \delta_A + \frac{\bar{q}_0 S b}{I_z} C_{N_{\delta_R}} \delta_R$$

$$N_y = \frac{\bar{q} S}{m g} \left[C_{y_\beta} \beta + C_{r_{\delta_R}} \delta_R \right] + \frac{R_{\dot{r}} \dot{r}}{57.3\, g}$$

These equations of motion are described in Chapter II of Reference 10 and standard symbols are employed. In the mechanization of these equations relays were used to permit fast switching between any two flight conditions. The roll channel was included in this mechanization in the hope that time would permit observation of the effect of aileron deflection, δ_A .

The transfer functions of the other system components in the lateral loop have been listed in the text. The components of the roll loop and their transfer functions are;

Aileron Actuators	$\frac{20}{(s + 20)}$	$\pm$ 55 deg (position)
Roll AFCS Actuators	$\frac{60}{(s + 60)}$	$\pm$ 40 deg/sec (rate)
Roll Rate Gyro	$\frac{15800}{(s^2 + 176s + 15800)}$	

The settings of the potentiometers for the various flight conditions are tabulated in Table XVIII. The flight conditions noted on these potentiometer setting sheets correspond to conditions 1 through 6 as follows:

A1---- Condition 1

A2---- Condition 2

A3---- Condition 3

B1---- Condition 4

B2---- Condition 5

C1---- Condition 6

Prior to data recording, the steady state values of the aircraft equations were checked. Then the control loops were closed and dynamic response data collected at each flight condition for each response analyzed.

When this phase of the analog study was completed, the Adaptive Controller was mechanized in order to test its performance and characteristics. The diagram of this mechanization, as well as a switching logic table, are contained in Fig. 53. The stepping relay timer was connected to and operated standard eleven pole step switches from a digital voltmeter. This complete mechanization with the Adaptive Controller connected to modify the variable loop gain provided the facilities to completely check out the logic, operating parameters, and aircraft performance. Recording equipment was included as needed throughout this study.

TABLE XVIII

POT SETTINGS

#1 FLIGHT CONDITION

#3 Pot. No.	A.1.	A.2.	A.3	B.1.	B.2	C.1.
1	.177		1.038			.187
2		.496		.841	.093	
3	.138		.000			.035
4		.057		.001	.128	
5	.010		.109			.013
6		.072		.126	.009	
7	.022		.073			.093
8		.059		.540	.033	
9	.170		2.025			.290
10		.865		.760	.282	
11	.005		.991			.196
12		.123		.801	.021	
13	.132		.644			.079
14		.250		.498	.053	
15	.247		.000			.037
16		.062		.001	.170	
17	.147		.000			.050
18		.217		.016	.028	
19	.059		.971			.172
20		.200		.412	.073	
21	.056		-3.400			.153
22		.685		.180	.000	
23	.030		.711			.176
24		.114		.700	.043	
25	.130		.437			.057
26		.199		.332	.050	
27	.680		.152			.055
28		.360		.100	.208	
29	.500		.500		.500	.500
30		.500		.500	.500	.500
31	.020		.103			.009
32		.038		.066	.009	
33	.035		.503			.180
34		.097		.579	.042	
35	.026		.593			.147
36		.093		.578	.038	

A. Very Low Altitude
1. Low Velocity, Low α
2. Moderate " , Moderate α
3. High " , High α

B. High Altitude
1. High Velocity, Very High α
2. Low Velocity, Low α

C. Very High Altitude
1. High Velocity, Moderate α

Switched Cases: A.1. ⟷ B.1
A.3 ⟷ A.2
C.1 ⟷ B.2.

12ND 6173

TABLE XVIII

#2 FLIGHT CONDITION

POT No.	A.1.	A.2.	A.3.	B.1.	B.2.	C.1.		
37	↑							
38								
39	CADS GAINS (SET TO 0 FOR PROBLEM)							
40	↓							
41	.500 →	→	→	→	→	→		
42	β GUST (VARIED)							
#43	.0163R°							
44	.035							
45	.158							
46	.158							
47	.100							
48	.800							
49	$K_{n_z}/400$							
50	.800							
51	ψ_K							
52	.223							
53	.400							
54	.395							
55	1.000							
56	$\phi_K/5$							
57	K_{SA}							
58	K_{SA}							
59	.600							
60	.500							
61	L = -35°							
62	L = 20°							
63	L = -20°							
64	L = 35°							
65	L = -10°							
66	L = +10°							
67	L = -40°/SEC							
68	L = +40°/SEC							
69	L = -40°/SEC							
70	L = +40°/SEC							
71	L = -40°/SEC							
72	L = +40°/SEC	→	→	→	→	→		

12ND 6173

TABLE XVIII

#3

FLIGHT CONDITION

POT. No.	1.	2.	3.	4.	5.	6.		
73	L = +45°							
74	L = -45°							
75	L = 20°/SEC							
76	L = -20°/SEC							
77	NOT USED							
78	"							
79	"							
80	"							
81	KI/50							
82	.500							
83	D.C. REF.							
84	THRESHOLD							
85	SERVO GAIN							
86	.200							
87	.167							
88	.100							

12ND 6173

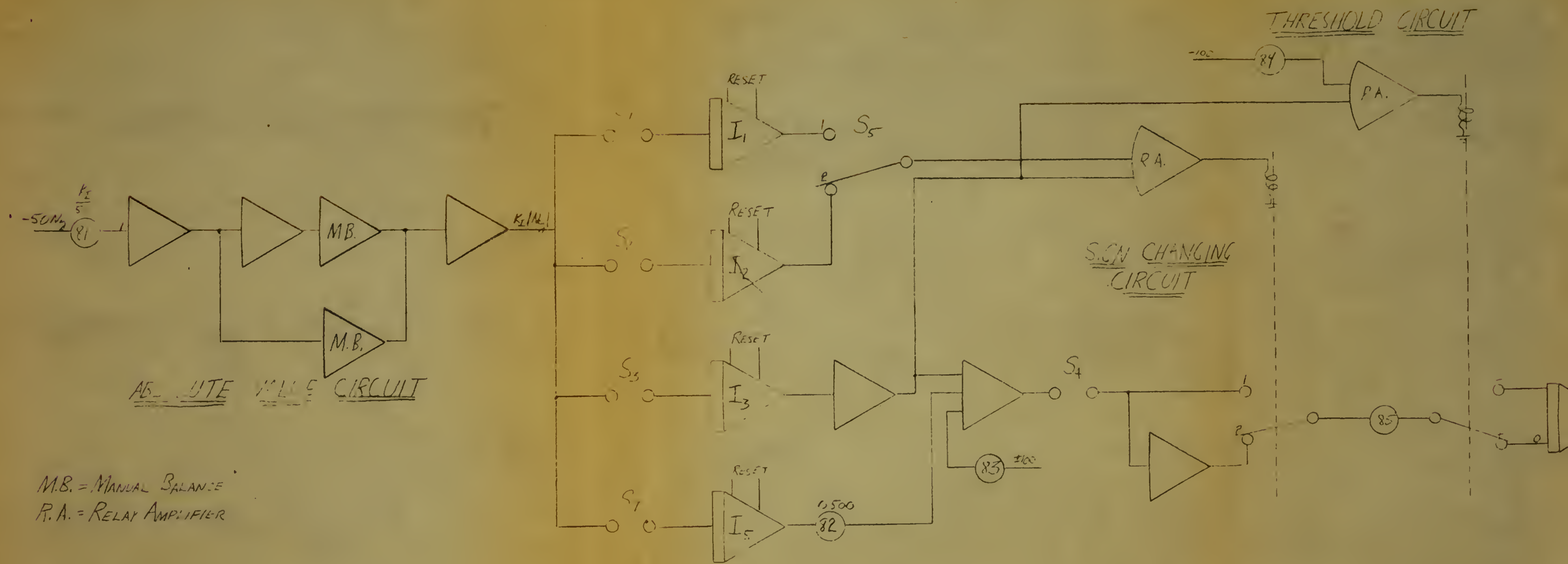

SELF-ADAPTIVE COMPUTER

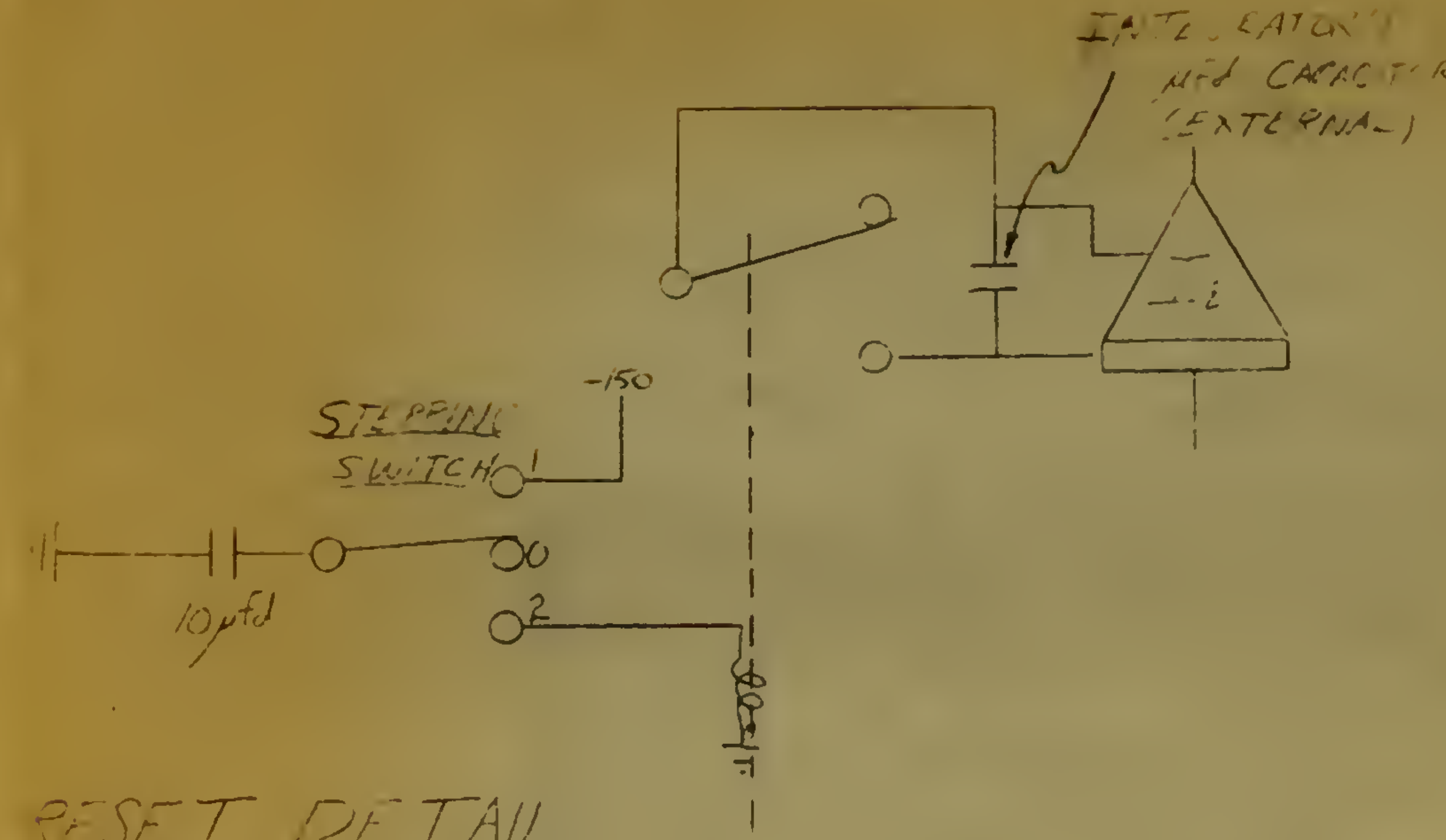

RESET DETAIL
(4 SETS)

0 = OPEN
1 = CLOSED OR POSITION 1
2 = POSITION 2

POSITION 2 FOR INTEGRATORS = RESET
0 OR 1 = INTEGRATE
11 RECHARGES RELAY-THROW CAPACITORS)

CYCLE DESIGNATION	TIME (SEC)	STEPPING POSITION	S_1	S_2	S_3	S_4	S_5	S_7	I_1	I_2	I_3	I_5	S_*
t_{10}	0	1	0	1	1	0	1	1	0	0	0	0	0
	1	2	0	1	1	0	1	1	0	0	0	0	0
t_{11}	2	3	0	0	0	1	1	0	1	0	1	1	0
	3	4	0	0	0	1	1	0	0	0	0	0	0
t_{12}	4	5	0	0	0	0	2	1	2	0	2	2	0
	5	6	0	0	0	0	2	1	2	0	2	2	0
t_{20}	6	7	1	0	1	[illegible]	[illegible]	1	0	0	0	0	0
	7	8	1	0	1	[illegible]	[illegible]	1	0	0	0	0	0
t_{21}	8	9	0	[illegible]	0	1	2	0	0	1	1	1	0
	9	10	0	0	0	1	2	0	0	0	0	0	0
t_{22}	10	11	0	0	0	0	1	1	0	2	2	2	1
	11	11	0	0	0	0	1	1	0	2	2	2	1
t_{30}	12	1	0	1	1	0	1	1	0	0	0	0	0
	13	2	0	1	1	0	1	1	0	0	0	0	0
t_{31}	14	3	0	0	0	1	1	0	1	0	1	1	0

STEPPING SWITCH LOGIC

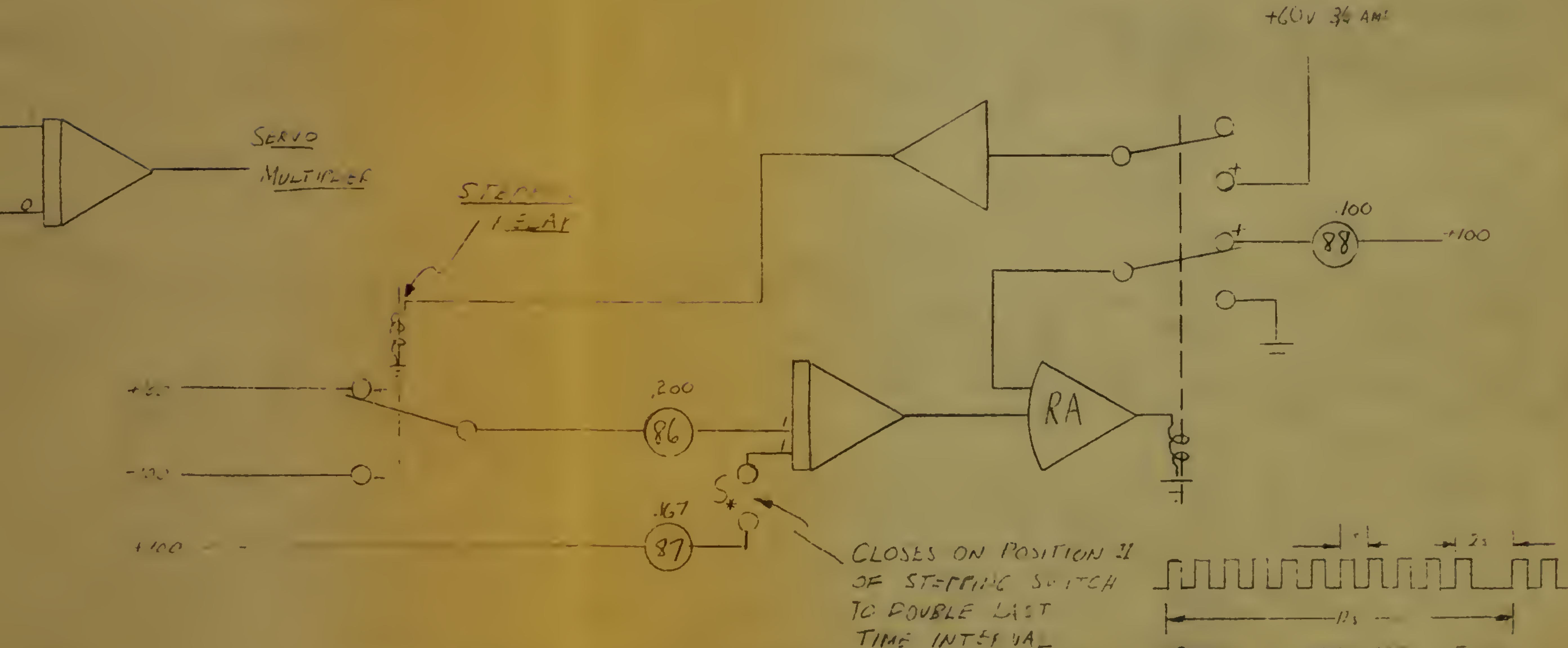

TIMING CIRCUIT FOR STEPPING RELAY

Figure 53

References and Bibliography

1. Smyth, R. K., Unpublished Lecture Notes and Comments; Autonetics Division, North American Aviation, Inc., 1959.

2. Minneapolis Honeywell Company, Aero Division, A Study to Determine an Automatic Flight Control Configuration to Provide a Stability Augmentation Capability for a High Performance, Supersonic Aircraft; WADC Report 57-349, May 1958.

3. Whitaker, H. P., Yamron, J., and Kezer, A., Design of Model Reference Adaptive Control Systems for Aircraft; Massachusetts Institute of Technology, September 1958.

4. Dandois, M., Self Adaptive Control Systems; Convair FZM-1242, September, 1958.

5. Lathrop, R. C. and Graham, D., The Synthesis of Optimum Transient Response; Criteria and Standard Forms; AIEE Technical Paper 53-249, Applications and Industry, November, 1953.

6. Merriam, C. W., III, Use of a Mathematical Error Criterion in the Design of Adaptive Control Systems; Presented at 1959 Annual Convention AIEE, January, 1959.

7. Merriam, C. W., III., Synthesis of Adaptive Controls; Servomechanism Laboratory, Massachusetts Institute of Technology, February, 1959.

8. Rath, Raymond R., Summary and Status of Adaptive Control System Program; Flight Control Laboratory, Wright Air Development Center, September 1958.

9. Li, Y. T., Adaptive Control Systems Philosophy; (publishing information on paper not available).

10. Norair, Dynamics of the Airframe; Buaer Report AE-61-4 II, Northrop Corporation, 1959.

11. Chalk, Charles R., Additional Flight Evaluation of Various Longitudinal Handling Qualities in a Variable Stability Jet Fighter; WADC TR 57-719 July, 1958.

12. Harper, Robert P., Jr., Flight Evaluation of Various Longitudinal Handling Qualities in a Variable Stability Jet Fighter; WADC TR 55-299, July 1955.

13. Moore, J. R., Open Cycle-Closed Cycle Systems; Proceedings of IRE, Vol. 39, 1951.

14. Campbell, G., Use of an Adaptive Servo to Obtain Optimum Response; Cornell Aero Laboratory, R-84, February 1957.

15. Whitaker, H. P., Design of Automatic Rudder Coordination System for Aircraft; MIT Instrumentation Laboratory, T-151, AD 97159, August, 1956.

16. Bairnsfather, R. R., A Self Adjusting Control System; MIT Instrumentation Laboratory, T-102, June, 1956.

17. Sperry Gyroscope Company, Feasibility Study for Automatic Optimizing Systems; WADC TR 58-243, Reports 1-4, AD 157970, AD 155576, 1957 and 1958.

18. Aeroneutronics Systems, Inc., Feasibility of a Self Optimizing Automatic Flight Control System; Reports 1-4, AD 149375, AD 149376, AD 149846, 1957 and 1958.

19. RCA Airborne Systems Laboratory, Techniques for Advanced Flight Control; Section 6, Adaptive Systems, AD 134443, June 1956.

20. Draper, C. S., and Li, Y. T., Principles of Optimalizing Control Systems and an Application to the Internal Combustion Engine; ASME Publication, September, 1951.

21. Tsien, H., Engineering Cybernetics; McGraw-Hill, 1955.

22. Dandois, M. and Lowes, A., Analysis and Synthesis of a Linear, Self Adaptive Stability Augmentation System; Convair FZA 271, January 1959.

23. Smyth, R. K., Autonetics Adaptive Flight Control System for an Advanced Flight Test Vehicle; Autonetics EM 1766, North American Aviation, Inc., 1959.

24. Thaler, G. J., Unpublished notes for a class in Advanced Linear Servomechanisms; Department of Electrical Engineering, U. S. Naval Postgraduate School, October 1958.